# Characterisation of Noradrenergic Inputs in the Myenteric Plexus of the Human Colon

**Dominic Robert Parker, MBBS**

*Thesis submitted to Flinders University for the degree of*

**Master of Surgery (by Research)**

College of Medicine and Public Health

August 2021

Flinders UNIVERSITY

FLINDERS MEDICAL CENTRE

# Table of Contents

## Summary

The sympathetic nervous system inhibits human colonic motility largely by releasing noradrenaline in the myenteric plexus, causing presynaptic inhibition of the release of acetylcholine. It is unclear whether noradrenergic inputs preferentially target specific cell types in a “hard-wired” fashion, or release noradrenaline diffusely by volume transmission. The objective of these studies was to characterise the relationship of noradrenergic nerve terminals (varicosities) with intrinsic myenteric neurons.

Healthy colonic tissue was retrieved from colorectal resection specimens and small squares were dissected and fixed to expose the myenteric plexus. Multiple layer immunohistochemistry, confocal microscopy and 3D reconstruction identified noradrenergic varicosities (labelled with tyrosine hydroxylase, TH) close to nerve cell bodies labelled for HuC/D, choline acetyl transferase (ChAT) and nitric oxide synthase (NOS). Enkephalin (Enk) varicosities were used as a positive control because they have recently been shown to have an association with cholinergic neurons. Subsequent calculation of varicosity density within ±1µm of individual cells enabled a statistical comparison between cell types using a mixed effects model.

From 7 patients, 486 myenteric nerve cell bodies were analysed. The density of noradrenergic varicosities was significantly greater close to ChAT+/NOS- (cholinergic) compared to ChAT-/NOS+ (nitrergic) cells (median density ratio 1.35 varicosities/1000µm$^3$, 95% credible interval 1.04-1.69). This suggests that noradrenergic inputs preferentially target cholinergic neurons in the myenteric plexus. Enkephalin varicosities also showed preferential targeting of ChAT+/NOS- compared to ChAT-/NOS+ neurons (median density ratio 1.51 varicosities/1000µm$^3$, 95% credible interval 1.23-1.83) in keeping with results of previous studies. TH and Enk varicosity baskets were found surrounding cholinergic neurons, supporting the quantitative analysis and validating the novel method. A small population of catecholaminergic (likely dopaminergic) TH-immunoreactive myenteric neurons accounted for approximately 1% of all neurons in the myenteric plexus; these cells were ChAT-immunoreactive and hence likely to be cholinergic.

This study has further defined the pathway of sympathetic inhibition of colonic motility via the myenteric neurons of the enteric nervous system, demonstrating preferential connectivity between noradrenergic inputs and intrinsic cholinergic cells. Further research is required to determine the

specific neurochemical code and functional class of cells targeted by sympathetic axons.

## Declaration

I certify that this thesis does not incorporate without acknowledgement any material previously submitted for a degree or diploma in any university; and to the best of my knowledge and belief, does not contain any material previously published or written by another person except where due reference is made in the text.

Dr Dominic Parker

# List of Tables

# List of Figures

# List of Abbreviations

| | |
|---|---|
| 3D | 3-Dimensional |
| 5-OHDA | 5-Hydroxydopamine |
| 5-HT | 5-Hydroxytryptamine |
| AXR | Abdominal X-ray |
| ACh | Acetylcholine |
| ATP | Adenosine Triphosphate |
| AF488 | AlexaFluor 488 |
| AMCA | Aminomethylcoumarin |
| ANS | Autonomic Nervous System |
| CGRP | Calcitonin Gene-Related Peptide |
| COMT | Catechol-O-methyltransferase |
| CCK | Cholecystokinin |
| ChAT | Choline Acetyl Transferase |
| CT | Computed Tomography |
| CY3 | Cyanine Dye 3 |
| Cy5 | Cyanine Dye 5 |
| Dmaps | Diameter Maps |
| DOPA | Dihydroxyphenylalanine |
| DBH | Dopamine Beta-Hydroxylase |
| EM | Electron Microscopy |

| | |
|---|---|
| ENS | Enteric Nervous System |
| GABA | Gamma-aminobutyric acid |
| GIT | Gastrointestinal Tract |
| GLP-1 | Glucagon-like Peptide 1 |
| HRM | High Resolution Manometry |
| ICC | Interstitial Cells of Cajal |
| IPAN | Intrinsic primary afferent neurons |
| L-NOARG | L-Nitro-L-Arginine |
| LDCV | Large Dense Core Vesicle |
| MMC | Migrating Motor Complex |
| MAO | Monoamine Oxidase |
| MPO | Myenteric Potential Oscillations |
| NSE | Neuron Specific Enolase |
| NPY | Neuropeptide Y |
| NOS | Nitric Oxide Synthase |
| NA | Noradrenaline |
| NAT | Noradrenaline Transporter |
| PFA | Paraformaldehyde |
| PD | Parkinson's Disease |
| PBS | Phosphate Buffered Solution |
| PGP 9.5 | Protein Gene Product 9.5 |

| | |
|---|---|
| SSRI | Selective Serotonin Reuptake Inhibitor |
| STC | Slow Transit Constipation |
| SCV | Small Clear Vesicle |
| SDCV | Small Dense Core Vesicle |
| SOM | Somatostatin |
| SP | Substance P |
| TK | Tachykinin |
| TH | Tyrosine Hydroxylase |
| VIP | Vasoactive Intestinal Peptide |
| VAChT | Vesicular Acetylcholine Transporter |
| VMAT1 | Vesicular Monoamine Transporter 1 |
| VMAT2 | Vesicular Monoamine Transporter 2 |

## Acknowledgements

Many kind people have contributed to the completion of this research and deserve great thanks:

Professor Phil Dinning, my principal supervisor, for his guidance in the practical aspects of research, and ensuring I stayed on track.

Professor Simon Brookes, for formulating the concept for this project and directing the study throughout its course.

Professor David Wattchow, for introducing me to the world of Neurogastroenterology, linking my project to postoperative ileus and his overwhelming support.

Dr Tiong Cheng Sia, who has been through all this not long ago, for taking me under his wing and providing advice and friendship.

Dr Lukasz Wiklendt, for developing the novel computer software necessary for quantitatively calculating varicosity density from 3D reconstructed data and providing many of the related figures.

Lauren Jones, who is completing her own PhD, for teaching me how to use confocal microscopy and Imaris software.

All of the researchers in the Brookes laboratory, including Wei Ping Gai, Rochelle Petersen, and in particular Bao Nan Chen and Adam Humenick, who taught me the fundamentals of tissue dissection, immunohistochemistry, and how to work in a lab.

My family, for their continuing encouragement in all of my endeavours.

And my wife Jessica, for her ongoing support now and into the future.

# Chapter 1 Introduction and Literature Review

The objective of this thesis is to characterise the physiological connections between the sympathetic nervous system and neurons of the myenteric plexus of the human colon, with a view to understanding how colonic motility is modulated by sympathetic activity. A detailed appreciation of the specific relevant aspects of the physiology of the gastrointestinal and nervous system is required in order to demonstrate this and is discussed in the introduction. Of the three divisions of the autonomic nervous system, the sympathetic division and enteric nervous system are examined closely, while the parasympathetic division will not be examined here. The literature review presents what is already known regarding the noradrenergic innervation of the colon in animal and human models and sets the scene for this body of research. The way in which sympathetic modulation of motility manifests clinically in medicine and surgery is also considered.

## 1.1 The Gastrointestinal Tract

The overall function of the gastrointestinal system is to provide vital nutrients and energy to the body, broken down from ingested food and fluid. To achieve this, several essential functions are required: digestion of food macromolecules into smaller absorbable molecules, secretion of hormones and enzymes, absorption of nutrients, water, electrolytes and vitamins, movement of content through the length of the tract and excretion of waste produced in the process (Barrett et al., 2016). The gastrointestinal tract (GIT) is a continuous tubular structure comprised of the mouth, pharynx, oesophagus, stomach, small intestine, large intestine (colon and rectum) and the anus, each of which perform specific roles in the digestion and propulsion of luminal content (Hall and Hall, 2016b). Gastrointestinal physiology is complex, involving multiple organs and levels of regulation, and therefore is the subject of considerable research to attain an understanding that can be used to promote health and treat disease.

### 1.1.1 Basic Layers of the Intestinal Wall

Four main layers of the intestinal wall are present in the GIT from the oesophagus to the anus: mucosa, submucosa, muscularis propria and serosa. The innermost layer is the mucosa, which itself contains a glandular epithelium, a lamina propria and muscularis mucosae. In the small intestine, plicae circulares (circular folds), are a feature of the epithelium, as well as small projections into the lumen of the bowel called villi, which are covered with absorptive enterocytes interspersed with goblet cells; these structures increase the surface area for absorption. Crypts of Lieberkuhn are present also in the small bowel and the cells within these crypts have a secretory function. They also contain the stem cells from which new epithelial cells are constantly generated. The submucosa is a layer of connective tissue which serves to support the mucosa, and contains a network of vasculature, nerves and some lymphatics. The muscularis propria has two layers of smooth muscle cells running perpendicular to one another: the inner circular muscle running circumferentially, and the longitudinal muscle, which runs along the length of the bowel. This contractile smooth muscle is responsible for propulsive movement of luminal content along the length of the intestine. Striated muscle is present in the external anal sphincter as well as the proximal oesophagus, in which it transitions to smooth muscle over the middle third. A thin layer of mesothelial cells makes up the serosa, which is contiguous with the visceral peritoneum and the mesentery. Functionally, these four layers perform different roles, which vary depending on the region of the gastrointestinal tract (Bass and Wershil, 2016; Hall and Hall, 2016b).

### 1.1.2 Anatomy and Physiology of the Human Colon

Compared to the small intestine, the colon has a larger diameter but is shorter in length, being approximately one metre long. The luminal surface does not contain plicae circulares as in the small intestine. Three thick bands of longitudinal muscle called taeniae coli converge proximally at the appendix and distally at the terminal part of the sigmoid colon forming the rectum. Haustra are segmental features of the colon that are formed by the relatively shorter length of the taeniae coli in comparison to the rest of the colonic wall, giving rise to a series of out-pouchings. The colon receives approximately 1.2 to 1.5 litres per day of small intestinal content (chyme) delivered from the terminal ileum and through the ileocaecal junction (Dinning et al., 2016a). This content passes sequentially through the caecum, ascending, transverse, descending and sigmoid colonic segments, before entering the rectum and finally being eliminated as formed faeces through the anus, with a volume of approximately 200-400mL per day (Sinnatamby, 2011). Because it is a site of absorption of water and electrolytes, the colon has a significant role in maintaining fluid balance. Short-chain fatty acids, primarily butyrate, are additionally absorbed by the colon following fermentation of indigestible content by resident colonic bacteria. Movements of the colon mix the faecal content within haustra to promote better absorption. The colon, in particular the sigmoid and rectum, also acts as a reservoir for faeces. Faeces must eventually be excreted, and the colonic musculature propels stool distally along its length (propulsion) and finally expels faeces under voluntary control by the anal sphincter complex and pelvic floor musculature (defaecation) (Dinning et al., 2016a).

## 1.2 Gastrointestinal Motility

Gastrointestinal motility refers to the movement of content in the intestinal tract and the motor patterns that produce this. The activity of intestinal smooth muscle is controlled by myogenic mechanisms that cause spontaneous activity, and also by neurogenic mechanisms that have a significant effect in augmenting and altering this action (Dinning et al., 2016a).

### 1.2.1 Spontaneous Myogenic Activity

Smooth muscle cells in the muscularis propria act together to create coordinated contraction as a syncytium rather than as individual cells. Intermediate junctions join individual cells mechanically, while gap junctions allow electrical transmission between cells, enabling synchronised movement. The Interstitial Cells of Cajal (ICCs) are modified smooth muscle cells and are the pacemakers for the intrinsic activity of the circular and longitudinal layers of the muscularis propria. The ICCs allow for spontaneous rhythmic activity that can be considered the basic motor patterns of myogenic activity. Additionally, neural inputs may act initially on intermediary ICCs in order to alter myogenic activity (Spencer et al., 2016). There are two predominant types of spontaneous myogenic activity detailed below.

Slow waves in the intestine occur at a range of frequencies, decreasing from approximately 12 per minute in the human duodenum, to 8-9 per minute in the terminal ileum and to 2-8 per minute in the colon (Hall and Hall, 2016b). In the colon, these are generated from ICCs residing in the submucosal border of circular muscle (Rae et al., 1998). These waves propagate both orally and anally along the intestine and by themselves do not elicit smooth muscle contraction in the intestine, but produce an undulating membrane potential. Only once the electrical potential reaches a set electrical threshold does the muscle contract (Dinning et al., 2016a). Beginning in a separate pacemaker region of ICCs in the myenteric plexus of colon, myenteric potential oscillations (MPOs, or spike potentials) have a higher frequency of 12-20 per minute and are true action potentials. The summation of MPOs with slow waves and enteric neuronal input leads to electrical membrane potential reaching threshold (> -40mV) and muscular contraction occurring (Dinning et al., 2016a; Hall and Hall, 2016b).

It is important to note that while these myogenic mechanisms can cause muscular contraction independently, neurogenic coordination is required for large propulsive activity leading to significant movement of content. Experiments in which tetrodotoxin has been used to abolish

neural activity in the gut wall led to inhibition of propulsion of a bolus in isolated rabbit colon (Dinning et al., 2014b). However, the myogenic mechanisms may promote mixing of content in the small and large intestine (Spencer et al., 2016).

### 1.2.2 Neurogenic Activity

Neurogenic mechanisms interact with and alter spontaneous myogenic activity. The Enteric Nervous System (ENS) and its associated extrinsic inputs are responsible for exerting neurogenic control on the intestinal muscle. The ENS provides a network of neural circuitry within the intestinal wall. In the intestine, enteric excitatory motor neuron activity brings the slow waves toward the set threshold to cause significant smooth muscle contraction (Furness, 2006). Additionally, the ENS is able to coordinate larger propulsive movements of the bowel, enabling "mass movement" of intestinal content (Dinning et al., 2016a).

Bayliss and Starling described a fundamental concept they called the "law of the intestine" in 1899, whereby excitation and contraction occur oral to a bolus, and inhibition with relaxation below the level (aboral) of the bolus, resulting in anterograde movement of the content in a wave called peristalsis, which they initially considered to be a simple reflex (Bayliss and Starling, 1899). Trendelenburg developed a method to study peristaltic reflexes in guinea-pig small intestine caused by distension of the lumen early in the 20$^{th}$ century (Trendelenburg, 2006). Costa and Furness added to this phenomenon in their studies on isolated guinea-pig intestine/colon, in which a bolus placed in the lumen of the bowel triggered sensory neurons via luminal distension and subsequently activated polarised neural circuitry (Costa and Furness, 1976). Ascending excitatory motor neurons cause smooth muscle contraction proximal to the bolus, while descending inhibitory motor neurons cause active relaxation distal to the bolus. Motor neurons have action over short distances, while interneurons act over longer distances, synapsing with motor neurons 40mm maximally in the oral direction and over 70mm in the anal direction (measurements in human tissue) (Wattchow et al., 1995; Porter et al., 1997). The result of this was movement of bolus distally (aborally), and subsequently the content may activate the same polarised neuronal circuitry at its distal position to continue movement along the length of the bowel. Such polarity has been shown in human specimens for both motor neurons and interneurons (Wattchow et al., 1997).

While this movement of content aborally along the intestine is still commonly referred to as the peristaltic "reflex," a recent series of studies have proposed that the "law of the intestine" is a highly

adaptable process with speed of propulsion dependent upon the size and consistency of the content. As such, peristalsis is not an all or nothing reflex. This process was called the "neuromechanical loop hypothesis" of neural peristalsis (Dinning et al., 2014b). The neurogenic activity of the ENS is modulated by extrinsic input from the autonomic nervous system, including the sympathetic and parasympathetic divisions. These extrinsic neurons are also a part of a variety of gastrointestinal reflexes, which will be discussed later.

### 1.2.3 Small Intestinal Motor Patterns

Before moving to colonic motor patterns, it is worth briefly discussing the motor patterns of the small intestine. Peristalsis as described above occurs due to the coordination between the ENS and the smooth muscle and is an essential mechanism of propulsion of chyme through the small bowel.

After eating, the postprandial (or "fed") motility pattern takes over, triggered by luminal content in contact with the mucosa which induces vagal sensory signals and gastrointestinal hormonal action of cholecystokinin (CCK) and glucagon-like peptide 1 (GLP-1). The postprandial motor pattern produces "rhythmic segmentation," whereby contractions of the small intestine produce sequential segments, and then contractions in different areas divide the columns of luminal content into new segments and promote mixing. Additionally, this pattern may alternate with fast or slow peristalsis causing some limited propulsion of content. The importance of these motor patterns after eating a meal is in promoting mixing of food with the secreted enzymes for digestion, and bringing nutrients close to the mucosa for absorption (Rayner and Hughes, 2016).

In the fasting state, a distinct pattern takes over. The interdigestive motility pattern, labelled as the migrating motor complex (MMC), moves residual luminal content through the small intestine in a sweeping motion until reaching terminal ileum. This prevents bacterial stasis or migration of bacteria from the colon, which could otherwise cause small intestinal bacterial overgrowth (Miller et al., 2018). Finally, this pattern helps to remove epithelial cells that are regularly sloughed off from the intestinal wall (Furness, 2006). The MMC is responsible for the cyclical contractions that generally begin in the antrum of the stomach or the duodenum and move in an anterograde direction along the length of the small bowel, occurring at approximately 75-90 minute intervals in humans (Harris and Evers, 2017). There are four phases, beginning with a quiescent period (phase I), a period of random, irregular contractions (phase II), the period of greatest contractile activity (phase III, the "activity front") and finally decreasing contractions (phase IV) (Furness, 2006; Deloose

et al., 2012). The concept of the MMC was defined first by Szurszewski in dogs, who described the motor complex as the small intestinal interdigestive "housekeeper" (Szurszewski, 1969). The MMC is generated by the ENS, and extrinsic denervation does not prevent the MMC from occurring. Phase III is the most active period where high amplitude contractions occur resulting in propulsion and is likely to be induced by the action of the hormone motilin. After eating a meal which evokes the "fed" motor patterns, the interdigestive motor pattern resumes one to two hours later (Furness, 2006).

### 1.2.4 Colonic Motor Patterns

Colonic motility allows for storage, mixing and propulsion of luminal content. There are many colonic motor patterns described in animals and humans, and the descriptive terminology for these had been variable until a recent consensus paper was published from experts in the field (Corsetti et al., 2019). Studies of isolated animal colonic segments *in vitro* have demonstrated the following motor patterns: "neural peristalsis," being the long-distance anterograde propulsion of solid or liquid content; "ripples," which are chaotic myogenic contractions moving both orally and anally; "colonic motor complexes," that are likely neurogenic in origin and may migrate through the length of the colon; and "neural retrograde propagating contractions," that cause contractions moving content in the oral direction, and are neurogenic in origin (Corsetti et al., 2019).

Several modalities exist to examine the colonic motility in humans *in vivo*. Measurement of colonic transit studies, including radio-opaque marker studies, scintigraphy and wireless motility capsules provide insights into the movement of content, but provide no details on the motor patterns that move the content (Scott et al., 2020). While colonic manometry provides no information on the movement of content, it does measure intraluminal pressure and contact force of the bowel wall, allowing for the real time measurement of colonic contractions (Scott et al., 2020). Over the last 10 years, technological advances have allowed a significant increase in the number of sensors to be incorporated into manometry catheters, and these high-resolution manometry (HRM) studies have begun to reveal the types of contractile patterns that exist in the human colon (Dinning, 2018). These motor patterns have been summarised in a consensus document (Corsetti et al., 2019) and include the following:

1. Simultaneous pressure increases (also previously termed "colonic pressurisations") are recorded across every manometry recording sensor in the colon and may be related to anal

sphincter relaxation, rectal filling, and flatus.

2. Haustral boundary pressure transients are rhythmic contractions (3 per minute) that appear to occur at a haustral fold. These may correlate to the myogenic ripples seen in animals *in vitro*.
3. The cyclic propagating motor pattern consists of repetitive propagating contractions occurring at 2-6 per minute. While this motor pattern occurs throughout the colon, the majority of events originate at the recto-sigmoid junction and propagate through the sigmoid colon in a predominantly retrograde direction (Dinning et al., 2014a).
4. Low-amplitude propagating contractions produce pressure changes <50mmHg, generally moving anally and often during the daytime, approximately 40 to 120 times per day.
5. High-amplitude propagating contractions produce relatively larger pressure changes (>100mHg), can travel through the entire length of the colon, and occur between 4 to 23 times per day. Importantly, they are associated with colonic propulsion and defaecation.

Colonic motility represents the macroscopic picture of what is happening in terms of gastrointestinal transit in humans and may assist in the explanation of symptomatology in patients with functional bowel problems. The study of the enteric nervous system demonstrates the microscopic picture at a cellular and even biochemical level, which forms the functional units for colonic motor patterns and thus is integral to motility and assisting the diagnosis and treatment of such patients.

## 1.3 Modes of Neurotransmission

### 1.3.1 Overview of Neurotransmission

Neurotransmission refers to neuronal-neuronal or neuronal-effector communication. There is a hierarchy of modes of neurotransmission shown in Figure 1-1 (Goyal and Chaudhury, 2013). Two broad mechanisms exist: chemical transmission and electrical transmission. Electrical transmission is the physical communication between two neurons (or other cells) by way of gap junctions, so that electrical signals are transferred between cells rapidly. Between nerve cells, chemical transmission is much more common and involves the release of chemical neurotransmitters which bind and activate post-junctional or post-synaptic receptors. This is widespread in the autonomic nervous system (ANS) and ENS, so it is discussed in detail (Goyal and Chaudhury, 2013). Dale's Principle of chemical transmission states that all the axon terminals of an individual neuron will release the same chemical transmitter or transmitters (Eccles, 1976; Strata and Harvey, 1999). Chemical transmission may occur at a specialised synapse, or otherwise in a non-synaptic fashion that has been termed "non-synaptic diffusion" or "volume" transmission (Vanhatalo and Soinila, 1998). The alternate terminology of "wired" versus "volume" transmission has also been used, where "wired" refers to chemical and electrical transmission, and "volume" refers to the diffusion of transmitters through longer distances in the extracellular space (Agnati et al., 2010). Nerve terminals exist as three distinct types of endings: terminal boutons (common in the central nervous system), motor end-plates (in striated muscle), or as axonal varicosities. Varicose nerve fibres have long axons with bead-like varicosities occurring at close intervals along their length, which are the sites where neurotransmitters are concentrated and released. Adrenergic neurons often have varicose axons with thousands of varicosities along their length, as seen by Falck et al. in 1962 (Falck and Torp, 1962).

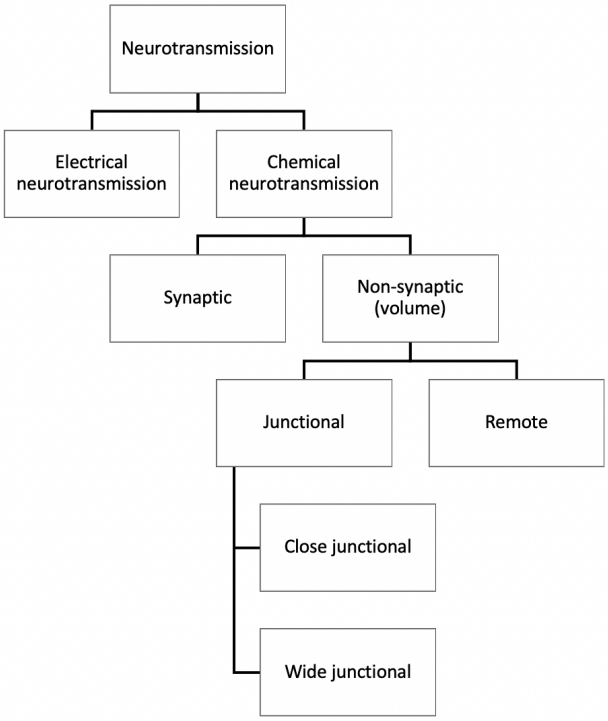


**Figure 1-1 Hierarchy of methods of neurotransmission (Goyal and Chaudhury, 2013)**

### 1.3.2 Neurotransmitters

Neurotransmitters are the substances liberated at neuronal release sites that then bind to receptors and cause a specific action. Classical criteria previously defined the characteristics of neurotransmitters:

- A substance synthesised within the neuron,
- Stimulation of that specific neuron causes release of the substance,
- The effect produced by the substance released by the neuron is similar to the effect of exogenous administration, and
- The action of the substance is terminated by removal or metabolism (Vanhatalo and Soinila, 1998).

There are many different neurotransmitters that may have action in the CNS, ANS or ENS. Small molecule transmitters include glutamate, gamma-aminobutyuric acid (GABA), glycine, acetylcholine (ACh) adenosine triphosphate (ATP) and the monoamines dopamine, noradrenaline (NA) adrenaline and serotonin. There are also large molecule transmitters such as substance P, enkephalin and vasopressin, which are neuropeptides (Barrett et al., 2016). Molecules such as nitric oxide (NO) also

act as neurotransmitters. Of these, ACh, NA and NO appear to be major transmitters in the ENS.

### 1.3.3 Synaptic Transmission

The process of chemical synaptic transmission involves an action potential travelling toward the terminal end of the presynaptic neuron, triggering voltage-gated calcium channels to open. This then causes liberation of a neurotransmitter into a synaptic cleft, typically by exocytosis of a vesicle storing the neurotransmitter. The neurotransmitter then acts on receptors on the postsynaptic neuronal membrane to cause an effect on that cell, producing either excitation or inhibition. In neuron-neuronal transmission, the end result is an excitatory post-synaptic potential (EPSP) or an inhibitory post-synaptic potential (IPSP) in the post-synaptic neuron. In the case of neuromuscular transmission these are called excitatory junctional potentials (EJP) or inhibitory junctional potentials (IJP). After causing an action, the neurotransmitter action is then terminated by several possible mechanisms: reuptake into the presynaptic neuron by a specific transporter, catabolism by an enzyme in the synaptic cleft, or diffusion out of the cleft. This is the "classical" chemical neurotransmission and occurs at specialised synapses (Barrett et al., 2016).

Certain features are present that characterise the presence of synaptic transmission. Morphologically, synapses on the presynaptic neuron have an active zone with vesicles clustered in this area, ready for release. There is often a density of fast acting ionotropic receptors on the adjacent post-synaptic membrane although slower acting metabotropic receptors may also be present. The synaptic cleft is a closed cavity, with a surface area usually approximating $1\mu m^2$. The resulting synaptic potential is usually fast, and the duration of response is typically from 10-30ms. Overall, synaptic transmission is precise and rapid, and tends to occur in neuron-neuron communication, although there is considerable variability between different synapses (Goyal and Chaudhury, 2013).

### 1.3.4 Non-synaptic (Volume) Transmission

The concept of non-synaptic transmission was first considered in the 1960s, before which all chemical transmission was thought to occur at synapses. In non-synaptic transmission, neurotransmitters released from a neuron may diffuse within the extracellular space and attach to receptors on neurons close or distant to the site of release; for this reason, it is also termed non-synaptic diffusion neurotransmission, or volume transmission. In this way, neurotransmitters may act on a neuronal population with close or distant spatial proximity to the site of release and the

appropriate receptor specificity (Vanhatalo and Soinila, 1998).

In some instances, liberated neurotransmitter can travel in the extracellular space, enter into the blood or cerebrospinal fluid, and have a remote action ("paracrine" or "neuro-endocrine" transmission). More commonly however, the neurotransmitter will act locally via non-synaptic transmission, and this has been called junctional transmission. Close junctional transmission occurs when the release site and the postjunctional receptors are spatially very close (10-20nm), however they do not have all the features of a synaptic active zone on electron microscopy described above, and the cleft is open to the extracellular space. The postjunctional receptors are often slower acting metabotropic receptors, and the response typically lasts 250ms-2.5s. Wide junctional transmission occurs across longer distances (100-2000nm), again without the characteristics pre- and postsynaptic specialisations. Receptor sites are widely spaced meaning the resulting action can be widespread. The action may last between seconds to minutes. Junctional transmission occurs neuron-neuron and also neuron-effector (e.g. smooth muscle or secretory cells) (Goyal and Chaudhury, 2013). Several factors determine the efficacy of neurotransmitters acting by volume transmission, including the amount of neurotransmitter released, the method of termination of the transmitter and the available space or volume extracellularly the transmitter can diffuse through (Vanhatalo and Soinila, 1998).

The type of vesicular packaging of neurotransmitter can give an indication of the type of transmission. Small clear vesicles (SCV) that contain the classical neurotransmitters ACh, glutamate, GABA and ATP are more likely to be involved in synaptic transmission, lining up at the active zone of the presynaptic neuron. Small or large dense core vesicles (SDCV and LDCV) contain amines and neuropeptides respectively, and are more likely to be involved in non-synaptic transmission.

In contrast to synaptic transmission, volume transmission may not have a direct one-to-one relationship to action potentials, is slower in causing an effect, can act on a much larger number of neurons at once (rather than a neuron sender/receiver ratio of 1:1), and may be more economical in terms of energy usage (Vanhatalo and Soinila, 1998). Another consideration is that neurotransmitters may diffuse out of a synaptic cleft and then have an action at other receptors sites, resembling junctional transmission. Catecholamines have been thought to act by volume transmission from non-synaptic varicosities, being released into the extracellular space and exerting an effect on multiple neurons simultaneously. Noradrenaline and dopamine have been considered as neurotransmitters with significant volume transmission effects, in particular in the central

nervous system (Sykova, 2004; Fuxe et al., 2015).

### 1.3.5 Other Aspects of Neurotransmission

Other relatively recently discovered concepts have contributed to our understanding of neurotransmission. Cotransmission refers to the release of multiple neurotransmitters at a synaptic cleft, dubbed a “transmitter cocktail.” This property has implications in research, whereby a single neuron imaged with immunofluorescence can be immunoreactive for two or more neurotransmitters which colocalise in the same varicosities. Interactions between neurons and glial supporting cells have become the focus of several research groups, and glial cells may play a more active role in neurotransmission than previously thought.

In “false transmission” a neurotransmitter or substance is taken up by a neuron that would not usually synthesise or release that substance; subsequent release of the aberrant neurotransmitter can cause a different effect to that normally produced (Vanhatalo and Soinila, 1998). A clinically relevant example of false transmission may occur with the use of the antidepressant class of serotonin re-uptake inhibitors (SSRIs). Due to the drug, there is an elevated amount of serotonin in the extracellular fluid which is taken up by a different class of neurons in the CNS, possibly catecholaminergic neurons, and then released in the brain causing anti-depressant effects, and in extreme cases, serotonin syndrome (Vanhatalo and Soinila, 1998).

## 1.4 The Autonomic Nervous System

The motor parts of the nervous system can be separated into a somatic component responsible for voluntary movement of skeletal muscle, and an autonomic component concerned with maintaining bodily homeostasis in an involuntary fashion for a large number of organ systems in the body. Langley was the first to define the Autonomic Nervous System (ANS) in 1898 (Langley, 1898). The ANS contains a sympathetic and a parasympathetic division, which generally act in opposition to regulate the function of viscera or effector organs. The relative actions of these two divisions change depending on the circumstance; the sympathetic branch is activated in times of stress ("fight or flight" conditions), whereas the parasympathetic branch is activated during times of relative quiescence to "rest and digest" (Costanzo, 2018). The Enteric Nervous System (ENS) is generally considered the third division of the ANS and is limited to the gastrointestinal tract and will be discussed separately. This section will review the ANS broadly and its general effects on major body systems. Content pertaining to the sympathetic modulation of gastrointestinal/colonic motility will be discussed in detail in section 1.6.

### 1.4.1 Layout of the Autonomic Nervous System in the Human Body

Pathways in the ANS always contain two neurons: a preganglionic neuron with its cell body contained within the central nervous system (CNS) localised within the lateral horn of the spinal cord grey matter or in the brainstem nuclei; and a postganglionic neuron with its cell body located within a peripheral ganglion and its terminal ending at or in the target organ. Efferent axons pass along preganglionic nerves from the CNS to an autonomic ganglion, where they may synapse with the cell body of the postganglionic neuron that will signal to the effector organ. Typically, the postganglionic neuron release neurotransmitters via axonal varicosities at the site of the effector tissue. These autonomic neurotransmitters bind to specific receptors on the effector cells to cause an action. The neuroanatomy of the sympathetic and parasympathetic divisions differs in several aspects. An understanding of these two components, the involved ganglia, the neurotransmitters involved, and their receptors enables an appreciation of how physiology can be modified by disease states and pharmacology (Costanzo, 2018).

### 1.4.2 Sympathetic Division of the Autonomic Nervous System

Sympathetic neurons are derived from neural crest cells and have preganglionic cell bodies in spinal cord segments T1 to L2, termed the thoracolumbar sympathetic outflow tract (McCorry, 2007).

Preganglionic fibres are short and project either to paravertebral ganglia in the sympathetic chain, a series of ganglia aligned longitudinally adjacent to the spinal cord, or to the prevertebral ganglia situated medially in front of the aorta including the coeliac ganglia, superior mesenteric ganglia and inferior mesenteric ganglia. These preganglionic fibres release ACh at the neuro-neuronal synapse in the ganglia, which then binds to nicotinic receptors on the postganglionic neuronal cell body. A single preganglionic fibre may excite many (up to 20) postganglionic fibres. Postganglionic sympathetic fibres are generally long and noradrenergic, releasing noradrenaline from the terminal varicosities onto the effector site, for example, vascular smooth muscle in a blood vessel wall. Many of these postganglionic fibres run with the vascular bundles to effector organs (McCorry, 2007).

Noradrenaline (NA) is the major neurotransmitter of most postganglionic neurons of the sympathetic division and acts on adrenergic receptors. The exceptions are sympathetic postganglionic neurons innervating sweat glands, which release ACh that acts on muscarinic receptors. Another variance is the medulla of the adrenal gland, made up of modified postganglionic neurons without axons which, instead of carrying an electrical current along a fibre, release the catecholamine neurotransmitters adrenaline (80%) and NA (20%) directly into blood circulation to act as hormones (McCorry, 2007). Many of these postganglionic sympathetic neurons contain an additional neurotransmitter, for example neuropeptide Y (NPY) or adenosine triphosphate (ATP), depending on the target organ, and the combination of neurotransmitters can be considered as a "chemical code".

There are several subgroups of adrenergic receptors, classified as alpha and beta, which also have subtypes: alpha-1, alpha-2, beta-1, beta-2 and beta-3. These receptors may have differing actions in different effector organs, and also have a differential response to noradrenaline and adrenaline. Alpha-1 receptors tend to be excitatory, are widely distributed, and are responsible for blood vessel vasoconstriction. Alpha-2 receptors have a more modulatory effect on tissues and are usually inhibitory. Of note, these receptors can be found on the presynaptic membrane of the postganglionic adrenergic neuron, and thus work in a feedback mechanism to regulate further release of noradrenaline. Beta-1 receptors are the predominant receptors on the heart, and when bound with adrenaline, they cause increased myocardial contraction and heart rate. Beta-2 receptors are generally inhibitory, for example they cause smooth muscle relaxation in vasculature and the bronchioles of the lung, leading to vasodilatation and bronchodilatation respectively. Beta-3 receptors reside in adipose tissue and result in lipolysis when activated. NA has greater action on

alpha receptors, but also binds and activates beta receptors to a smaller degree. Adrenaline acts on both alpha and beta receptors. Every organ will have a different combination of adrenergic receptors located on its cell membranes which determine the resulting action caused by NA or adrenaline (Hall and Hall, 2016a). Some of the overall "fight or flight" activity of sympathetic activity includes an increase in heart rate, vasoconstriction of blood vessels, raised blood pressure, bronchodilatation, raised blood glucose levels, sweating, and decreased gastrointestinal motility and secretion (McCorry, 2007).

### 1.4.3 Parasympathetic Division of the Autonomic Nervous System

The parasympathetic division begins in two regions: from brainstem nuclei and cranial nerves III, VII, IX and X, and from the sacral spinal cord, thus being called the craniosacral outflow tract. In contrast to short sympathetic preganglionic fibres, parasympathetic preganglionic fibres traverse a long course before reaching a ganglion, which is often located close to or within the effector organ. The vagus nerve (cranial nerve X, dubbed "the wanderer") courses through the thoracic cavity to supply the heart and lungs, and then into the abdominal cavity to innervate many of the gastrointestinal organs from foregut and midgut. 75% of the total parasympathetic nerve fibres innervating viscera are within the vagus nerve. All preganglionic fibres use ACh as a neurotransmitter and are thus cholinergic, with nicotinic receptors at the junction between pre and postganglionic fibres (McCorry, 2007).

Postganglionic fibres in the parasympathetic division are also cholinergic, however ACh binds to effector tissues via muscarinic receptors. In contrast to sympathetic postganglionic fibres, parasympathetic postganglionic fibres are shorter and located within the viscera, while the preganglionic fibres are relatively longer (Hall and Hall, 2016a). Within the GIT specifically, preganglionic parasympathetic inputs activate enteric neurons, which can be considered as "parasympathetic postganglionic neurons." ACh is the neurotransmitter of the parasympathetic preganglionic division, is synthesised in cholinergic neurons by the choline acetyltransferase (ChAT) enzyme from Acetyl-Co-A and Choline. ACh is broken down by acetylcholinesterase, terminating its action (Barrett et al., 2016). The "postganglionic" parasympathetic neurons, i.e. enteric neurons, release a wide range of other neurotransmitters. Some of the parasympathetic "rest and digest" effects include decreased heart rate, reduced blood pressure, bronchoconstriction, and generally increased gastrointestinal motility and secretion (McCorry, 2007).

### 1.4.4 Catecholamine Biosynthesis

The catecholamines dopamine, noradrenaline and adrenaline are synthesised in a chain of enzymatic reactions, beginning with the amino acid tyrosine. Tyrosine may be derived from dietary sources or from phenylalanine. Within neuronal cytoplasm, tyrosine is converted by the enzyme tyrosine hydroxylase (TH) to dihydroxyphenylalanine (DOPA). The enzyme amino acid decarboxylase then converts DOPA to dopamine. In noradrenergic neurons, dopamine moves into vesicles via the vesicular monoamine transporter (VMAT) and is then converted by dopamine beta hydroxylase (DBH) into NA. In the adrenal medulla, this pathway continues, with NA being converted once more into adrenaline by the enzyme phenylethanolamine-N-methyltransferase (see Figure 1-2) (Barrett et al., 2016). In cells that secrete primarily dopamine, the DBH enzyme is absent, preventing the conversion of dopamine to NA, thus dopaminergic cells will be immunoreactive for TH but not DBH, whereas noradrenergic cells will contain both TH and DBH.

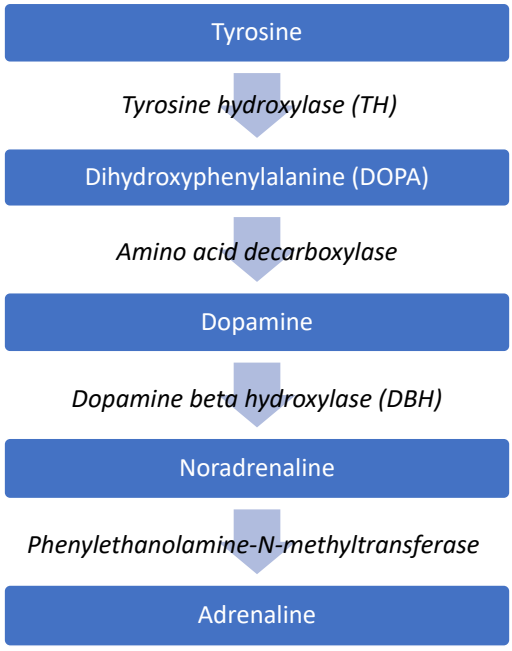


**Figure 1-2 Catecholamine Biosynthesis Pathway**

There are three possible fates for noradrenaline following release by a noradrenergic neuron and action on an adrenergic receptor. Firstly, there is a reuptake mechanism utilising noradrenaline transporter (NAT) on the presynaptic membrane of adrenergic neurons, accounting for the majority its removal. Some noradrenaline diffuses away from the synaptic cleft into the extracellular space and may act on other receptors or diffuse into the blood. Catecholamines may be oxidised into inactive metabolites by the monoamine oxidase (MAO) enzyme in adrenergic neurons. Another

enzyme, catechol-O-methyltransferase (COMT), is present in some tissues, specifically the kidneys, liver and smooth muscle, and can methylate catecholamines into inactive metabolites also (Barrett et al., 2016).

## 1.5 The Enteric Nervous System

The Enteric Nervous System (ENS) is considered the third division of the ANS and is an intrinsic neural network within the gastrointestinal tract. In humans, this neural circuitry is contained within several plexuses. The myenteric (Auerbach's) plexus resides between the longitudinal and circular smooth muscle layers, and there are two plexuses in the submucosa, including Schabadasch's plexus next to circular muscle, and Meissner's plexus next to the mucosa (Furness, 2012). It is estimated there are some 200-600 million neuronal cells in the ENS, similar to the number of neurons in the spinal cord (Furness, 2006). The ENS is significant and unique for its ability to function independently without connection to the central nervous system, which has led to the description of "brain in the gut" by various researchers (Gershon, 1998; Wood, 2011; Furness, 2012). Nerve cell bodies cluster together in discrete groups called ganglia, and ganglia are connected by internodal (or interganglionic) strands (Costa et al., 2000). Axons from neuronal cell bodies may project in a number of directions and there is a diversity of cell types. In the myenteric plexus, there is a primary plexus composed of the ganglia and internodal strands, a secondary plexus with fibres running parallel to circular muscle, and a tertiary plexus in which fibres are found between the primary plexus, closely associated with the longitudinal smooth muscle layer (Furness, 2006). The overall functions of the ENS are to regulate movements of the gastrointestinal smooth muscle, mucosal secretion and transport, local blood flow, and immune and endocrine functions (Furness, 2012). Hirschsprung's disease is an example of a developmental disorder in the newborn where absence of the ganglionated plexuses in the distal colon can lead to functional large bowel obstruction in the neonate, underpinning the importance of the ENS in relation to colonic motility (Chung, 2017).

### 1.5.1 Enteric Neuronal Cell Types

There are a multitude of enteric neuronal cell types present in both the myenteric and submucosal plexus. They may be categorised by location within the ganglia, by the shape, size or proportions of each cell, by the neurochemical markers they express, by the connections and projections within the ENS and by their function (Costa et al., 2000). Morphological types of enteric neurons were first described using silver staining in 1899 by Dogiel and divided broadly into three groups. Dogiel type I neurons contain only one long axon, and have short flat dendrites coming from a small to medium sized cell body; these may be interneurons and motor neurons. Dogiel type II neurons by comparison have multiple axons and a well-rounded larger cell body, and some of these may be intrinsic sensory neurons. Dogiel type III neurons have few, longer dendrites that branch extensively

with a single axon (Dogiel, 1899; Furness, 2006; Hu and Spencer, 2018).

Simplistically, enteric neurons may be afferent (sensory) neurons that detect a stimulus, interneurons that send signals between neurons, and efferent (motor) neurons that carry out excitation or inhibition on the appropriate effector cells. Much of the characterisation of the different types of enteric neurons was first carried out in the guinea-pig small intestine (Brookes, 2001).

- Intrinsic primary afferent neurons (IPANs): Dogiel type II morphology, with cell bodies located in the myenteric and submucosal plexus. These either directly or indirectly detect chemical or mechanical stimuli and then project to many other cells in the ENS.
- Excitatory circular muscle motor neurons: Dogiel type I morphology, with cell bodies in the myenteric plexus. They receive inputs from IPANs as well as ascending interneurons, and project to circular muscle, having excitatory action directly on smooth muscle cells or indirectly on the interstitial cells. Neurotransmitters include ACh and tachykinins.
- Inhibitory circular muscle motor neurons: Dogiel type I morphology, with cell bodies in the myenteric plexus. They also receive inputs from the IPANs and from non-cholinergic descending primary afferent neurons. Projections are to the circular muscle where they have an inhibitory action. Neurotransmitters include nitric oxide (NO), adenosine triphosphate (ATP), vasoactive intestinal peptide (ATP), and pituitary activating cyclic AMP (PACAP).
- Excitatory and inhibitory longitudinal muscle motor neurons: small neurons, with cell bodies in the myenteric plexus and short projections to the longitudinal muscle. Excitatory motor neurons have polarised ascending projections, however the inhibitory motor neurons have projections in both the oral and anal direction (Humenick et al., 2019).
- Ascending interneurons: Dogiel type I morphology, located in the myenteric plexus. These receive inputs from IPANS and other ascending interneurons, forming an ascending chain to send neural messages long distances. They project to other ascending interneurons and excitatory circular muscle motor neurons. Neurotransmitters include ACh, tachykinins and opioid peptides, e.g. enkephalin.
- Descending interneurons: neurons that form descending chains projecting anally. These can be subclassified into three separate types of descending interneurons based on cholinergic and nitrergic labelling.
- Secretomotor neurons: cholinergic cells, located within the myenteric and submucous

plexus, and projecting to the mucosa to affect the secretory function of the epithelium.

- Vasomotor neurons: non-cholinergic cells, again located in the myenteric and submucous plexus, projecting to the mucosa to have action on the intestinal wall vasculature, with the neurotransmitter VIP.
- Intestinofugal (viscerofugal) neurons: a unique cell type with cell bodies located in the myenteric plexus. These are sensory cells with axons that project to the prevertebral ganglia and are involved in intestino-intestinal reflexes, which will be described below (Furness, 2000).

### 1.5.2 The Myenteric Plexus and Motility

While the smooth muscle is the muscular equipment that produces contraction, the myenteric plexus houses most of the neural apparatus that controls this action. There are a multitude of motor neurons within the myenteric plexus, although most have short projections, generally ≤10mm in length. Interneurons however, have significantly longer projections, up to 40mm in the oral direction and 70mm in the anal direction in human specimens (Wattchow et al., 1997). Additionally, these interneurons have specific polarity related to function: descending (projecting anally) neurons are generally inhibitory and ascending (projecting orally) neurons generally excitatory. This arrangement enables proximal contraction and distal relaxation required for neural peristalsis and movement of an intraluminal bolus.

### 1.5.3 ChAT and NOS Immunoreactive Neurons

Prior to the 1990's, it had not been possible to clearly visualise cholinergic neurons. Steele et al. used immunohistochemical antibodies to the choline acetyltransferase (ChAT) enzyme to see these clearly in guinea-pig small intestine myenteric plexus for the first time in 1991 (Steele et al., 1991). ACh is synthesised by the ChAT enzyme, which is abundant in cholinergic neurons that are excitatory. A few years later, nitric oxide (NO) was recognised as a non-adrenergic non-cholinergic inhibitory neurotransmitter acting on the smooth muscle. It is synthesised in enteric inhibitory motor neurons and some descending interneurons (generally with Dogiel type I morphology) by neuronal nitric oxide synthase (NOS) (Sanders and Ward, 2019).

Just over a decade later, a study by Porter et al. set out to determine the immunoreactivity of ascending and descending interneurons to antibodies to ChAT and NOS in human ascending colon using retrograde labelling techniques (Porter et al., 2002). This research found that ascending

interneurons are almost exclusively ChAT+/NOS- (90%), and are thus cholinergic, with the remaining 10% being ChAT-/NOS-. Descending interneurons are more heterogenous, and may be ChAT-/NOS+ (46%), ChAT+/NOS- (20%) or positive for both of these markers (ChAT+/NOS+, 29%); these three immunochemical classes may reflect three separate functions of descending interneurons in the human colon. Importantly, the great majority of interneurons are labelled by antisera to ChAT and NOS (Porter et al., 2002).

In a later study by Murphy et al., antibodies to HuC/D were used to identify all neuronal cell bodies in human colonic myenteric plexus and these HuC/D antibodies were found to be more sensitive than previously used markers, such as neuron specific enolase (NSE). The HuC/D antigen is a protein than binds to RNA in neurons (Murphy et al., 2007). HuC/D labelling stained cell bodies but not cell processes, making visualisation and counting of neuronal somata easier in comparison to other pan-neuronal markers NSE or protein gene product 9.5 (PGP 9.5). Furthermore, there was no cross-reactivity of HuC/D staining with S100, a marker for glial cells. Thus, HuC/D labelling can be considered a pan-neuronal marker in the enteric nervous system. The relative proportions of ChAT and NOS-immunoreactive cells in human colonic myenteric plexus were quantified:

- ChAT+/NOS- neurons = 48% (+/-3%)
- ChAT-/NOS+ neurons = 43% (+/-2.5%)
- ChAT+/NOS+ neurons = 4% (+/-0.5%)
- ChAT-/NOS- neurons = 5% (+/-0.9%)

ChAT+/NOS- cells are likely to represent several different types of neurons in the myenteric plexus, including excitatory motor neurons to the longitudinal and circular muscle, ascending interneurons, some descending interneurons, primary afferent neurons, some vasomotor neurons and some secretomotor neurons. By comparison, ChAT-/NOS+ cells comprise fewer cell types, including inhibitory motor neurons to longitudinal and circular muscle, as well as some descending interneurons. ChAT+/NOS+ neurons are the final proportion of descending interneurons. Small ChAT-/NOS- cells were a novel class described in this study and could either represent unlabelled cholinergic cells or else longitudinal muscle motor neurons (Murphy et al., 2007).

## 1.6 Adrenergic Innervation of the Enteric Nervous System

### 1.6.1 Actions of the Sympathetic Nervous System on the Enteric Nervous System

The Sympathetic Nervous System performs three major functions in relation to the Enteric Nervous System:

1. Secretomotor: causing decreased mucosal secretomotor function by action on the submucosal plexus,
2. Vasoactive: causing vasoconstriction by action on the intestinal vasculature, and
3. Motility: causing inhibition of motility by action on the myenteric plexus and contraction of sphincter muscles.

There are very few adrenergic fibres innervating the mucosa directly, and some of these may have interaction with Peyer's patches, a form of lymphoid tissue (Lomax et al., 2010). Postganglionic sympathetic neurons arise from either the paravertebral ganglia (sympathetic chain) or the prevertebral ganglia, including the coeliac, superior mesenteric, inferior mesenteric and pelvic ganglia. Sympathetic neurons that have cell bodies within the paravertebral ganglia are almost all concerned with vasoconstriction, while neurons with cell bodies in the prevertebral ganglia may be concerned with any of the three major functions above (Lomax et al., 2010).

### 1.6.2 Subtypes of Sympathetic Postganglionic Neurons

In the guinea-pig, three distinct subtypes of postganglionic sympathetic neuron project from the prevertebral ganglia to the small intestine, and the chemical coding of each of these correlates with the target they innervate and their functional role. All of these neurons are noradrenergic (staining for DBH in the original study, demarcated here as NA+) and may contain somatostatin (SOM), Neuropeptide Y (NPY) or neither of these. NA+/SOM+ neurons project to the submucous ganglia and are likely to control mucosal secretomotor function. NA+/NPY+ neurons project to the intestinal blood vessels and are vasomotor in nature. NA+/NPY-/SOM- (not containing either NPY or SOM) neurons project to the myenteric ganglia and are concerned with motility (Costa and Furness, 1984). The same distribution of neurochemical combinations has not yet been identified in humans.

When examining the coeliac ganglion in a guinea-pig model, Macrae et al. found that adrenergic neurons made up 99% of neuron cell bodies in that ganglion with the composition as follows: NA+/SOM+ = 21%, NA+/NPY+ = 53%, NA+/NPY-/SOM- = 26% and NA+/NPY+/SOM+ = 1% (Macrae et

al., 1986). Interestingly, in this study vasoactive intestinal peptide (VIP) positive axons thought to be primary afferent fibres from the gut were seen to selectively terminate in the coeliac plexus around the NA+/SOM+ (secretomotor) and NA+/NPY-/SOM- (motility) positive cell bodies, but not around the NA+/NPY+ (vasoactive) positive cell bodies. This may demonstrate the pathway of an intestino-intestinal reflex that results in changes in motility and secretomotor function, but not in vasoconstriction (Macrae et al., 1986).

### 1.6.3 Sympathetic Activity in Relation to Secretomotor Function

From the submucosal plexus, excitatory secretomotor neurons innervate the crypts of Lieberkuhn of the mucosa and normally promote the secretion of electrolytes, mucus and water (Wood, 1999). Adrenergic fibres terminating in the submucosal plexus secrete noradrenaline, which when bound to alpha-2 noradrenergic receptors on the excitatory secretomotor neurons, will cause hyperpolarisation and thus suppress secretion of fluids, a postsynaptic inhibitory effect (Wood, 1999). Sympathetic activity, as a “fight or flight” response, may prevent secretions thus helping to maintain fluid balance and blood volume. These sympathetic neurons are thought to be tonically active. The predominant sympathetic innervation related to secretomotor function is to the submucosal plexus, rather than direct innervation of the mucosa (Lomax et al., 2010).

### 1.6.4 Sympathetic Activity in Relation to Vasoactive Function

Sympathetic postganglionic neurons are tonically active in relation to vasoactive function of intestinal blood vessels. During times of sympathetic activity, vasoconstriction occurs in the splanchnic bed in order to divert blood from the gut and provide more blood flow for vital organs, and conversely vasodilatation occurs during times of rest allowing more blood flow for digestion (Lomax et al., 2010). Splanchnic circulation may account for up to 25% of the cardiac output, therefore diversion to systemic circulation does significantly alter fluid balance (Wood, 1999). Though noradrenaline is the main neurotransmitter released by postganglionic sympathetic neurons, adenosine triphosphate (ATP) or related purine nucleotides have been shown to be major neurotransmitters released to cause submucosal arteriole vasoconstriction by postjunctional $P_{2X}$-purinergic receptors in guinea-pigs (Evans and Surprenant, 1992). NPY is also implicated in modulating vasoconstrictor function, acting at prejunctional Y2 receptors (Kotecha, 1998). Noradrenergic neurons innervating intestinal vasculature have cell bodies in both the paravertebral and prevertebral ganglia.

### 1.6.5 Sympathetic Activity in Relation to Intestinal Motility

Intestinal motility is the focus of this study and will therefore be discussed in depth. Sympathetic activity inhibits gastrointestinal motility by two mechanisms:

1. Contraction of gastrointestinal sphincters, and
2. Inhibition of contractility of gastrointestinal non-sphincteric smooth muscle.

Consequently, sphincter muscle and non-sphincter muscle are arranged and behave differently in their response to sympathetic stimulation.

#### *1.6.5.1 Sphincteric Smooth Muscle*

Sphincteric muscle is continuous with circular smooth muscle, and includes the lower oesophageal sphincter, pyloric sphincter, sphincter of Oddi, ileocaecal sphincter and internal anal sphincter. In some of these areas there is distinct thickening of the circular muscle (e.g. pylorus and internal anal sphincter) and in others there is not. Sympathetic fibres directly and densely innervate most sphincteric smooth muscle in the gut and are predominantly excitatory in nature, causing sphincter muscle to contract and thus preventing content progressing through the GIT (De Ponti et al., 1996).

Several immunohistochemical studies have demonstrated a dense innervation of smooth muscle at the sites of GIT sphincters, originating with a technique used created by Falck and Hillarp to stain adrenergic neurons (Falck et al., 1982). Costa and Gabella found dense innervation of adrenergic fibres in the muscular layers corresponding to the lower oesophageal sphincter and anal sphincter in guinea-pigs, rabbits and rats (Costa and Gabella, 1971). In another study using rats, a high density of adrenergic fibres was observed in the pyloric sphincter and in the anococcygeus muscle at the level of the anal sphincter (Gillespie and Maxwell, 1971). The rectum of the guinea-pig and cat have been extensively examined and found to have dense adrenergic innervation of the internal anal sphincter and also the anal accessory muscles (Furness and Costa, 1973; Howard and Garrett, 1973).

Functional animal studies support the concept of direct sympathetic inputs to sphincteric muscle causing excitation and contraction (Furness, 2006). In one example, Pahlin et al. examined the ileocaecal sphincter in cats, finding that lumbar colonic nerve and splanchnic nerve stimulation led to contraction of the ileocaecal sphincter that was prevented by blockade of alpha-adrenergic receptors with phenoxybenzamine, or depletion of noradrenaline stores in nerve terminals by guanethidine, which replaces noradrenaline in transmitter vesicles (Pahlin and Kewenter, 1976).

In sphincteric smooth muscle, the alpha-1 adrenergic receptors are involved in causing a contractile response to noradrenaline, while beta-adrenergic receptors are also present and can cause relaxation of the sphincters (Goyal and Rattan, 1978; De Ponti et al., 1996).

#### *1.6.5.2 Non-sphincteric Smooth Muscle*

In contrast, non-sphincter muscle is affected by sympathetic activity largely in an indirect fashion via the myenteric plexus, with some sparse direct innervation of the smooth muscle. Unlike secretomotor and vasoactive components, the sympathetic innervation to non-sphincter smooth muscle is not thought to be tonically active (Lomax et al., 2010). Prior to immunohistochemical labelling of the terminal endings of sympathetic fibres, it was thought that the enteric smooth muscle received direct dual innervation by both the sympathetic and parasympathetic divisions of the ANS (Lundgren, 2000). In 1964, Norberg et al. examined cat and rat intestine under fluorescence microscopy. They found adrenergic fibres terminating around cells in the ganglia of the myenteric plexus, however there were only few fibres to the circular and longitudinal smooth muscle layers. This study corrected the previous view that adrenergic fibres exert their inhibitory effect directly on the smooth muscle cells, but instead proposed an indirect inhibition via action on the myenteric ganglia cells. Norberg et al. initially suggested the presence of synaptic connections between adrenergic nerve terminals and excitatory enteric cells (Norberg, 1964). Jacobowitz confirmed the finding of dense adrenergic fibres in the myenteric plexus with relatively sparse innervation of the smooth muscle in cat intestine not long after. Additionally, he found that removing the coeliac ganglion resulted in those adrenergic fibres disappearing, supporting the origins of adrenergic neurons being located within the prevertebral ganglia (Jacobowitz, 1965).

In the following years there were many functional investigations into the interaction between the sympathetic nerves and the myenteric plexus. Kewenter's experiments with cat small intestine found that sympathetic nerve activity inhibited intestinal excitation mediated by cholinergic nerves and hence prevented intestinal contractions. However, contractions were not inhibited by noradrenergic nerves when exogenous ACh was applied to the bowel, suggesting that it targets ACh release (Kewenter, 1965). At this time, many researchers studied the effects of sympathetic nerve activation on the stomach in animals *in vivo*. Jansson et al. experimented on anaesthetised cats and similarly found that activation of the adrenergic fibres to the stomach inhibited the vagal-induced gastric smooth muscle contraction but did not prevent the myogenic tone or contractions produced directly by ACh (Jansson and Martinson, 1966; Jansson et al., 1969). Interestingly, another group did

similar experiments on cats *in vivo* and in contrast to the Jansson et al. studies they reported that adrenergic fibre stimulation also blocked the action of exogenous close intra-arterial injection of ACh to the stomach. This response was attributed to using a higher frequency of nerve stimulation to the adrenergic nerves (10 Hz vs. 2-4 Hz), and it was therefore suggested that the higher frequency may have caused a larger liberation of noradrenaline causing overflow of the neurotransmitter into the muscular layer to cause direct action on smooth muscle adrenergic receptors, or stimulate to a much greater degree the few fibres that sparsely innervate the muscularis propria (Furness, 2006). Two studies found analogous results in the colon, whereby noradrenergic nerve stimulation inhibited contractions induced by pelvic nerve/vagal stimulation, but did not affect contractions induced by direct application of ACh (Beani et al., 1969; Hulten, 1969; Furness, 2006).

Multiple studies then demonstrated that sympathetic nerve stimulation or application of NA leads to a quantifiable decrease in the release of ACh from the myenteric plexus. In guinea-pig longitudinal muscle, NA and adrenaline reduced the output of ACh by 80% with a dose-dependent effect (Paton and Vizi, 1969). The same research group found the same result in studies of guinea-pig and rabbit, and that this inhibition could be antagonised by phentolamine, an alpha-adrenergic antagonist (Knoll and Vizi, 1970) (Vizi and Knoll, 1971). A study by Del Tacca et al. at this time importantly showed that the same mechanism of noradrenergic inhibition of ACh output from the myenteric plexus exists in human descending colon also (Del Tacca et al., 1970).

Costa and Furness built on this work and questioned the presence of synapses between adrenergic neurons and enteric cells. From guinea-pigs, tissue from the duodenum, ileum and proximal colon was examined with fluorescence microscopy, demonstrating adrenergic fibres and enteric ganglion cells simultaneously for the first time. Costa et al. did not find any adrenergic axonal fibres surrounding enteric ganglia, or any special relationships between nerve terminals and enteric neuronal cells to suggest that synaptic connections, but instead *en passant* relationships, with adrenergic axons passing through the ganglia. They concluded that the inhibitory action of adrenergic nerve terminals was not due to neuro-neuronal synapses, but rather from the specificity of adrenergic receptors being present on the effector enteric neuronal cells, to which diffusely released noradrenaline would bind and have action (i.e. volume transmission) (Costa and Furness, 1973).

The involvement of presynaptic inhibition was introduced by Nishi and North in 1973 using intracellular electrodes in guinea-pig small intestine preparations. They found that exogenous NA

caused presynaptic inhibition of transmitter release from cholinergic neurons (Nishi and North, 1973; Furness, 2006). The following year, Hirst and McKirdy, again using intracellular electrode recordings, found that stimulating sympathetic adrenergic fibres caused the same decrease in transmission (Hirst and McKirdy, 1974).

### 1.6.6 Noradrenergic Connectivity to the Intrinsic Enteric Neurons of the Myenteric Plexus

From the 1980s it was clear that sympathetic postganglionic (adrenergic) fibres densely innervate ganglia in the myenteric plexus, sparsely innervate non-sphincteric smooth muscle, and cause presynaptic inhibition of the release of ACh, which results in decreased contraction of the longitudinal and circular smooth muscle layers and overall inhibition of motility. The specific connectivity of adrenergic fibres to individual cells of the myenteric plexus however, still remains unclear. Compared to the high output of research occurring in the late 1960s to early 1970s investigating the functional mechanism of sympathetic inhibition of non-sphincteric muscle, comparatively few studies have investigated adrenergic connectivity to the myenteric plexus. These few studies are discussed below and are greatly heterogenous, crossing a range of species in varying GIT regions, and utilising various methods to elucidate connectivity.

Manber and Gershon performed several *in vitro* experiments to assess determining connectivity and hypothesised the existence of an axo-axonic adrenergic-cholinergic interaction in the myenteric plexus. In the first studies using isolated rabbit jejunum, the evoked release of ACh and NA was tested. Perivascular nerve stimulation inhibited the release of ACh which was an already known finding, however ACh was also found to inhibit release of NA from adrenergic axons, an effect that could be blocked by atropine, suggesting muscarinic presynaptic inhibition. This signified reciprocal noradrenergic-cholinergic inhibition. The second study used jejunum from rabbit and guinea-pig to examine adrenergic axons morphologically by radioautography and electron microscopy (EM). The majority of adrenergic axons were seen at the edges of the myenteric ganglia. There also appeared to be adrenergic varicosities contacting varicosities of another type; possibly cholinergic fibres based on the presence of characteristic 50nm small clear vesicles, though there were no markers of cholinergic neurons applied to the preparation as there were none available at that time. No specialised synaptic membrane structures were seen on EM, however the method of fixation precluded visualisation of these, therefore the authors suggested the ultrastructural features were evidence for likely adrenergic-cholinergic axo-axonic synapses in mammals (Manber and Gershon, 1979).

Llewellyn-Smith et al. published two studies in the early 1980s looking specifically at the ultrastructural detail of noradrenergic fibres in the enteric plexuses. The first of these used guinea-pig small intestine and three methods to identify noradrenergic neurons: the chromaffin reaction, dopamine beta-hydroxylase localisation with horse-radish peroxidase antibody and loading with 5-hydroxydopamine (5-OHDA). With light and electron microscopy, adrenergic axons were reportedly concentrated at the periphery of myenteric ganglia. Varicosities were seen near nerve cell bodies, however there were no axo-somatic synapses or synapses between axons and cell processes at the ultrastructural level. However, there were some synapses onto neuronal cell processes in the submucous plexus (Llewellyn-Smith et al., 1981). Gordon-Weeks' study a year later with electron microscopy of guinea-pig ileum, distal colon and rectum also did not find any noradrenergic contacts consistent with synapses (Gordon-Weeks, 1982). In conflict with the previous two mentioned studies, Gershon and Sherman reported axo-axonic contacts between noradrenergic and intrinsic serotonergic neurons in guinea-pig small intestine by EM. Another experiment in the same paper demonstrated functionally that exogenous NA antagonised serotonin release mediated by alpha adrenergic receptors, while endogenous NA (released from stimulated nerve terminals) facilitated serotonin release mediated by beta adrenergic receptors (Gershon and Sherman, 1982).

A subsequent study by Llewellyn-Smith translated their methods from guinea-pig to human small intestine. Noradrenergic fibres were again concentrated at the periphery of the myenteric ganglia, however in contrast to the findings in guinea-pig, there were several varicosity "baskets" identified around myenteric neurons, but few synaptic connections between noradrenergic varicosities and nerve processes, and even fewer synapses with the neuron cell bodies themselves (Llewellyn-Smith et al., 1984). Similar to previous studies, there was sparse direct innervation to the muscularis propria.

Gershon and Sherman continued their work in guinea-pig intestine with EM, and in 1987 found axo-somatic close appositions between noradrenergic terminals and serotonergic cells. No other intrinsic neurons were found to have noradrenergic contacts to cell bodies. Specialised synaptic membranes were not definitively seen, possibly due to their loss in the permanganate fixation technique used, though the authors proposed that these contacts function like synapses. Thus, it was thought that noradrenergic interaction with serotonergic neurons is a highly significant factor in the regulation of motility from the myenteric plexus (Gershon and Sherman, 1987).

At the turn of the millennium Tassicker et al. examined guinea-pig small intestine *in vitro* using a

novel method of biotinamide anterograde tracing from mesenteric nerves, which showed all fibres arising from the extrinsic nerves with confocal microscopy (Tassicker et al., 1999). Colocalisation of biotinamide labelled fibres with TH showed that most of these extrinsic fibres were noradrenergic. Additionally, there were pericellular baskets of adrenergic varicosities around a few myenteric cells, strongly suggestive of synaptic inputs to those cells, though these made up less than 1% of all myenteric neurons. With double-labelling immunohistochemistry, many baskets (~50%) were found around 5-HT (5-hydroxytryptamine) positive cells, serotonergic neurons previously identified as descending interneurons. Many baskets (~60%) were around ChAT-immunoreactive cells (which may also be 5-HT positive, overlapping populations).

Electron microscopy was performed in 2008 using immunogold-silver staining for TH in rat duodenum to demonstrate adrenergic terminals at the ultrastructural level. Most TH-immunoreactive varicosities (70%) had close contact *en passant* relationships to enteric distal dendrites without synapses being present, however 16% made asymmetric synaptic contacts with cell bodies or dendrites of the myenteric ganglionic neurons (Hayakawa et al., 2008).

Building on the work of Tassicker, Tan et al. also used Biotinamide anterograde tracing of mesenteric nerves with confocal microscopy and examined the innervation of sensory (calcitonin gene-related peptide, CRGP stained) and sympathetic nerves related to the jejunal myenteric plexus in *in vitro* mouse studies. 43% of all Biotinamide labelled fibres were TH-immunoreactive and these projected circumferentially and anally. Interestingly, the TH fibres formed *en passant* contacts and close appositions with NOS positive cells in the myenteric plexus likely to be inhibitory motor neurons. This finding was not previously observed and conflicted with the results obtained by Tassicker et al.; the difference was attributed to inter-species variation (Tan et al., 2010).

In another study, prevertebral ganglia (coeliac and superior mesenteric) were injected *in vivo* with biotin and the small intestine and stomach removed nine days later and stained with TH. 60% of individual adrenergic fibres and their subsequent arbors (tree-like branches) innervated both the myenteric plexus and the smooth muscle. This study presents a swing back towards the idea of significant direct inhibition of the circular and smooth muscle layers, as well as indirect inhibition via the myenteric plexus which has been well established. The authors of this paper also asserted that noradrenergic varicosities did not have closed synaptic clefts or postsynaptic densities indicative of synapses, and could rather be considered to act by junctional neurotransmission (Walter et al., 2016).

In summary, these studies illustrate noradrenergic connectivity to the intrinsic neurons of the myenteric plexus. Guinea-pig studies with EM have provided some indirect evidence of limited contacts between noradrenergic terminals and cholinergic axons, (Manber and Gershon, 1979) and also noradrenergic terminals surrounding serotonergic nerve cell bodies and cell processes, (Gershon and Sherman, 1982; 1987) backed up by an anterograde labelling study of extrinsic nerves (Tassicker et al., 1999). Few studies have looked at connectivity in the colon, and only one study was performed in human small intestine (Llewellyn-Smith et al., 1984).

### 1.6.7 Adrenergic Receptors in the Myenteric Plexus

The particular adrenergic receptor subtype that mediates intestinal inhibition in the myenteric plexus enables researchers to use selective agonists and antagonists to modify gut function. Noradrenaline is thought to have its action in the myenteric plexus largely by binding to alpha-2a receptors on the presynaptic aspect of cholinergic excitatory neurons, thereby suppressing the release of acetylcholine and other excitatory neurotransmitters (Wood, 1999). Previously alpha-adrenergic receptors have been categorised as alpha-1 if they are present postsynaptic membranes and alpha-2 if present on the presynaptic membrane.

Using adrenergic receptor agonists and antagonists in guinea-pig ileum, Drew first determined that presynaptic receptors in the small intestine were of the alpha-2 subtype. Clonidine, an alpha-2 adrenergic receptor agonist caused significant inhibition of twitch response, and oxymetazoline and xylazine had the same effect but were less potent. Phentolamine, yohimbine, piperoxan and tolazoline acted as alpha-2 antagonists, preventing the effect of clonidine (Drew, 1978). Stebbing et al. found in 2001 that in guinea-pig small intestine the alpha-2a adrenergic receptors located on cells of the excitatory ascending motor pathway, including ascending interneurons and also on the ascending intrinsic sensory neurons (IPANs), are responsible for the inhibition of intestinal motility caused by noradrenaline. Additionally, the alpha-2 antagonist idazoxan blocked the inhibitory effect, and the alpha-2 agonist UK14,304 mimicked the inhibitory effect (Stebbing et al., 2001). A study with a very different design using alpha-2a adrenergic receptor deficient (knockout) mice also concluded that this was the receptor involved in sympathetic inhibition of intestinal motility, and also that these receptors must be present on the cholinergic motor neurons. Knockout mice had slower gastrointestinal transit and no response to medetomidine (an alpha-2 adrenergic receptor agonist), while in wild type mice medetomidine slowed transit. Phentolamine prevented the inhibitory effect of medetomidine in the wild type mice (Scheibner et al., 2002). Later studies have

shown by immunohistochemistry on guinea-pig, mouse and rat tissue from ileum and colon that many of the adrenergic receptors are widely present in the myenteric plexus, including beta-1, beta-2 and alpha-2 receptors. Glial cells also had adrenergic receptors in some species (Nasser et al., 2006).

Importantly, the various subtypes of adrenergic receptors are present throughout the body in many other organs. For instance, beta-1 and beta-2 adrenergic receptors are abundant in the heart and are responsible for increasing heart rate and myocardial contractility; beta-2 receptors are involved in bronchodilation of airways in the lungs; alpha receptors are present in vasculature causing vasoconstriction (McCorry, 2007). For these reasons, many of the respective agonists and antagonists of adrenergic receptors used in a research setting on isolated preparations of a single organ (e.g. in the small or large intestine) cannot be used safely *in vivo* due to risk of causing significant systemic adverse effects, for example severe tachycardia leading to haemodynamic instability, bronchoconstriction with airway compromise or profound hypotension.

### 1.6.8 Sympathetic Gastrointestinal Reflexes

There are two significant physiological reflexes that utilise the sympathetic pathways and inhibitory effect on motility. They are the intestino-intestinal inhibitory reflex and the generalised sympathetic inhibitory reflex and may be activated in isolation or simultaneously. Functional animal studies have demonstrated many of these.

#### *1.6.8.1 Sympathetic intestino-intestinal reflexes*

In this reflex, stimulation by distension of a distal region of the intestine alters the activity in proximal regions, causing a delay in transit. Distension in an intestinal region activates intestinofugal neurons, with cell bodies located in the myenteric plexus and axons projecting to the prevertebral ganglia. Intestinofugal neurons are mechanosensitive and can act as first order neurons (primary afferent) in response to mechanical distension, however they can also be activated by synaptic connections from enteric neurons and therefore also act as second order neurons (interneurons) (Hibberd et al., 2012).

Synapses in prevertebral ganglia enable intestino-intestinal reflexes to occur between remote segments of bowel, without involvement of the CNS. Intestinofugal terminals synapse onto postganglionic sympathetic neurons in the prevertebral ganglia, which run in the mesenteric

extrinsic neurons, preferentially to more proximal regions to act on the myenteric plexus and cause inhibition of motility at that remote location (Furness, 2006). Szurszewski and Miller investigated the role of the prevertebral ganglia in this reflex, and demonstrated that intestinofugal neurons are responsible for monitoring volume changes in the colon, and that this information is relayed to and monitored via the prevertebral ganglia (Miller and Szurszewski, 2002; Szurszewski et al., 2002).

In the 1940s Kuntz showed the reflex in experiments on cats, whereby the intestine was cut between the point of stimulation (distension) and point of recording, with the mesenteric nerves and prevertebral ganglia kept intact, but the prevertebral ganglia separated from the CNS. When distension was applied in the distal ileum or colon, motility of the proximal ileum was inhibited. Nicotine applied to the coeliac ganglia prevented this reflex, because the afferent-efferent connection was cholinergic (Kuntz and Van Buskirk, 1941; Kuntz and Saccomanno, 1944). Notably, this study identified this reflex prior to the understanding of the postganglionic sympathetic efferent pathway or the intestinofugal afferent pathway. By creating lesions in various neural structures, it was found that the prevertebral ganglia are the relay centre for this reflex (i.e. cutting the vagus and paravertebral sympathetic chains did not affect the reflex, but removing the prevertebral ganglia abolished it) (Kuntz, 1938). Other animal studies have substantiated the finding that the prevertebral ganglia act as a relay centre by various different methods (Semba, 1954; Gibbins et al., 2003). This pathway of the intestino-intestinal reflex can be seen in Figure 1-3. The intestino-intestinal reflex has been applied to region specific areas also, including the enterogastric reflex causing gastric inhibition of motility in response to acid detected by the duodenum mucosa, and the "ileal brake" in which high fat content in the ileum causes inhibition of proximal intestinal motility (Schapiro and Woodward, 1959; Lin et al., 2003; Lomax et al., 2010).

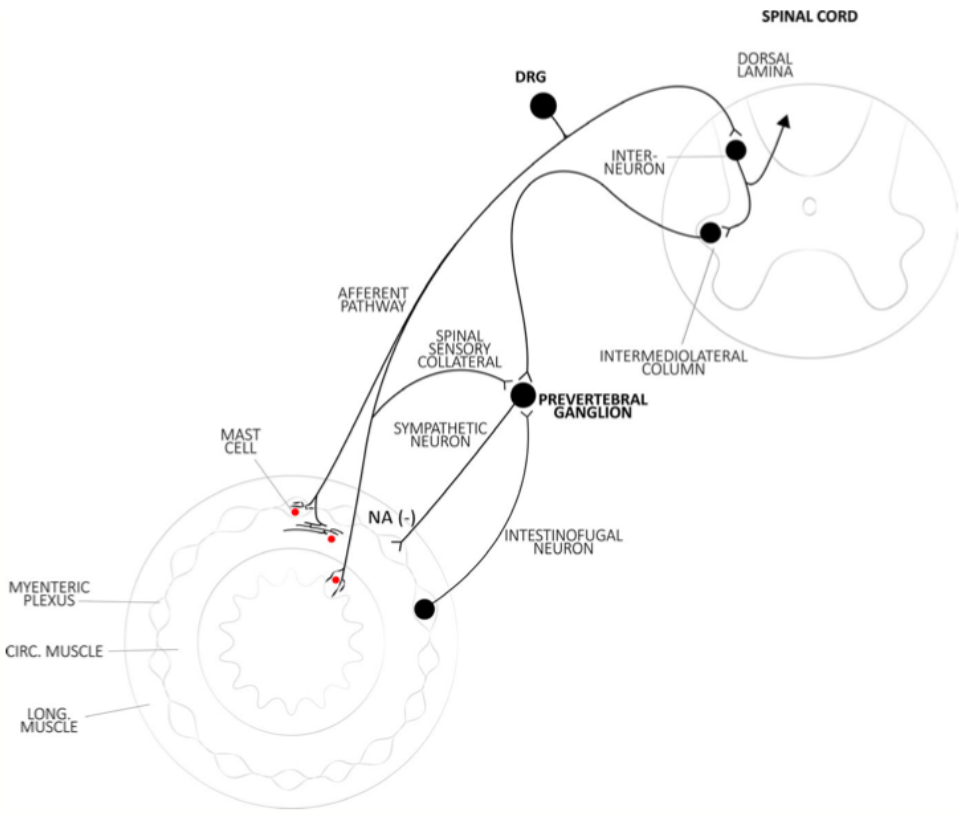


**Figure 1-3 The Intestino-Intestinal Reflex.**

**Diagram reproduced with permission from Wattchow et al. and Wiley Company. Intestinofugal neurons in the myenteric plexus receive sensory information and project to the prevertebral ganglion, synapsing with the sympathetic neurons which project back to the myenteric plexus at various levels along the length of the intestine and cause inhibition by release of noradrenaline (NA) (Wattchow et al., 2020).**

#### *1.6.8.2 Generalised inhibitory reflexes*

The generalised sympathetic inhibitory reflex is evoked in response to extensive irritative or painful stimuli to the GIT or the abdominal structures, mediated via the spinal cord and causes significant global inhibition of gut motility. Noxious stimuli, such as abdominal incision or pain from abdominal structures (e.g. peritoneum, urinary tract, testes) also elicit the reflex (Furness, 2006). This phenomenon is pivotal to the understanding of postoperative ileus and may also be caused by intra-abdominal sepsis and peritonitis. It was described initially in the seminal paper by Bayliss and Starling in 1899, whereby handling of the intestine lead to cessation of movements of the gut. Furthermore, it was found that cutting the extrinsic nerves to the gut prevented this generalised inhibition of motility, which we now understand is due to removal of the sympathetic pathways (Bayliss and Starling, 1899). Lesions or chemical modification at various sites can abolish the reflex,

which reveals details of the pathway: cutting the dorsal root nerve fibres interrupts the spinal afferent neurons; damaging or anaesthetising the spinal cord prevents the afferent to efferent relay via interneurons; and inhibiting noradrenaline systemically with guanethidine removes the efferent output via the sympathetic postganglionic neurons (Furness, 2006).

### 1.6.1 Noradrenergic Inhibition and Colonic Motor Patterns

A study published in 2018 gave some intriguing new insights into the effect of noradrenaline on colonic motor patterns. This was an *ex vivo* study of rabbit colon in an organ bath, and spatiotemporal diameter maps were examined following the application of noradrenaline and adrenergic receptor-active drugs. Interestingly, noradrenaline selectively abolished propulsive motor patterns. These "long-distance contractions" and "fast propagating contractions" may correspond to the human motor patterns "high-amplitude propagating pressure waves" and "simultaneous pressure waves," respectively (see section 1.2.4). However, noradrenaline did not impact upon the haustral boundary contractions (this pattern is involved in segmenting movements), and in fact actually increased myogenic ripple frequency. The major propagating motor patterns could be re-instated by administration of the alpha-2 adrenergic receptor antagonist yohimbine but did not return after the beta adrenergic receptor antagonist propranolol was added. The authors concluded that sympathetic pathways selectively inhibit propulsive colonic motor patterns (Hanman et al., 2019). This conclusion may be of importance in relation to neural connectivity, because yet again it points towards specifically targeted action on individual neuronal cell types, rather than diffuse inhibition of all cell types. However, it should be noted that exogenous noradrenaline was applied to the whole preparation, so the effects of sympathetic nerve activation may not be accurately replicated.

## 1.7 Intrinsic Catecholaminergic Neurons in the Myenteric Plexus

Over many years, small numbers of catecholaminergic neurons have been identified in the gastrointestinal tract of various species. The nature of these cells and their function are still being elucidated. In 1971, Costa and Furness identified adrenergic neurons in guinea-pig proximal colon that appeared similar to those in sympathetic nerves (Costa and Furness, 1971). Four years later, Krokhina found neurons that demonstrated catecholamine fluorescence in the enteric ganglia in the cat GIT (Krokhina and Chuvil'skaia, 1975). Schultzberg et al. in 1980 tested a raft of immunochemical markers on gastrointestinal specimens from rats and guinea-pigs, and among these used Dopamine Beta-Hydroxylase (DBH). DBH is the enzyme responsible for conversion of dopamine to noradrenaline, therefore the presence of this enzyme indicates cells that noradrenergic rather than dopaminergic. A few DBH positive neuronal cell bodies were seen in the myenteric plexus of the guinea-pig stomach, and the myenteric plexus of the rat oesophagus, stomach and colon. The authors themselves questioned these results as it was thought that no DBH could be detected in intestinal specimens that had been denervated (Schultzberg et al., 1980). Later that decade it was suggested that there may be dopaminergic neurons within the gut. On the premise that noradrenergic innervated tissue (e.g. the spleen) has a constant dopamine to noradrenaline ratio, levels of those two neurotransmitters were measured from specimens of GIT from mice. Studies concluded there were dopaminergic intrinsic neurons in the myenteric plexus of mice, based on indirect measurements of higher dopamine/noradrenaline ratios compared to control tissue, and the presence of a dopamine metabolite (Eaker et al., 1988).

In the first study investigating intrinsic catecholaminergic neurons in humans, Wakabayashi et al. examined human GIT specimens from autopsy and used Tyrosine Hydroxylase (TH) labelling to identify catecholaminergic neurons. There were TH-immunoreactive cell bodies seen in all parts of the GIT in low proportions, in both the myenteric and the submucosal plexuses. The myenteric plexus of the lower oesophagus was the region with the greatest frequency of intrinsic TH positive cells. In the myenteric plexus of the colon, the majority of TH-immunoreactive cells were identified in the ascending colon (compared with the transverse, descending colon and rectum) in four out of five specimens (Wakabayashi et al., 1989).

Following from this, links between possible dopaminergic neurons in the GIT and the gastrointestinal dysfunction experienced in sufferers of Parkinson's Disease (PD) were made. A cohort study investigated the proportions of dopaminergic neurons in the GIT of patients with PD

compared with normal controls as well as individuals with constipation (without PD). Protein Gene Product 9.5 (PGP9.5) was used to quantify the denominator for all intrinsic neurons in both groups, and a monoclonal mouse antibody to neuronal dopamine used to identify dopaminergic cells. Overall, there were markedly fewer dopaminergic neurons in the myenteric plexus of PD patients compared with controls and other constipated patients (mean 0.4% vs. 6.9% vs. 5.7%, respectively). Interestingly, there was no difference in the proportion of TH positive neurons between groups, and TH was thought not to be specific for dopamine in this experiment. Additionally, there were lower levels of dopamine in the muscularis propria layer in PD patients registered by high performance liquid chromatography. These results suggest that the pathophysiology of gastrointestinal function in PD (e.g. constipation) may be related to loss of dopaminergic neurons, and in turn imply that dopaminergic neurons may have a role in intestinal motility (Singaram et al., 1995).

Anlauf et al. conducted a study investigating the neurochemical coding of intrinsic neurons in various regions of the human GIT, including regions from the stomach, duodenum, small intestine and colon. The vast majority of these neurons were cholinergic, with 50-70% of neurons immunoreactive for Vesicular Acetylcholine Transporter (VAChT), and a large proportion of those co-reactive for Vasoactive Intestinal Peptide (VIP). 13-20% of enteric ganglionic neurons were immunoreactive for TH. The proportion of these decreased along the length of the gastrointestinal tract, to 0-6% in the distal small intestine and colon. A large proportion of these were co-reactive with Vesicular Monoamine Transporter 2 (VMAT2) a marker for monoaminergic neurons and nerve fibres. However, none of these were reactive for DBH (dopamine beta-hydroxylase), indicating that these intrinsic TH positive cells are probably dopaminergic rather than noradrenergic. There were, however, many extrinsic neurons varicosities and axon fibres that were positive for both TH and DBH, representing the postganglionic sympathetic noradrenergic fibres innervating the ENS (Anlauf et al., 2003).

Li et al. found intrinsic dopaminergic neurons present within mouse intestine using immunohistochemistry, immunoblots, and reverse-transcription polymerase chain reaction (PCR) (Li et al., 2004). The same group later identified dopaminergic receptors ($D_1$ – $D_5$) through the mouse GIT, as well as demonstrating that dopamine may have a motility inhibiting function. Knockout mice lacking the $D_2$ dopaminergic receptor had abnormally increased motility, which gives some insight to the role of this neurotransmitter in the ENS. Additionally, dopamine may be involved in the development of the enteric nervous system during embryology, suggested by early expression of

dopaminergic receptors (Li et al., 2006). Organ bath studies of mouse distal colon have shown that dopamine acts as an inhibitor of colonic motility via $D_1$ and $D_2$ receptors, by decreasing acetylcholine release in the ENS, and by inhibiting spontaneous activity of circular smooth muscle (Auteri et al., 2016).

To summarise, intrinsic catecholaminergic neurons in the ENS have been largely defined as dopaminergic, while noradrenaline seems to be released into the ENS exclusively by the extrinsic postganglionic sympathetic neurons coming from the prevertebral ganglia. Based upon data from animal studies, dopaminergic neurons are likely to play an inhibitory role in gastrointestinal motility. Further insight into the exact nature of these neurons in the colon may provide targets for research or therapy of neurological disorders such as Parkinson's disease that have gastrointestinal manifestations or assist in understanding the mechanism of action of drugs acting on the dopaminergic system, including domperidone, a dopaminergic antagonist (Natale et al., 2017).

## 1.8 Enkephalin Varicosity Baskets

In my study, varicosities immunoreactive for Enkephalin were used as a positive control. Enkephalin is an endogenous opioid and has been largely localised to excitatory ascending pathways in human colon (Humenick et al., 2021). Stored in ascending cholinergic neurons, Enkephalin likely modulates the release of ACh and therefore modulates the timing and contractile response of the ascending excitatory reflex (Allescher et al., 2000). In human small and large intestine, the morphological and neurochemical characteristics of Enkephalin-immunoreactive neurons were studied by Brehmer et al (Brehmer et al., 2005). They reported that 8.3% and 7.9% of all neurons (demarcated by HuC/D) were Enkephalin positive in the ascending colon and transverse colon, respectively. Regarding their morphology, 97.5% were "stubby" neurons with small cell bodies, short dendrites and a single axon. In just over half (50.4%), the axon was running orally, whereas in 29.4% neurons the axon was running aborally, while in the other 20.2% the direction could not be traced. The conclusion from this study was that most Enkephalin-immunoreactive stubby neurons have features consistent with ascending interneurons or smooth muscle motor neurons.

Recently, long ascending and long descending interneurons were examined by retrograde tracing techniques in segments of human colon. Of the cholinergic long ascending pathways, the majority (>90%) were immunoreactive for Enkephalin, whereas there were very few long descending interneurons containing Enkephalin (<5%). A subset of these (approximately a third) colocalised for Substance P (Humenick et al., 2020) in contrast to studies in mouse ENS where most Enkephalin immunoreactive cells colocalised with Substance P (Wright et al., 2021). Notably, it was found that Enkephalin positive neurons form "baskets" that were seen visually, in which varicosities are arranged densely and very close to specific myenteric cell bodies (Humenick et al., 2020). Baskets indicate "targeted wiring" where it is more likely that synaptic neurotransmission occurs. Previous studies to determine neuron to neuron appositions with electron microscopy and light microscopy have shown dense pericellular baskets form synaptic connections to those cell bodies (Pompolo and Furness, 1995).

The same research group also used multi-layer multiplexed immunohistochemistry to determine the cell types that gave rise to Enkephalin-immunoreactive baskets. From all the myenteric neurons coded, 93.6% of cells with a surrounding Enkephalin basket were ChAT-immunoreactive, suggesting strong synaptic inputs between Enkephalin nerve terminals and cholinergic cell bodies (Brookes et al., 2020). An example of such an Enkephalin basket is seen in Figure 1-4. This visual finding of

Enkephalin baskets around cells representing synaptic transmission is of significant relevance to the current research looking to characterise noradrenergic inputs to the myenteric plexus. A method that could properly quantify the density of these close-contacting varicosity baskets could therefore recognise “wired” synaptic connections in the enteric nervous system and allow mapping of the connectivity of neurons labelled immunohistochemically by their neurotransmitters.

Enkephalin is being used in this study because it is a relatively selective marker for a population of ascending cholinergic neurons and Enkephalin varicosities form baskets preferentially around specific types of enteric neurons. These Enkephalin baskets are being used as a comparator in order to validate our method of quantifying varicosity densities in close apposition to individual neuron cell bodies presented in Chapter 2 is robust and in keeping with what is seen overtly by visual observation.

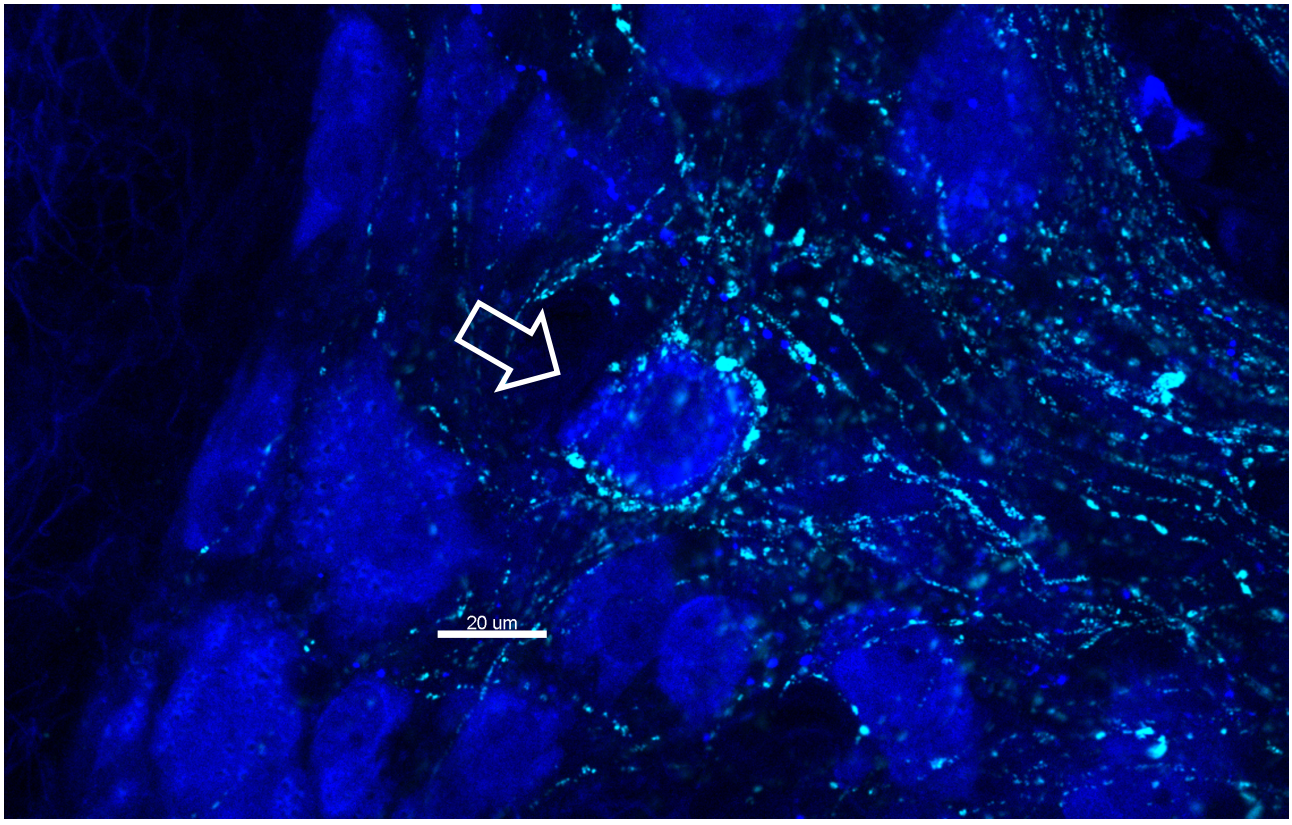


**Figure 1-4 Enkephalin Basket.**

**Enkephalin varicosities forming a basket around a cell body (arrow). Confocal 20x magnification image of a single slice of human descending colon from a 63 year old male. Neuronal cells of the myenteric plexus shown in blue and Enkephalin varicosities seen in cyan. This Enkephalin basket is an example of “targeted wiring.”**

## 1.9 Clinical Relevance to Gastrointestinal Surgery

Comprehension of the mechanism and pathway of sympathetic inhibition of intestinal motility goes beyond simply an appreciation of the physiology. There are several clinical areas where this research can be translated into a better understanding of the pathophysiology, and targets for further research or therapy.

Individuals with refractory gastrointestinal symptoms, such as chronic diarrhoea, faecal incontinence or severe constipation, are likely to come to the attention of a gastroenterologist. Where no structural cause or overt medical condition is identified to account for such symptoms, these patients are deemed to have "functional" colonic disorders. Often this is an unsatisfying diagnosis for patients because there is no clear explanation for their symptoms and in many instances effective treatment is limited. Psychological illness has been found to be associated with functional gastrointestinal disorders and delayed transit (Bennett et al., 2000). Post-traumatic stress disorder (PTSD) is associated with a range of non-malignant gastrointestinal disorders, (Gradus et al., 2017; Glynn et al., 2021) including irritable bowel syndrome specifically (Ng et al., 2019). In extreme cases, chronic debilitating constipation that significantly detract from quality of life may result in the patient requiring a total colectomy with ileorectal anastomosis or alternatively formation of an ileostomy, a highly morbid operation with significant risks. Abnormalities of the autonomic and enteric nervous system are likely to play a large role in some cases of functional gastrointestinal disorders.

Additionally, postoperative ileus is a relatively common occurrence following gastrointestinal surgery. It is frustrating for both the patients who experience it and the surgeons who are tasked with appropriately managing the problem. Sympathetic inhibition in postoperative ileus is an established component and should be addressed.

### 1.9.1 Slow Transit Constipation

Constipation as a symptom may be described by patients as reduced frequency of defaecation, needing to strain to defaecate, a sense of incomplete evacuation, hard stools, or bloating and abdominal pain (Mahmoud et al., 2017). A "normal" stool frequency is difficult to define, ranging from three times per day to three times per week. The Rome IV criteria have been devised to assist in the diagnosis of functional gastrointestinal problems such as constipation (Drossman and Hasler, 2016; Mearin et al., 2016). Slow transit constipation (STC) is a severe form of functional constipation

with demonstrated delayed pan-colonic transit (Tillou and Poylin, 2017). The condition is more common in females and there is an association between STC and concurrent psychiatric disorders and/or a history of sexual abuse. Importantly, STC is debilitating and reduces quality of life. Some patients may have coexisting causes for constipation that make management exceptionally difficult, such as pelvic floor disorders, or dysmotility elsewhere in the GIT (Frattini and Nogueras, 2008).

After diagnosis, medical management is attempted first with a "bowel regime" of laxatives and enemas. Other medications that have previously been used include colchicine, misoprostal, erythromycin (a prokinetic motility receptor agonist) and 5-$HT_4$ (5-hydroxytryptamine) agonists, for example prucalopride (Tillou and Poylin, 2017). In the majority of patients with STC, most of these pharmacological agents are ineffective or partially effective. For those with refractory symptoms, surgery can become an option and often requires subtotal or total colectomy (Serra et al., 2020). An ileorectal anastomosis or rarely an ileal pouch may be created to achieve continuity to the bowel, otherwise an ileostomy can be formed. Surgical management is fraught with the possibility of postoperative complications, as well as the longer-term chronic gastrointestinal symptoms that may persist, including diarrhoea, incontinence, bloating or recurrent constipation, and for these reasons surgery is the last resort in treatment of these patients (Tillou and Poylin, 2017).

The pathophysiology of STC is poorly understood and there are several proposed mechanisms. A commonly cited result is a reduced number of interstitial cells of Cajal, implicating the pacemakers of myogenic motility in the pathophysiology (He et al., 2000; Lyford et al., 2002). In manometry studies there are fewer high amplitude propagating contractions (HAPCs) seen in the colon of patients with STC. One study has found a decrease in the number of excitatory nerve fibres immunoreactive for tachykinins and enkephalin in the colonic circular muscle of patients with STC compared to healthy human controls (Porter et al., 1998). Some researchers have considered that a diffuse abnormality of the ENS and autonomic modulation as a possible cause (Frattini and Nogueras, 2008).

Two papers directly relevant to my thesis are discussed here. Highlighting the importance of functional cell types in the ENS, a study of colonic tissue retrieved from patients with STC demonstrated there were fewer neurons per unit of colon in total, but a higher proportion of nitrergic cells compared to cholinergic cells (Wattchow et al., 2008). A recent study using high resolution manometry (HRM) examined the contractile motor patterns of the large bowel of four patients with STC both *in vivo* and then *ex vivo* after the colon was removed during a colectomy

(Dinning et al., 2016b). The *in vivo* recordings indicated that there were significantly fewer propagating motor patterns compared to healthy controls, however once removed from the body and placed in an organ bath the STC colonic tissue demonstrated regular propagating motor patterns at 1 per minute. The authors concluded that dysmotility present *in vivo* is not seen *ex vivo*, and that extrinsic nerves may be implicated in the pathophysiology of slow-transit constipation. These last findings are of great interest, because they may suggest that the symptoms experienced in STC *in vivo* may be related to inhibition of motility via the sympathetic fibres in the extrinsic nerves, which when cut during resection, allow the gut to function appropriately.

Overall it remains difficult to define the pathophysiology of STC. There have been multiple differences found in the colon of STC patients compared to normal controls, however currently it is impossible to tell if these are primary changes responsible for symptoms or secondary to another underlying process yet unknown.

### 1.9.2 Postoperative ileus

Postoperative ileus is the temporary cessation of gastrointestinal motility following a surgical procedure. Ileus leads to increased length of stay in hospital, associated healthcare costs and morbidity for patients, most significantly being the risk of aspiration pneumonia (Wattchow et al., 2020). The reported incidence of postoperative ileus following a gastrointestinal procedure ranges between 3 to 33% (Vather et al., 2013).

#### *1.9.2.1 Clinical features of postoperative ileus*

Patients with ileus may have obstipation, abdominal distension and discomfort, troublesome nausea and vomiting, and be unable to tolerate oral intake. These clinical features typically develop 2-3 days after a gastrointestinal operation, and in some may be short-lived, while for others will linger on for weeks before spontaneously resolving. Examination findings include a distended abdomen and the absence of bowel sounds apparent on auscultation of the abdomen with a stethoscope. Imaging studies with a plain abdominal X-ray (AXR) or computed tomography (CT) of the abdomen and pelvis will reveal distended loops of small and large bowel in the absence of mechanical obstruction, though this last detail can sometimes be difficult to discern. Usually, postoperative ileus will resolve, and supportive care is required in the meanwhile, including intravenous fluid administration, parenteral nutrition if required, and in some cases a nasogastric tube to decompress the stomach and reduce the risk of aspiration (Wattchow et al., 2020).

#### *1.9.2.2 Pathophysiology of postoperative ileus*

The pathogenesis is multifactorial, however it is believed there are several contributing factors. The first major component is that of early neurogenic sympathetic inhibition of motility. Second is the late phase of intestinal inflammation, involving activation of mast cells and macrophages in the gut wall, and release of cytokines locally and systemically, all of which perpetuates the sympathetic inhibition and leads to prolonged ileus. Third is the role of pharmacological interference, in particular opioid medications used for analgesia which activate mu and kappa opioid receptors and inhibit gut motility via a different pathway. Additionally, electrolyte disturbances such as hypokalaemia may be implicated (Behm and Stollman, 2003; Bauer and Boeckxstaens, 2004).

The sympathetic and neurogenic component of postoperative ileus centres around the generalised sympathetic reflex detailed in Section 1.6.8.2. Operative events that trigger this reflex may include handling of the bowel, manipulation of any of the intra-abdominal structures such as organs and the peritoneum, and in some instances skin incision. Drugs that act on the sympathetic and parasympathetic divisions of the ANS are an attractive option to manipulate the enteric nervous system and motility, and thus prevent or treat ileus. However, to date the treatment efficacy in humans from various trials remains poor. These trials in animals and humans are discussed below.

#### *1.9.2.3 Animal studies investigating manipulation of the autonomic nervous system for therapy in postoperative ileus*

Several instructive animal studies to demonstrate the pharmacology of adrenergic-interactive drugs are discussed here.

Tanila et al. studied the effects of alpha-2 adrenergic agonist medetomidine and antagonist atipamezole in rats *in vivo*, measuring the passage of Evans blue dye in the GIT. Medetomidine expectedly delayed small bowel transit, and atipamezole caused a reversal of that effect. Additionally, atipamezole reversed the delayed motility induced by laparotomy in rats (Tanila et al., 1993). Another study using rats measured the inhibition of motility (also using Evans blue dye) caused by various surgical interventions: skin incision, laparotomy and laparotomy with mechanical gut stimulation. Interestingly, skin incision did not delay transit. However, the other two interventions did, and inhibition was more significant after extirpation of the caecum and small bowel. The authors then applied reserpine, an inhibitor of adrenergic neurotransmission which blocks the VMAT2 transporter: this completely resolved the delayed transit produced by laparotomy

and partially reduced the inhibition caused by the more invasive laparotomy with gut manipulation. They also tested L-nitro-L-arginine (L-NOARG, a nitric oxide synthase inhibitor) which fully resolved the delayed motility in that latter group, in addition to reserpine. These findings confirmed the involvement of noradrenergic pathways in ileus, but also suggested a role for inhibition induced by nitric oxide (De Winter et al., 1997).

A study by Fukuda and colleagues merits attention. In rats subjected to laparotomy, coeliac ganglionectomy caused an improvement in GIT and colonic transit. An improvement in GIT motility was also seen after application of guanethidine (a non-selective adrenergic antagonist) and yohimbine (a selective alpha-2 adrenergic antagonist) both at early and late timepoints, 3 and 27 hours post-operation respectively. Propranolol (a beta-adrenergic antagonist) did not change GI transit (Fukuda et al., 2007). Overall, animal studies indicate that adrenergic inhibition can reverse or reduce the delayed motility in postoperative ileus, suggesting that sympathetic neural pathways may play an important role.

#### *1.9.2.4 Human studies investigating manipulation of the autonomic nervous system for therapy in postoperative ileus*

There have been a number of human studies investigating sympathetic and parasympathetic actions on intestinal motility. Neely and Catchpole (1971) documented results from 30 patients at a time where understanding of the enteric nervous system lagged far behind the present. Their logical approach was to inhibit the noradrenergic response, and then activate a cholinergic response by a combination of pharmacological agents. They tested several regimens:

1. Guanethidine and Bethanechol (the latter is a parasympathomimetic, causing stimulation of muscarinic receptors): guanethidine was administered first, and then bethanechol given when bowel sounds were present in repeated doses until the passage of flatus. The authors reported slight hypotension as well as abdominal discomfort as mild adverse effects.
2. Guanethidine and Prostigmine (an acetylcholinesterase inhibitor): similarly, guanethidine was administered first, and prostigmine given after bowel sounds resumed. Abdominal pain after the administration of prostigmine appears to be the major adverse effect documented.
3. Phentolamine (a non-selective alpha-adrenergic antagonist) and Prostigmine: phentolamine was given in place of guanethidine, and prostigmine is given as above.

In the case reports, these regimens gave excellent results in relieving established postoperative

ileus, while having few significant adverse effects (Neely and Catchpole, 1971).

A later double-blinded randomised trial incorporating 40 patients tested the efficacy of propranolol, a beta-adrenergic receptor antagonist, administered intravenously. The time to first stool postoperatively was used to define the period of ileus. Patients in the propranolol group (20 subjects) had a modest, but statistically significantly shorter duration of ileus compared to controls given placebo: 82 ± 11hrs in the low dose (4mg) propranolol group, 79 ± 8h in the high dose (10mg) propranolol group, compared to 110 ± 9h in the control group (p value <0.01). There was no difference if propranolol was given 30 minutes prior to the operation compared to the first morning postoperatively, but the effect was larger in those having surgery in the distal colon and in patients over 60 years of age. There were no significant adverse cardiorespiratory effects observed in the treatment group (Hallerback et al., 1987b). In the same year these authors trialled propranolol in combination with neostigmine (an acetylcholinesterase inhibitor) as a treatment for ileus in patients undergoing open cholecystectomy. In this randomised controlled trial, ileus was shortened in those patients being administered propranolol and neostigmine compared to controls, but not in those receiving neostigmine alone (Hallerback et al., 1987a).

A Brazilian group examined the outcomes in relation to ileus of 35 patients requiring operative intervention for schistosomiasis with gastrointestinal bleeding related to oesophageal varices in a randomised-controlled trial, with propranolol given preoperatively. Operative management included splenectomy, division of left gastric vein and sclerosis of the oesophageal varices performed endoscopically. Propranolol is indicated for schistosomiasis, portal hypertension and upper GIT bleeding, making this a convenient study. As well as clinical observation, colonic myoelectric activity was recorded by electrodes in the seromuscular layer in the large bowel. There were no significant differences between the propranolol treatment group and the control group, either clinically or seen by myoelectric activity, and so the authors concluded that there was no benefit to propranolol in postoperative ileus (Ferraz et al., 2001). This is consistent with the understanding that alpha receptors have the predominant effect in inhibition in motility rather than beta receptors.

More recently, Stakenborg et al. investigated the effects of prucalopride, a 5-HT4 receptor agonist, on intestinal inflammation and postoperative ileus in both a mouse model and a pilot trial of patients undergoing pancreaticoduodenectomy (Whipple) procedure. In the human pilot trial of 30 patients, prucalopride administered prior to abdominal surgery improved postoperative recovery

times related to ileus, including nasogastric tube output, tolerance of oral intake and length of stay. The animal model in the same publication suggests that prucalopride acts on the alpha-7 nicotinic receptor on macrophages to decrease their activation and thereby decrease inflammation and ileus (Stakenborg et al., 2019).

Neostigmine alone has been assessed as a therapy for ileus in a multicentre retrospective study also including patients with colonic pseudo-obstruction and refractory constipation (n = 182). Neostigmine benefits patients with pseudo-obstruction. The drug was given via the subcutaneous route rather than intravenously in an attempt to reduce adverse effects. The median time to bowel motion following administration of subcutaneous neostigmine was 29 hours (interquartile range 12.18 – 56.84hrs), however there was no control group to compare to, making it difficult to appreciate any improvement in outcomes. There were few adverse events noted, though the authors advocate for telemetric monitoring of possible bradycardia and avoiding the drug in those with new or second-degree heart block (Kram et al., 2018). In the setting of pseudo-obstruction, recent studies have suggested that cardiac monitoring may not be required routinely with the use of subcutaneous neostigmine (Frankel et al., 2019).

Summarising these studies of human subjects, there is no strong conclusive evidence for a pharmacological agent to treat postoperative ileus by action on the noradrenergic or cholinergic pathways which is both efficacious and safe in humans. Although Neely and Catchpole were optimistic regarding their dual drug regimens, medications such as guanethidine, phentolamine and bethanechol are seldom used widely in human populations in the current era because of profound systemic, and specifically cardiovascular, adverse events, especially profound hypotension.

## 1.10 Summary

### 1.10.1 Overview

Though much research has been conducted into the relationship between extrinsic sympathetic fibres and enteric neurons of the myenteric plexus, our understanding is still incomplete. It is well established that the sympathetic extrinsic nerves exert their main effect on motility by releasing noradrenaline from varicosities in the myenteric plexus. This noradrenaline binds to alpha-2a adrenergic receptors on enteric neurons causing presynaptic inhibition, preventing the release of acetylcholine and other transmitters and thus limiting activation of excitatory pathways that would normally cause non-sphincteric smooth muscle to contract. However, the specific neural connectivity between noradrenergic nerve terminals and myenteric neurons remains unclear.

Animal studies have reported conflicting results regarding the presence of synapses or not between sympathetic postganglionic varicosities and intrinsic neurons. The single human study has suggested there are synaptic connections onto cell processes and few cell bodies of myenteric cells. Furthermore, it is unclear whether sympathetic inputs make targeted connections to specific cell types, and there are reports of noradrenergic terminals forming connections to cholinergic neurons, serotonergic neurons and nitrergic neurons in the literature.

This current research project will assess the density of postganglionic sympathetic varicosities close to individual intrinsic myenteric neurons to quantitatively determine if noradrenergic neurons preferentially target one specific cell type over another in the myenteric plexus of human colon, and in doing so will characterise the connectivity that dictates the inhibitory action on motility. The presence of targeted cells would suggest that particular components of the enteric nervous system may be preferentially subjected to noradrenergic inhibition.

A variety of research methods and opportunities will be utilised, including access to human colon provided by the colorectal surgeons at Flinders Medical Centre, multi-layer immunohistochemistry, high resolution confocal microscopy, 3D reconstruction software and a novel way to calculate the density of varicosities around cells. Cholinergic and nitrergic cell types were compared because together they constitute almost 100% of intrinsic myenteric neurons and these broad groups contain known functional classes of cells. Interestingly, both cholinergic and nitrergic cells have been stated to be targets of noradrenergic terminals in animal studies.

Quantitatively analysing varicosity density close to numerous cells presents a challenge and a new method of doing so had to be validated. Enkephalin-immunoreactive varicosity baskets were used as an opportune positive control to test a new method of density analysis. The high density of varicosities within such baskets should translate into a quantitatively higher density of varicosities around cholinergic cells compared to nitrergic cells, based on recent unpublished data. This study is unique on two fronts: it is the first study to investigate the presence or absence of noradrenergic targets in the myenteric plexus in human bowel, and also the first to use sophisticated density analysis afforded by 3D reconstruction of cells in the enteric nervous system.

In addition to the quantitation of density of varicosities, tyrosine hydroxylase (TH) labelling also allowed the identification of the small population of TH positive intrinsic neurons in the myenteric plexus in the same human colonic specimens. Previous literature has suggested these cells are dopaminergic rather than noradrenergic, representing a distinct group of neurons from the TH positive axons derived from postganglionic sympathetic fibres in the extrinsic colonic neurons. Dopaminergic neurons are likely to have an inhibitory role in motility of the colon. Multi-layer immunohistochemical labelling ascertained whether these intrinsic TH cells are cholinergic or nitrergic and assist in better defining this rare cell type, which has not been done previously in human or animal tissue.

### 1.10.2 Experiments and Aims

**Experiment 1: Characterisation of Noradrenergic Inputs to the Myenteric Plexus of the Human Colon**

Aim: To determine if noradrenergic (postganglionic sympathetic) varicosities preferentially target specific neurons (ChAT-immunoreactive versus NOS-immunoreactive) in the myenteric plexus of the human colon.

Hypothesis: Sympathetic varicosities are not associated with any one particular cell type over another, but rather release noradrenaline diffusely throughout the myenteric plexus.

Clinical relevance: Sympathetic inhibition is implicated in motility disorders of the gastrointestinal tract such as postoperative ileus and slow transit constipation, therefore an understanding of the underlying connectivity is required to develop treatments for these patients or drive further research.

**Experiment 2: Characterisation of Enkephalin-immunoreactive varicosity associations in the myenteric plexus of the human colon**

Aim: To quantitatively analyse the density of Enkephalin-immunoreactive varicosities close to myenteric neurons in the human colon and compare varicosity density between cholinergic and nitrergic cell types.

Hypothesis: Enkephalin varicosities have a greater quantitated density surrounding cholinergic neurons compared with nitrergic neurons.

Clinical relevance: Enkephalin-immunoreactive varicosities largely arise from cholinergic ascending interneurons and act in ascending cholinergic pathways. Presently this relationship has been seen only visually and not quantitated. Furthermore, quantitative analysis of Enkephalin varicosities will demonstrate if our method of density analysis fits what is seen visually.

**Experiment 3: Classification of Intrinsic Tyrosine Hydroxylase-immunoreactive Cells in the Myenteric Plexus of the Human Colon**

Aim: To classify intrinsic tyrosine hydroxylase-immunoreactive cells in the myenteric plexus of the human colon into the broad groups of cholinergic and nitrergic cells.

Hypothesis: Intrinsic TH positive cells are cholinergic cells.

Clinical relevance: Intrinsic TH positive cells are likely to be dopaminergic and involved in inhibition of intestinal motility. These cells may be implicated in gastrointestinal disorders attributable to Parkinson's Disease.

# Chapter 2 Methods and Materials

The sections in this chapter give a broad methodological overview of the components used in this research. The major study, *Characterisation of Noradrenergic Inputs to the Myenteric Plexus of the Human Colon*, used almost all of these techniques, while studies on varicosity baskets and TH positive intrinsic cells did not require the sophisticated density analysis performed.

## 2.1 Ethics Approval and Patient Consent

Human tissue was acquired from patients undergoing surgical colonic resection. Ethics approval was obtained for this project (Southern Adelaide Clinical Human Research Ethics approval number 207.17). Every patient involved in this study had the process of tissue donation clearly explained to them during the surgical consent process, were given a detailed information sheet on the study and also signed a consent form. Informed consent for tissue donation was administered by a member of the surgical team. Patients were informed that no additional length of bowel would be removed for research purposes; only that required for an oncological resection was resected. It was explained that the patient would derive no direct benefit or payment by agreeing to take part in the study. The consent form was filed in the patient's clinical case records held by the hospital. The only data recorded for patients were age, sex, date of operation, the surgeon's name, region of bowel and reason for operation, in order to ensure confidentiality. All patients were being treated by the Colorectal Surgical Unit within a single institution, Flinders Medical Centre.

## 2.2 Colonic Tissue Collection

Colonic tissue was taken from the healthy margin of resection specimens from patients requiring removal of a colorectal cancer. The indication for colonic resection was considered prior to collecting tissue, and those with diffusely diseased bowel (for example, inflammatory bowel disease or diverticulitis) were not included in this study. Additionally, tissue was not taken from bowel that was obstructed for any reason, or tissue from a stoma.

The colonic tissue was retrieved from the operating theatre as soon as possible once the en bloc resection specimen was separated from the patient in order to reduce ischaemic time. A small, approximately 2cm length ring of tissue was cut from an uninvolved resection margin well distant (usually proximal) from the site of the tumour with minimal mesentery attached, at the surgeon's

direction. If there was concern for the tumour being close to the resection margin, no specimen was taken. The tissue was placed into oxygenated Krebs solution (pH; 7.4, NaCl; 118mM, KCl; 4.8mM, $CaCl_2$; 2.5mM, $MgSO_4$; 1.2mM, $NaHCO_3$; 25mM, $NaH_2PO_4$; 1.0mM, glucose; 11mM, with 95% $O_2$ and 5% $CO_2$ bubbled) and taken to the Neurogastroenterology Laboratory within the same hospital building. Tissue specimens were given a record number and de-identified, and details were recorded regarding the age and sex of the patient, as well as the part of the bowel the tissue was resected from. This process required collaboration between the research team, the colorectal surgical team and theatre staff to ensure timely retrieval of the specimen. The Anatomical Pathology staff also knew of, and approved, the collection of samples.

## 2.3 Colonic Tissue Preparation

### 2.3.1 Primary Dissection and Fixation

The colonic tissue was then pinned out in a petri dish lined with Sylgard (Dow Corning, USA, Silicone Elastomer Kit) under a dissecting microscope, and oxygenated Krebs solution (as above) was regularly replaced approximately every 10 minutes to keep the tissue oxygenated. The mucosa and submucosa were dissected from the inner surface of the colonic tissue, and large parts of the serosa with any attached mesentery were dissected from the outer surface, taking care to preserve the smooth muscle layers. After the initial dissection, the tissue was stretched out in the petri dish using entomological pins, then immersed in 4% paraformaldehyde (PFA) fixative (pH 7.2, 4% formaldehyde in 0.1 M phosphate) and kept in a fridge overnight at 4°C. The following morning, the tissue was unpinned and immersed in a solution of 4% PFA at room temperature on a mixer to complete a 24-hour period of fixation. This method of fixation is per the laboratory protocol. It allows the pinned out colonic tissue to retain a stretched structure when being fixed initially. Importantly the warmer temperature also ensures penetration of the fixative.

### 2.3.2 Secondary Dissection

Next, the colonic tissue was removed from fixative and washed repeatedly in 1% phosphate buffered solution (PBS), with five washes of at least five-minute intervals. Secondary dissection was performed under the dissecting microscope with the tissue pinned out in a petri dish lined with Sylgard, this time immersed in PBS 1%. The circular muscle fibres were carefully removed from the specimen in strips by sharp dissection with microscissors, avoiding damage to the myenteric plexus. On the other side, as much of the serosa was removed as possible, while preserving the longitudinal

muscle layer. The clearest areas were cut into rectangular pieces approximately 15mm$^2$, with a small cut on an edge in order to easily reidentify each individual specimen. Wherever possible, an inter-taenial region was selected, because the thick longitudinal muscle in the taenial regions makes visualisation of the myenteric plexus more difficult. The end result was a rectangular wholemount of longitudinal muscle and myenteric plexus with a variable thin layer of circular muscle adhering.

## 2.4 Multi-layer Immunohistochemistry and Imaging

### 2.4.1 First Layer Immunohistochemistry

Immunohistochemical staining was performed at multiple time points through this study. In order to permeabilise cell membranes to optimise antibody penetration (clearing), the tissue was placed into PBS/0.5% Triton™ X-100 overnight. Before each layer of immunohistochemical staining, the specimen was washed in 1% PBS five times for five minutes.

The colonic tissue was immersed in 400µL antibody solution in an Eppendorf tube (Argos, 1.5mL), ensuring the tissue was not folded, stuck to itself or the wall to promote good antibody penetration. Primary and secondary antibodies used in the first layer of immunohistochemistry are shown in Table 2-1. Between staining with antibodies, the tissue was subjected to thorough washing in 1% PBS, as above. Importantly, HuC/D antibody was first incubated with a Biotinylated secondary antibody for a 6-hour period, followed by Streptavidin AMCA (aminomethylcoumarin) overnight, which enables the high affinity Biotin-Streptavidin binding that is resistant to antibody elution.

Fluorophores used in this study included AMCA (blue, excitation max 350nm, emission max 450nm), AF488 (Alexa Fluor 488, green, excitation max 490nm, emission max 525nm), Cyanine Dye 3 (CY3, orange-red, excitation max 550nm, emission max 570nm) and Cyanine Dye 5 (CY5, far red, excitation max 650nm, emission max 670nm). Eppendorf tubes were kept in the dark to prevent fading of the fluorophore due to external light. After a final wash following the secondary antibody, the specimens were immersed in successively increasing concentrations of filtered phosphate buffered glycerol, 50%, 70% and 100%, for 10 minutes in each, prior to being mounted on a slide and cover-slipped with the myenteric plexus facing upwards.

**Table 2-1 First layer immunohistochemistry primary and secondary antibodies**

| | Species | Manufacturer | Ref number | Concentration used | Duration | Reference |
|---|---|---|---|---|---|---|
| *Primary antibodies* | | | | | | |
| **HuC/D** | Mouse | Molecular Probes | A-21271 | 1:200 | 3 days | (Murphy et al., 2007) |
| **Leu-Enk** | Rabbit | ImmunoStar | 20066 | 1:1000 | 3 days | (Heinicke and Kiernan, 1990) |
| **TH** | Sheep | Millipore | AB1542 | 1:1000 | 3 days | (Kaestner et al., 2019) |
| *Secondary antibodies* | | | | | | |
| **Biotin** | Donkey anti-mouse | Jackson | 62976 | 1:100 | 6 hours | N/A |
| **Streptavidin AMCA** | | Jackson | 54773 | 1:100 | Overnight (16-18 hours) | N/A |
| **AF488** | Donkey anti-rabbit | Alexa Fluor | Ref A21206<br>Lot 1480470 | 1:1000 | Overnight (16-18 hours) | N/A |
| **CY5** | Donkey anti-sheep | Jackson | 87481 | 1:200 | Overnight (16-18 hours) | N/A |

*Leu-Enk = Leu-Enkephalin, TH = Tyrosine Hydroxylase, AMCA = aminomethylcoumarin, AF488 = Alexa Fluor 488, CY5 = cyanine dye 5*

### 2.4.2 Confocal Microscopy

Prior to taking the preparations to the confocal microscope, every specimen was first viewed on a conventional epifluorescence microscope (Olympus IX71) to check for adequate staining, and to identify the most appropriate ganglia to image. If there was poor quality immunohistochemistry, then the tissue specimen was excluded. Ganglia were chosen based on the quality of immunohistochemistry, the absence of background staining and artefacts, and in areas that were free from tissue damage. A variety of different sized ganglia with varied appearances were chosen to avoid biasing the results.

Formal imaging was performed using a confocal microscope (Zeiss LSM880). Specimens were loaded and the preselected individual ganglia located in the preparation. Several trial runs were done to develop the most appropriate settings to view ganglia with various different staining combinations, specifically relating to magnification (20x), resolution, averaging, imaging speed, laser power and laser gain. Laser power and gain were adjusted for each individual fluorophore. Once determined, those parameters were kept uniform for each specimen throughout the experiment.

A ganglion was imaged using the Z-stack function, enabling multiple consecutive slices to be imaged, with the Z-step of 1µm thick. The number of Z-steps was determined by the first and last slices containing varicosities related to the ganglia, to ensure that all varicosities related to the ganglia were captured and could be included in the analysis. This led to images with a Z-dimension of approximately 25µm, which included the height of cell bodies. Images of 6-7 ganglia from each specimen were taken and the Z-stacks were saved to a hard-drive in ".czi" format. Confocal microscopy parameters are detailed in Table 2-2.

**Table 2-2 Confocal microscopy parameters**

| **Parameter** | **Parameter Settings** | | | |
|---|---|---|---|---|
| **Objective** | 20x | | | |
| **Numerical aperture** | 0.8 | | | |
| **Frame size** | 2048 x 2048 | | | |
| **Speed** | 8 seconds | | | |
| **Averaging** | 8 | | | |
| **Z-stack thickness** | 1.00µm | | | |
| **Laser parameters** | *Laser power* | *Gain* | *Digital offset* | *Digital gain* |
| **Hu – Biotin-Streptavidin AMCA** | 1.5 | 650 | 0 | 1 |
| **Enk – AF488** | 1.8 | 600 | 0 | 1 |
| **TH – CY5** | 5 | 700 | 0 | 1 |
| **NOS – AF488** | 1.4 | 600 | 0 | 1 |
| **ChAT – CY3** | 1.5 | 600 | 0 | 1 |

*Enk = Enkephalin, TH = Tyrosine Hydroxylase, ChAT = choline acetyl transferase, NOS = nitric oxide synthase, AMCA = aminomethylcoumarin, AF488 = Alexa Fluor 488, CY5 = cyanine dye 5, CY3 = cyanine dye 3*

### 2.4.3 Antibody elution

Antibody elution removes the primary antibody from the tissue specimen, meaning another "layer" of antibodies can be tested, with no species cross-reactivity between layers. Therefore, instead of being limited to testing a maximum of four antibody labels on a single tissue preparation, antibody elution allows many more to be tested in multiple layers to examine the same cells.

A 2-mercaptoethanol/sodium dodecyl sulphate buffer (2-ME/SDS) buffer was most effective in antibody elution and was used throughout the study to remove layers of antibodies (Gendusa et al., 2014). Fortuitously, it was found that despite removing all other antibodies, the Biotin-Streptavidin high-affinity bonding was not removed by the 2-ME/SDS buffer. In this study, this characteristic was utilised to maintain HuC/D staining of myenteric neuron cell bodies between layers of immunohistochemistry, so it could be used as a reference point to re-identify the same individual cells.

The method of antibody elution used was modified from the study by Gendusa et al. using the 2-mercaptoethanol/sodium dodecyl sulphate (2-ME/SDS) buffer (Gendusa et al., 2014). Twenty millilitres of filtered water was mixed with 2g of powdered SDS (Sigma) until dissolved, and then added to a solution of a further 67.5mL filtered water and 12.5mL of Tris-HCl (0.5 M, pH 6.8, Sigma T1503) to form a 100mL solution. Once mixed, this solution was divided into two 50mL allotments in centrifuge tubes (50mL, Corning) and 0.4mL 2-ME added to each under cover of a fume hood. Colonic tissue was immersed in the solution, the centrifuge tube sealed, then placed into a pre-heated waterbath (56°C) and allowed incubate for one hour with agitation at 60rpm. Afterwards, the colonic tissue was removed and washed in PBS-Tween (Sigma) three times at 10 minute intervals, before then being washed in standard 1% PBS, as above.

To ensure the elution had been effective at removing the antibodies from the specimen, the treated tissue preparation was mounted and viewed on the standard immunofluorescence microscope, and photographs taken to document there was no staining in those fluorophores. Additionally, HuC/D staining was checked to ensure this remained after elution, as the HuC/D cells would later be used as a reference point. Specimens were then taken off the slide and washed thoroughly with PBS 1% before undergoing the next layer of immunohistochemistry.

### 2.4.4 Second layer Immunohistochemistry

After washing, clearing with PBS/0.5% Triton™ X-100 overnight and a further wash with PBS 1%, the colonic tissue was immersed in antibody solution for the second layer of immunohistochemistry in order to determine the cell types of ChAT and NOS. Primary and secondary antibodies are listed in Table 2-3. Immunohistochemistry was performed in the same fashion as in the first layer.

After removal of the colonic tissue from the antibody solution, washing in PBS 1% and mounting in glycerol as previously described, each specimen was examined first under a conventional immunofluorescent microscope to check for appropriate staining of the secondary antibodies. Next, the same ganglia were imaged on the confocal microscope, once again with uniform settings between each specimen.

**Table 2-3 Second layer immunohistochemistry primary and secondary antibodies**

| | Species | Manufacturer | Ref number | Concentration used | Duration | Reference for primary antisera |
|---|---|---|---|---|---|---|
| *Primary antibodies* | | | | | | |
| **ChAT** | Rabbit | Schemann | P3YEB | 1:1000 | 3 days | (Schemann et al., 1993) |
| **NOS** | Sheep | Emson | K205 | 1:5000 | 3 days | (Olsson et al., 2006) |
| *Secondary antibodies* | | | | | | |
| **CY3** | Donkey anti-rabbit | Jackson | 711-165-152 | 1:200 | Overnight (16-18 hours) | N/A |
| **AF488** | Donkey anti-sheep | Jackson | 713-545-147 | 1:1000 | Overnight (16-18 hours) | N/A |

*ChAT = choline acetyl transferase, NOS = nitric oxide synthase, CY3 = cyanine dye 3, AF488 = Alexa Fluor 488*

## 2.5 3-Dimensional Reconstruction using Imaris Imaging Software

With the computer software Imaris (Bitplane AG, Imaris x64, version 8.4.1), a 3D reconstruction of structures can be produced enabling the distance between rendered varicosities and cell body surfaces to be measured accurately. The automated functionality of Imaris also allows recognition and inclusion of many thousands of varicosities at one time, and so an entire ganglion could be assessed.

### 2.5.1 Process of 3D Reconstruction

Z-stack images taken using the confocal microscope were loaded onto Imaris software to allow 3D reconstruction of the enteric ganglia which was performed one ganglion at a time. A total of two ganglia were reconstructed for each specimen. The process of reconstruction was performed with reference only to the first layer of immunohistochemistry, i.e. the HuC/D, TH and Enk staining. This allowed homogeneity in reproducing the myenteric neurons, and also blinded the investigator to ChAT and NOS immunoreactivity.

#### *2.5.1.1 3D Rendering of HuC/D-immunoreactive Cell Bodies as a Surface*

Firstly, HuC/D cells were reconstructed using the "surface" function in order to create a 3D rendering of neuronal cell bodies. Because HuC/D labelling shows only cell bodies, long neuronal processes were not reconstructed. Multiple pilot trials were performed to develop suitable parameters and an algorithm that would consistently produce a surface representative of HuC/D cells. The surface detail was set at 1µm in every reconstruction and this was constant throughout the study. The "intensity threshold" is the control that essentially produces a rendered surface when the colour intensity of the underlying immunohistochemical staining reaches this value, which is set by the user. In this study, the intensity threshold was set at a level whereby the edges of rendered cell matched the edges of the immunohistochemically defined cell as closely as possible. This was assisted by having the rendered surface overlying a 3D projection of the series of Z-stacks of HuC/D immunohistochemical staining, and in this way, comparing the reconstructed cells to the photographed image. If the intensity threshold was set too high, then the created surface did not cover the whole cell, whereas if the intensity threshold was set too low, the created surface was too large and also began to render background noise present in the immunohistochemical staining. Inappropriately sized cells would skew the distance of varicosities to the cell surface, therefore the intensity threshold was very carefully chosen. Due to differential immunohistochemical staining of

human tissue, it was impossible to rigidly apply the same parameters to each specimen, but parameters were kept the same for ganglia reconstructed within the same specimen.

The 3D rendered surface often replicated the individual cells well, but in some cases overlapping or touching cells were reconstructed as a single object. Using the "cut" function, this erroneously large object could be accurately divided into two separate cell surfaces, in many cases. Additionally, the cut function could remove parts of the surface that were not cellular, for example where an intense filament overlay a cell and was included in its surface. Any surface rendered from non-cellular material was deleted.

Using these tools, each individual cell body was reconstructed as an individual surface object recognised by Imaris, and from which various details can be measured (distance to other objects, area, volume).

#### *2.5.1.2 3D Rendering of TH and Enk-immunoreactive Varicosities as Spots*

Using the channel with either TH or Enk labelled varicosities present, the "spots" function was utilised to produce a spot (appears as a sphere) representing each individual varicosity. Rigorous test runs were performed on Imaris to determine the best way to reproduce varicosities as spots. The confocal image was visible behind the reconstruction to guide the generation of spots. Thresholding remained the greatest challenge: too high an intensity threshold resulted in spots being omitted, whereas too low an intensity threshold resulted in false positive spots. An appropriate balance had to be established and individual parameters were set and used consistently within each specimen but changed between specimens. The values for TH varicosities were different to those of the Enk varicosities due to different secondary antibody fluorophores, variable background noise, and a size difference between varicosities (TH varicosities were slightly larger than Enk varicosities, on average).

Once the spots were created, approximately 10% fell within the boundary of the reconstructed HuC/D cell surfaces. Although some of these could be artefacts, it was considered that many of these spots were true varicosities that were either very close to the cell surface or sitting within a fold of the cell membrane not detected by Imaris. As mentioned, the cell surface has a surface detail of 1µm, therefore it is possible that varicosities within a cleft of the cell might appear within the reconstructed cell surface. Because these represent the closest appositions, it was felt important to capture them in the dataset and therefore varicosities registering within 1µm of the inside surface

of the cell were included in analysis.

#### *2.5.1.3 Data Extraction for Density Analysis*

At this time, several sets of data were extracted for the density analysis. Each individual cell surface was numbered so it could be re-identified later. For the rendered cells, the following data was extracted:

- Designated cell number (e.g. Cell [1], Cell [2], etc.),
- Position of the cell in space (x, y, z coordinates),
- The specific 3D cell shape (exported as a .iv file, consisting of the data encoding the many triangle vertices that produce the 3D shape),
- Cell surface area ($\mu m^2$), and
- Cell volume ($\mu m^3$).

For the rendered varicosities, the positions in space (x, y, z coordinates) were extracted and later used for density analysis. Enk and TH varicosity "baskets" were readily observed on the confocal images. After being designated a cell number, any cell with an Enk or TH basket was recorded on the same Excel spreadsheet.

## 2.6 Identifying Cell Types Using ChAT and NOS Immunoreactivity

Following the second layer of immunohistochemistry and confocal imaging, HuC/D cells could be readily identified as ChAT and/or NOS-immunoreactive. Each HuC/D cell was therefore designated a category:

1. Cell type 1: ChAT + / NOS -
2. Cell type 2: ChAT - / NOS +
3. Cell type 3: ChAT + / NOS +
4. Cell type 4: ChAT - / NOS -
5. Cell type 5: Excluded cells

In some cases, it was recognised that the surface reconstruction did not accurately represent the respective cell body, therefore criteria were devised to systematically define which cells should be excluded and designated "cell type 5":

- Surfaces not representative of the underlying neuronal cell (e.g. misshapen with holes),
- Incomplete surfaces (e.g. on the edge of the preparation), and
- Surfaces which represented two or more cells grouped together that could not be easily separated, in particular those with a broad face.

Although these “cell type 5” would eventually be excluded from statistical analysis, data was extracted for density analysis, because the varicosities associated with them would otherwise be falsely attributed to other cell types.

This data on cell types was then added to the data extracted for density analysis in an Excel spreadsheet.

## 2.7 Varicosity Density Analysis

Density of TH and Enk varicosities is the dependent variable that is being tested to quantify close appositions between nerve terminals can cell bodies. A study by Zhang et al. is an example of how this has been done in a similar way: this group investigated the density of cholinergic varicosities within 3um of activated and non-activated neurons in the prefrontal cortex of rats and found that repeated stimulation of these neurons led to a significant increase in density of the cholinergic varicosities on the axonal fibres with *en passant* relationships to the cells (Zhang et al., 2011). There are several steps involved in the analysis of varicosity density.

Novel tailored software was developed in house (by Dr Lukasz Wiklendt) to measure the density of varicosities around cells using data exported from Imaris. To acquire varicosity density, information was extracted from Imaris for the triangles defining the cell surfaces and the positions of varicosity spots (both TH and Enk, x, y and z coordinates). Calculating density relied on the following formula for number density:

$$\rho_N = N / V$$

where $\rho_N$ is the number density of varicosities, N is the number of objects (varicosities), and V is containing volume ($\mu m^3$). Therefore, to know the density of varicosities the containing volume must be first known.

### 2.7.1 Determining the Volume of Containing Shells

A 3D grid of points with uniform spacing and a known density (8 grid points per $\mu m^3$) was generated in the bounding box of the ganglion (the frame of the 3D reconstruction, i.e. a flat rectangular prism containing all of the reproduced varicosities and cells of the ganglion).

Next, every grid point that was outside of a set distance range from an individual cell surface, or that was closer to another cell surface, was filtered out, leaving only those grid points within the set distance (e.g. 0µm - 1µm) and associated only with the cell of interest (Figure 2-1).Therefore, with a known density and counting the number of grid points in that range (e.g. between 0µm at the cell surface and distance 1µm) the volume of a shell around the cell surface can be calculated, using the same equation rearranged as below:

$$V \text{ (volume of shell)} = N \text{ (counted grid points)} / \rho_N \text{ (known pre-specified density)}$$

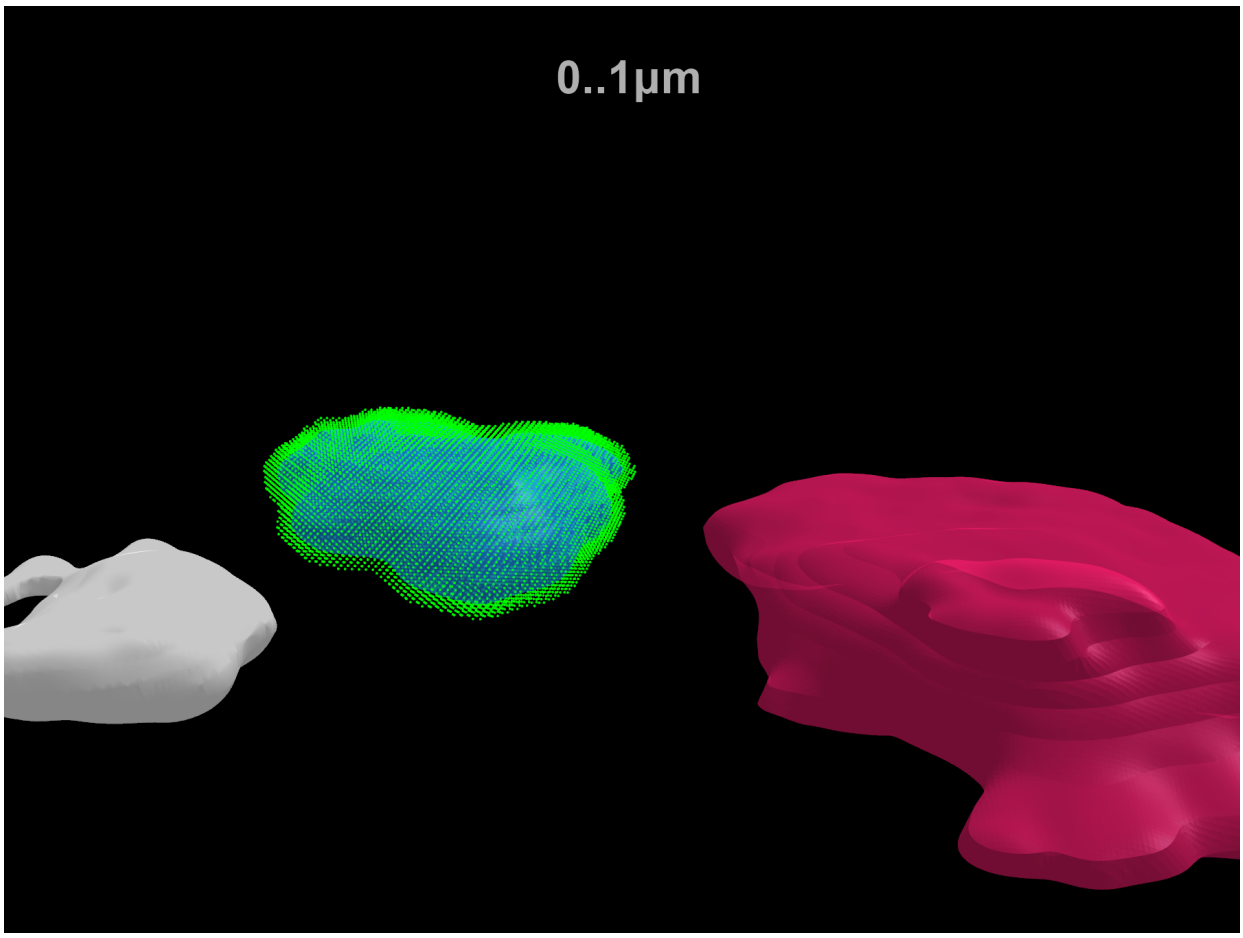


**Figure 2-1 Example of a 1µm thick shell.**

**Example of calculating the volume of a 1µm thick shell from 0µm at the cell surface to 1µm distance from the cell surface, using grid points with a predefined density. The number of varicosities within this shell divided by the volume of this shell gives the density of varicosities in varicosities/µm$^3$.**

### 2.7.2 Counting Varicosities within Shells

The positions of varicosities exported from Imaris were used to count the number of varicosities within the shells at various distances, e.g. at 0µm to 1µm, 1µm to 2µm, etc. Additionally, to include varicosities appearing within 1µm of the cell surface, a shell from -1µm (appearing inside the cell surface) to 0µm (at the cell surface) was produced and varicosities in that range counted. In order to avoid double-counting of varicosities, each shell grid point and varicosity was attributed to only the one cell it was closest to. An example of a shell where grid points have been removed because they are closer to another cell is shown in Figure 2-2.

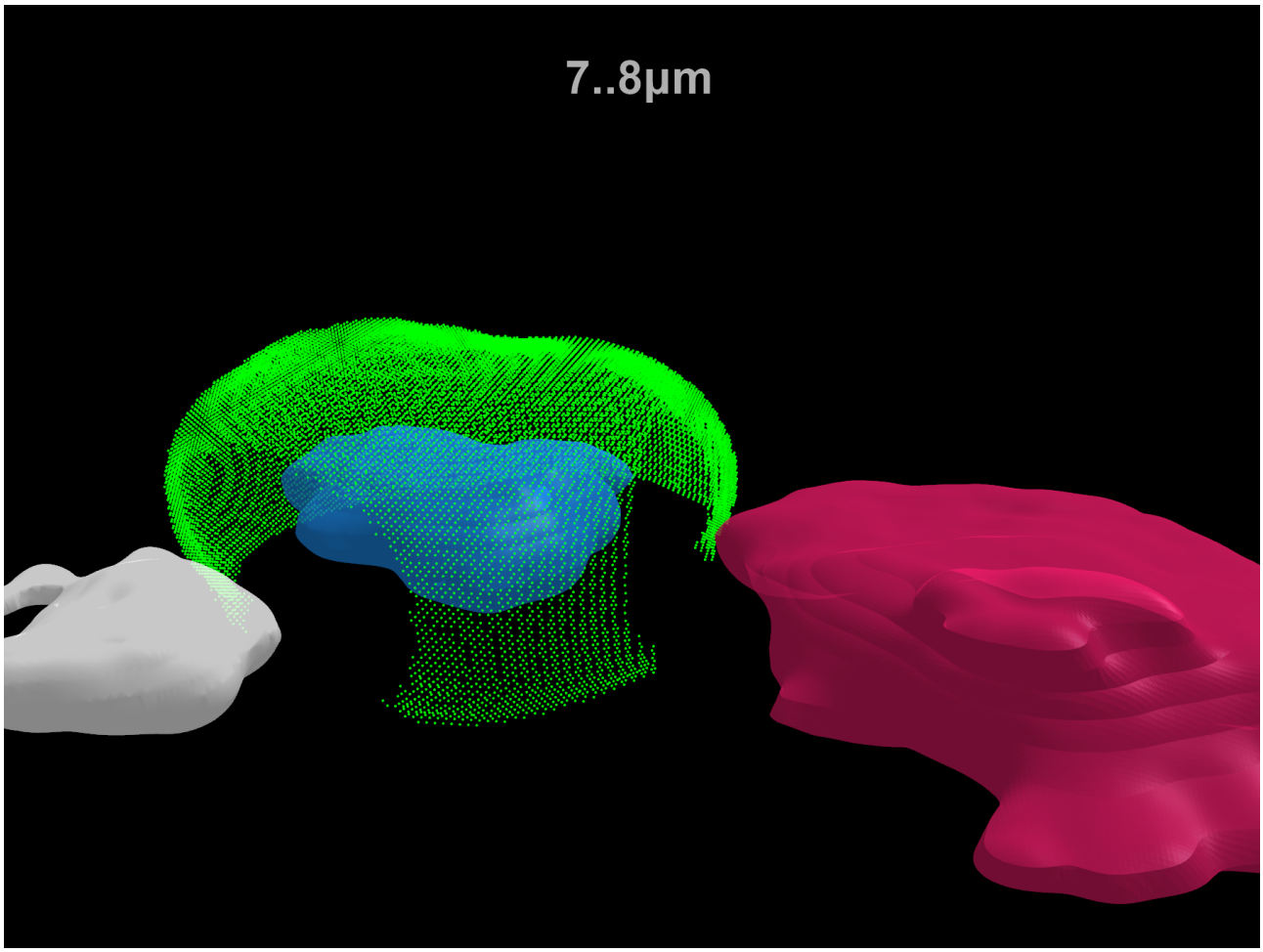


**Figure 2-2 Example of a more distant concentric shell.**

**Example of the 1µm shell of grid points created from 7µm to 8µm distance from that cell. Grid points or varicosities closer to the other adjacent cells are removed to avoid double-counting.**

### 2.7.3 Summarising Data for Statistical Analysis of Varicosity Density

In this study it was decided that the closest appositions are likely to be the most functionally important, therefore only varicosities within -1µm to 1µm were counted, i.e. the closest 2µm-thick shell to each cell's rendered surface.

Overall, every cell had the following data that was used for statistical analysis:

- Subject (patient number) and ganglia,
- Cell type: valid types 1, 2, 3, 4,
- Volume of the closest 2µm thick shell (from -1µm to 1µm) in $\mu m^3$,
- Number of Enk varicosities within the 2µm-thick shell, and
- Number of TH varicosities within the 2µm-thick shell.

### 2.7.4 Statistical Analysis of Varicosity Density

Statistical analysis was performed by a statistician in the research group (Dr Lukasz Wiklendt). Only ChAT+/NOS-, ChAT-/NOS+ and ChAT+/NOS+ cells were analysed and compared. The ChAT-/NOS- were removed from analysis as it is possible they may simply be poorly stained ChAT cells (Murphy et al., 2007).

To compare the counts of varicosities between three cell types (ChAT+/NOS-, ChAT-/NOS+ and ChAT+/NOS+), a generalised linear mixed-effects model of a negative-binomial family with log-link was used. A negative-binomial distribution model accounts for the potential overdispersion of counting varicosities within the 2µm thick shell, in contrast to a Poisson model. The 2µm-thick shell volume was used as a multiplicative offset for each cell, which allows the regression coefficients to be effectively converted to varicosity densities.

The brms R package was used to fit the model (Bürkner, 2017). The formulae below were used:

Count ~cell_type * varic_type + (cell_type *varic_type | subj/gang) + offset(log(volume))

Shape ~ cell_type * varic_type

A prior of normal (0, 1) for coefficients, and LKJ(2) for correlations was used. Four chains were sampled, retaining 1000 samples per chain following 1000 warmup samples. Diagnostics did not show any divergences and showed an Rhat close to 1.

To then compare the relative distributions of varicosity density close to cell types, a density ratio was calculated with 95% credible intervals (density of varicosities close to one cell type divided by the density of varicosities around a different cell type). This method of statistical analysis was used only to compare varicosity densities between ChAT+/NOS-, ChAT-/NOS+ and ChAT+/NOS+ cells.

## 2.8 Identification of Varicosity Baskets Around Cells

Data related to varicosity baskets was collected after reconstruction of the HuC/D cells with the first layer of immunohistochemistry. A varicosity basket was identified visually and defined as a ring of closely spaced and directly apposed varicosities surrounding an individual cell. Only cells that were used for the density analysis were analysed for varicosity baskets. These data were collected for both TH and Enk varicosities.

Numbered HuC/D cells with either TH or Enk varicosity baskets in the first layer of immunohistochemistry were noted and then classified with the second layer of immunohistochemistry by ChAT and NOS labelling. Cell types with TH or Enk baskets were counted and presented as a percentage of the total number of cells with baskets. Statistical differences in the number of baskets surrounding cells were calculated using the Fisher Exact Test.

## 2.9 Classification of Tyrosine Hydroxylase Positive Cells

An analysis of Tyrosine Hydroxylase (TH) positive myenteric nerve cell bodies was also carried out. A total count of all TH-immunoreactive intrinsic neuronal cell bodies was made using the HuC/D labelling in the first layer of immunohistochemistry. The position of the cell body in the ganglion (within the ganglion or peripherally located), and the number of axons were recorded.

2-dimensional size of the cell bodies was calculated with Image J software (Version 2.0.0), using maximum projection images (all Z-stacks combined) of TH and HuC/D labelling. The TH positive cell was identified and then an outline of the corresponding HuC/D cell body was drawn to determine the area in $\mu m^2$.

Next, using the second layer immunohistochemistry with ChAT and NOS labelling the same TH positive cells were identified and classified again into four groups of:

- ChAT+/NOS-,

- ChAT-/NOS+,
- ChAT+/NOS+, and
- ChAT-/NOS-.

Intrinsic TH positive cells of each cell type were counted and presented as a percentage of the total number of TH positive cells.

## 2.10 Summary of the Methods used in Chapters 3 to 6

For ease, the methods have been summarised in Table 2-4. Many of these steps are common to all of the results Chapters, while others are specific to only one or two. The corresponding results chapters are listed below:

- Chapter 3: Patient Demographics and Cell Type Distribution
- Chapter 4: Characterisation of Noradrenergic Inputs in the Myenteric Plexus of the Human Colon
- Chapter 5: Baskets of Varicosities within the Myenteric Plexus of the Human Colon
- Chapter 6: Intrinsic Catecholaminergic Cells in the Myenteric Plexus of the Human Colon

**Table 2-4 Steps in Analysis of Cell Type Proportion, Surface Area and Volume**

| Steps | Details | Chapters |
|---|---|---|
| **1. Colonic Specimen Collection** | Transport from theatre to laboratory in oxygenated Kreb's solution | 3, 4, 5, 6 |
| **2. Primary Dissection and Fixation** | Removal of mucosa, most submucosa and some serosa. Fixation with PFA 4% for 24h | 3, 4, 5, 6 |
| **3. Secondary Dissection** | Removal of submucosa, circular muscle and serosa | 3, 4, 5, 6 |
| **4. First Layer Immunohistochemistry** | Primary antisera: HuC/D, TH and Enk<br>Confocal microscopy | 3, 4, 5, 6 |
| **5. Antibody Elution** | Using 2-ME/SDS solution (see Chapter 2 Methods)<br>Verify antibody staining removed (but HuC/D retained) | 3, 4, 5, 6 |
| **6. Second Layer Immunohistochemistry** | Antibodies: ChAT, NOS<br>Confocal microscopy | 3, 4, 5, 6 |
| **7. 3D Reconstruction of First Layer Images** | HuC/D cell bodies, TH varicosities and Enk varicosities reconstructed using Imaris software<br>HuC/D cell bodies designated a cell number in order to be re-identified. | 3, 4, 5 |
| **8. Identification of Varicosity Baskets** | TH and Enk baskets were identified and the designated cell number noted | 5 |
| **9. Identification of TH Positive Intrinsic Cells** | TH-immunoreactive cells in the myenteric plexus of all imaged ganglia were identified and the designated cell number noted | 6 |
| **10. Identification of Cell Types** | Colocalisation of HuC/D cell bodies with ChAT and NOS staining | 3, 4, 5, 6 |

| | | |
|---|---|---|
| **11. Analysis of Cell Type Proportions** | Calculate the total numbers of each cell type.<br><br>Presented as % ± SEM for each cell type. | 3 |
| **12. Analysis of Cell Surface Area and Volume** | Cell surface area and volume averaged per specimen. Presented as a mean ± SEM for each cell type.<br>One-way ANOVA statistical test followed by Tukey's post hoc test to determine difference in average volume and surface area between cell types | 3 |
| **13. Calculation of Varicosity Density** | Data extracted from Imaris<br>Newly designed software used to determine the density of varicosities around each individual cell | 4 |
| **14. Statistical Analysis of Varicosity Density** | Mixed effects model to compare varicosity density between cell types | 4 |
| **15. Statistical Analysis of Varicosity Baskets** | The number of TH or Enk baskets surrounding individual cell types were counted and compared using the Fisher Exact Test | 5 |
| **16. Counting of TH positive intrinsic cells** | The number of TH positive cells colocalising with individual cell types with respect to ChAT and NOS immunoreactivity were counted | 6 |

*PFA 4% = Paraformaldehyde 4%; 2-ME/SDS = 2 mercaptoethanol/sodium dodecyl sulphate; TH = tyrosine hydroxylase; Enk = Enkephalin; ChAT = choline acetyltransferase; NOS = nitric oxide synthase; SEM = standard error of the mean; ANOVA = analysis of variance.*

# Chapter 3 Patient Demographics and Cell Type Distribution

## 3.1 Introduction

Cholinergic and nitrergic cells, identified by their immunoreactivity to the enzymes ChAT and NOS, make up 95% of all myenteric neurons labelled by the pan-neuronal marker HuC/D. The relative proportions of these cells in the human colon myenteric plexus have been documented in several dedicated studies (Murphy et al., 2007; Wattchow et al., 2008; Beck et al., 2009). Another study has determined these proportions specifically in the descending colon and rectum (Ng et al., 2018).

The work in this chapter formed a critical test of the validity of the major study characterising noradrenergic inputs to the myenteric cells by demonstrating that human enteric neurons could be reliably classified into similar populations of cholinergic and nitrergic cells from a small sample of subjects. Additionally, reconstructions of cholinergic and nitrergic cells provide detailed information on the 3-dimensional surface area and volume that has not been previously reported and can help to characterise further the size of these cell types.

## 3.2 Methods

The method detailed in Chapter 2, section 2.1 to 2.6, was followed to identify four cell types: (1) ChAT+/NOS-, (2) ChAT-/NOS+, (3) ChAT+/NOS+ and (4) ChAT-/NOS-. In general, the most completely and evenly labelled ganglia were chosen for analysis; poorly labelled ganglia with adhering muscle tissue were avoided. Cells were studied in 3D reconstructions created from confocal images stacks. Incompletely rendered cells at the edge of the image frame and cells that could not be separated from neighbours were discarded (“type 5” cells). Then from the remaining pool of cells the relative proportions of each cell type were calculated. Data for the surface area and volume of individual cells was exported from Imaris and averaged for every patient.

Proportions of different ChAT and NOS-immunoreactive neurons were simply reported as the total number of cells of each cell type and the overall percentage of the group with the standard error of the mean. Cell volume and surface area were averaged for each patient and then statistically compared using the one-way analysis of variance (ANOVA), followed by Tukey’s honestly significant difference (HSD) post hoc test to determine differences between cell types. Statistical analysis for this chapter was performed using Prism version 8.4.1 for Mac, GraphPad Software, La Jolla, CA, USA,

www.graphpad.com. P values <0.05 were considered statistically significant.

## 3.3 Results

### 3.3.1 Patient Demographics

Specimens from eight patients were collected for this study. Due to poor immunohistochemistry in the first layer, tissue from one patient could not be analysed (H2243, 50 year-old male, anterior resection for cancer, segment of sigmoid colon). Therefore, seven specimens were analysed and patient demographics and the specimen colonic region are shown in Table 3-1. In each specimen, six to seven ganglia were imaged on confocal microscope. The median patient age was 66 years (range 37 to 90), and five of the patients were female. All colonic tissue was retrieved from specimens from non-obstructing cancer resections.

### 3.3.1 Cell Type Proportions

A total of 673 HuC/D-immunoreactive cell bodies were reconstructed from 14 ganglia from the 7 specimens. 190 (38%) of these neurons were ChAT+/NOS-, 205 (42%) were ChAT-/NOS+, 58 (12%) were ChAT+/NOS+ and 33 (8%) were ChAT-/NOS- (Table 3-2). 187 reconstructed cells were excluded from the density analysis because they were incomplete, inadequate reconstructions, or unable to be separated from neighbouring cells ("type 5 cells;" criteria in Chapter 2, section 2.6).

Immunohistochemistry quality was generally very intense in all included specimens, and examples of the first and second layer from specimen H2239 are shown in Figure 3-1, Figure 3-2 and Figure 3-3. An example of the elution of antibodies from specimen H2244 is shown in Figure 3-4, with images captured using a standard epifluorescence microscope (Olympus IX71). A 3-dimensional reconstruction of the same ganglion is shown in Figure 3-5. An example of how an individual cell was coded based on immunoreactivity for ChAT and NOS is shown in Figure 3-6.

### 3.3.2 Cell Type Surface Area

The surface area of each cell body was calculated (see Table 3-3, and Figure 3-7). ChAT+/NOS+ cells had the largest mean surface area (3871 ± 494$\mu m^2$ SEM), followed by ChAT+/NOS- cells (3127 ± 428$\mu m^2$ SEM), ChAT-/NOS+ cells (2299 ± 371$\mu m^2$ SEM) and lastly ChAT-/NOS- cells (1610 ± 238$\mu m^2$ SEM). There was a statistically significant difference in surface area between cell types (one-way ANOVA test, $F(3,18) = 24.61$, $p = <0.0001$). Using Tukey's post hoc test, ChAT+/NOS+ cells were larger

than ChAT-/NOS- cells (p = 0.001) and ChAT-/NOS+ (p = 0.0013). ChAT+/NOS- cells were larger than ChAT-/NOS- cells (0.0045). Other differences between cell type surface are were not significant (see Figure 3-8).

### 3.3.3 Cell Type Volume

The mean cell volume showed a similar relative order to the surface area: ChAT+/NOS+ (6078 ± 391µm$^3$ SEM), ChAT+/NOS- (4566 ± 404µm$^3$ SEM), ChAT-/NOS+ (3178 ± 390µm$^3$ SEM) and ChAT-/NOS- cells (2156 ± 265µm$^3$ SEM) (see Table 3-4 and Figure 3-9). There was a statistically significant difference in volume between cell types (one-way ANOVA test, $F(3,18) = 47.09$, $p = <0.0001$). With Tukey's post hoc test, ChAT+/NOS+ cells had a larger volume than all other cells types (vs. ChAT-/NOS- $p = <0.0001$; vs. ChAT-/NOS+ cells $p = <0.0001$; vs. ChAT+/NOS- cells $p = 0.03$). Additionally, ChAT+/NOS- cells were larger than ChAT-/NOS- cells ($p = <0.0011$) (see Figure 3-10).

**Table 3-1 Included Specimen Demographics**

| | Age | Gender | Operation | Indication | Segment |
|---|---|---|---|---|---|
| **H2211** | 66 | Female | Right hemicolectomy | Cancer | Ascending colon |
| **H2234** | 90 | Female | Right hemicolectomy | Cancer | Ascending colon |
| **H2236** | 67 | Male | High anterior resection | Cancer | Descending colon |
| **H2239** | 45 | Female | Low anterior resection | Cancer | Sigmoid colon |
| **H2241** | 66 | Female | Right hemicolectomy | Cancer | Transverse colon |
| **H2242** | 37 | Male | Left hemicolectomy | Cancer | Transverse colon |
| **H2244** | 80 | Female | Anterior resection | Cancer | Descending colon |

**Table 3-2 Cell Type Raw Numbers and Percentages of Total for Each Colonic Specimen**

| Specimen | ChAT+/NOS- (%) | ChAT-/NOS+ (%) | ChAT+/NOS+ (%) | ChAT-/NOS- (%) | Total no. of cells |
|---|---|---|---|---|---|
| **H2211** | 19 (37) | 17 (33) | 10 (20) | 5 (10) | **51** |
| **H2234** | 13 (30) | 19 (44) | 5 (12) | 6 (14) | **43** |
| **H2236** | 29 (37) | 40 (51) | 5 (6) | 4 (5) | **78** |
| **H2239** | 22 (34) | 29 (45) | 12 (19) | 1 (2) | **64** |
| **H2241** | 29 (41) | 30 (43) | 5 (7) | 6 (9) | **70** |
| **H2242** | 44 (42) | 44 (42) | 15 (14) | 3 (3) | **106** |
| **H2244** | 34 (46) | 26 (35) | 6 (8) | 8 (11) | **74** |
| ***Total cells*** | ***190*** | ***205*** | ***58*** | ***33*** | ***486*** |
| **% Mean ± SEM** | ***38 ± 2.0*** | ***42 ± 2.3*** | ***12 ± 2.1*** | ***8 ± 1.7*** | |

*Results presented in this table are after the removal of incomplete or excluded cells. ChAT = choline acetyl transferase; NOS = nitric oxide synthase; SEM = standard error of the mean*

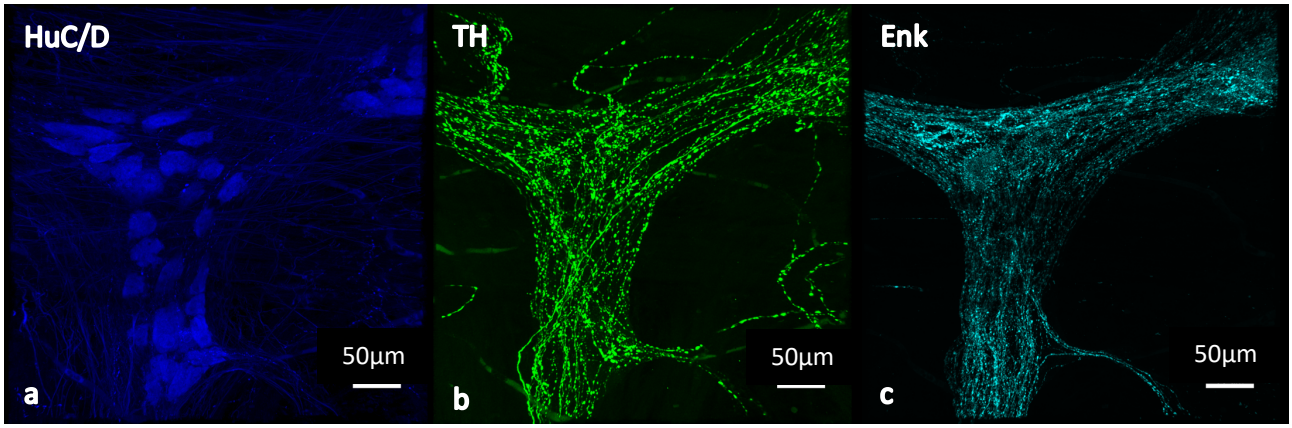


**Figure 3-1 1st Layer Immunohistochemistry.**

**Images taken with confocal microscopy of a single ganglion in the myenteric plexus from the sigmoid colon of a 45 year old female, subject H2239. (a) HuC/D-immunoreactive nerve cell bodies are shown in blue and serving as a pan-neuronal marker. (b) Tyrosine Hydroxylase (TH) varicosities are shown in green, and label catecholaminergic axons and nerve terminals, the vast majority of which are noradrenergic. (c) Enkephalin (Enk) varicosities are shown in cyan and appear smaller than TH varicosities. These will act as a positive control when examining the relationship between varicosities and cell bodies.**

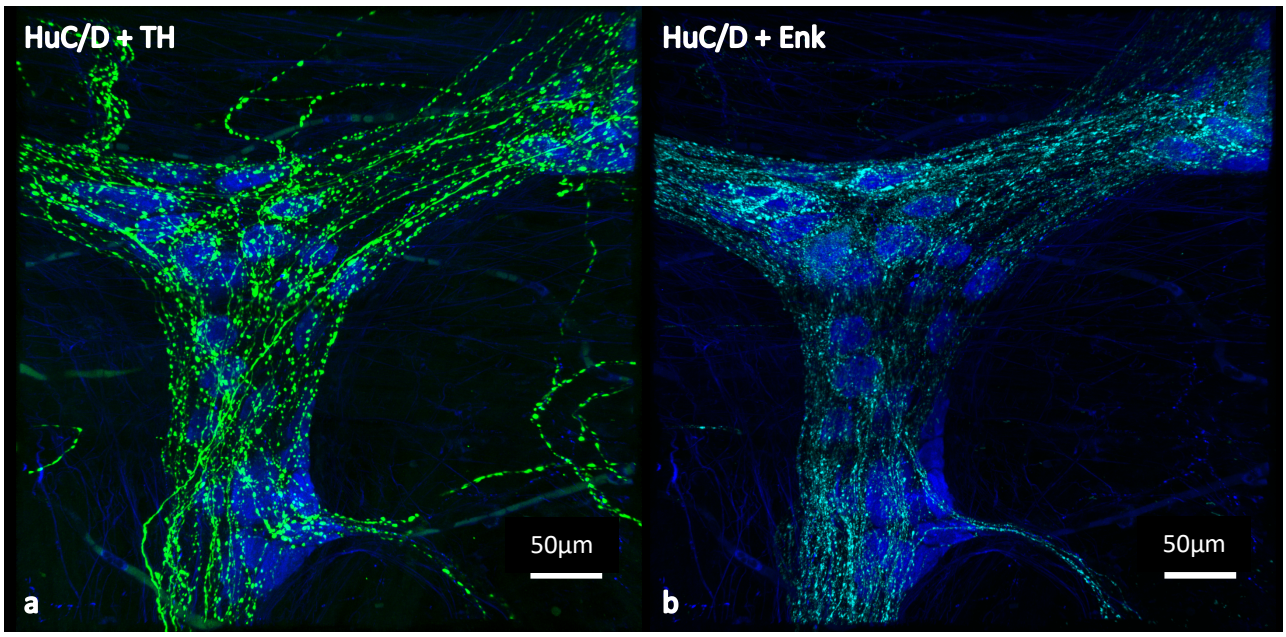


**Figure 3-2 Varicosity and Neuronal Cell Body Images Combined.**

**This is same ganglion shown in Figure 3-1. HuC/D-immunoreactive nerve cell bodies are in blue; (a) Tyrosine Hydroxylase (TH) varicosities in green, and (b) Enkephalin (Enk) varicosities in cyan. The relationship between varicosities and nerve cell bodies can be observed in this way.**

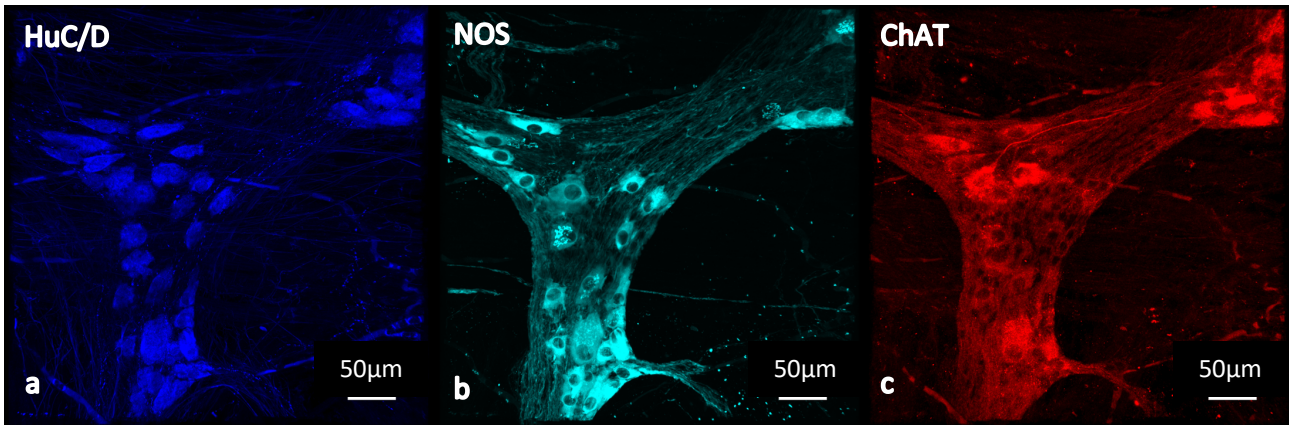


**Figure 3-3 2nd Layer Immunohistochemistry.**

**2nd Layer Immunohistochemistry from the same myenteric ganglion from subject H2239. The 1st layer of immunohistochemistry has been removed by the elution process with 2-mercaptoethanol/sodium dodecyl sulphate (2-ME/SDS), and then restained with a 2nd layer of immunohistochemistry. (a) HuC/D immunoreactivity intentionally remains despite elution with 2-ME/SDS due to the high affinity Biotin-Streptavidin bonding, and the cell bodies seen in Figure 3-1a can easily be reidentified and used as a reference point between layers. (b) Nitric Oxide Synthase (NOS) immunoreactivity shown in cyan; the cell bodies are well discriminated from the background. (c) Choline Acetyl Transferase (ChAT) immunoreactivity shown in red and is sometimes more difficult to appreciate compared to NOS. Antisera to ChAT and NOS will stain 95% of the nerve cell bodies found with the pan-neuronal marker HuC/D. By this method of multiple layer immunohistochemistry, the same individual myenteric nerve cell body can be examined for its relationship to TH and Enk varicosities in the 1st layer and its neurochemical code with respect to ChAT and NOS determined in the 2nd layer.**

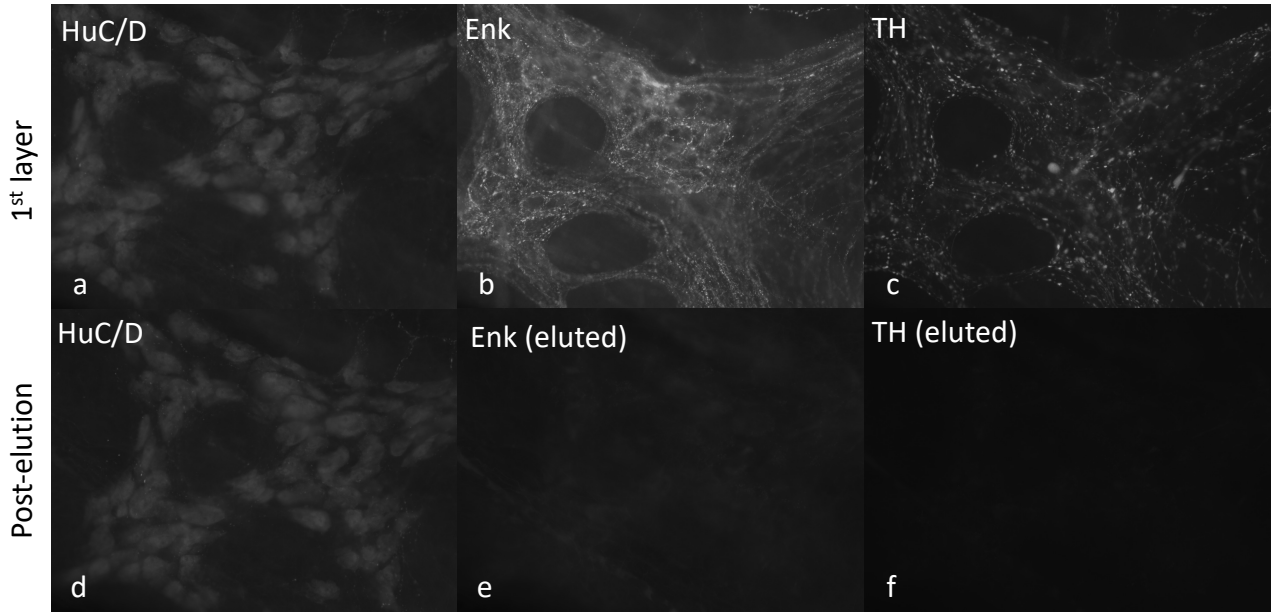


**Figure 3-4 Antibody Elution Technique.**

**Images of a ganglion from specimen H2244 using epifluorescence microscopy. This was used to check that the HuC/D staining had remained through the elution process, but that the Tyrosine Hydroxylase (TH) and Enkephalin (Enk) antibodies had been removed to allow for a second layer. First layer immunohistochemistry: (a) HuC/D at 500ms; (b) Enk at 100ms; (c) TH at 1000ms. Post-elution: (d) HuC/D at 500ms, retained through the elution process due to the high affinity Biotin-Streptavidin binding; (e) channel 2 at 100ms, Enk has been removed; (f) channel 4 at 1000ms, TH has been removed.**

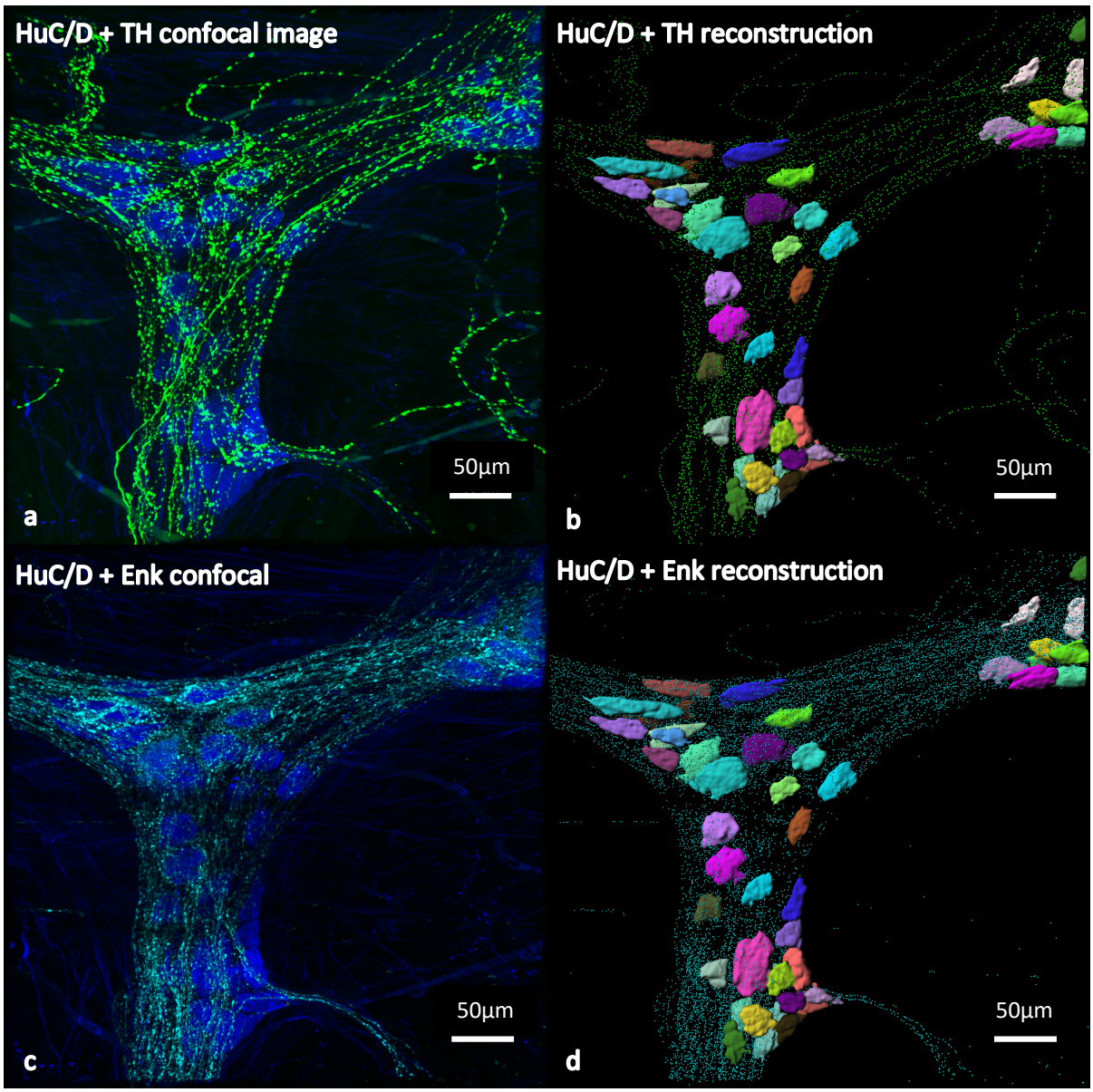


**Figure 3-5 Images of 3D Reconstruction using Imaris.**

**3D rendering from the same myenteric ganglion from H2239. (a) Confocal maximum projection image of TH (green) and HuC/D cells (blue); and (b) the corresponding Imaris 3D reconstruction, with each individual cell now being demarcated as a "surface" in a different colour to help distinguish overlapping cells. The green varicosities in (a) have been reconstructed as small spherical markers called "spots" in (b). Using the 3D reconstruction of nerve cell bodies as surfaces and varicosities as spots, the Imaris program can determine distances between all of these objects, and also map out their 3D coordinates in space, which will later be used to identify varicosities close to cells and then the varicosity density in relation to an individual cell. (c) Confocal maximum projection image of Enk (cyan) and HuC/D cells; with (d) respective reconstruction, with the same population of cells demarcated as multicoloured surfaces and the Enk varicosities as cyan spots. The relationship between Enk varicosities/spots and HuC/D cell bodies/surfaces will be investigated in the same way as TH varicosities and HuC/D cell bodies.**

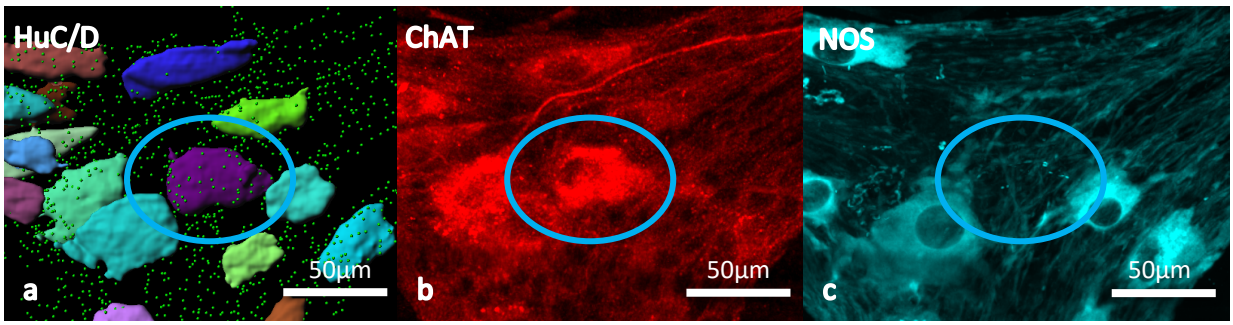


**Figure 3-6 Example of Identifying Individual Cell Types.**

**In Imaris, each individual HuC/D cell body represented by a surface is designated a number, e.g. HuC/D cell [1], and then compared with the 2nd layer of immunohistochemistry images to determine the chemical code with respect to Choline Acetyl Transferase (ChAT) and Nitric Oxide Synthase (NOS). (a) Zoomed image of an individual HuC/D-immunoreactive cell body reconstructed by Imaris (cell of interest within blue circle) with TH-immunoreactive varicosities replaced by green spots. (b) ChAT immunoreactivity; the corresponding cell of interest is ChAT positive. (c) Nitric Oxide Synthase (NOS) immunoreactivity; the cell of interest is NOS negative. Therefore, the cell of interest, designated HuC/D cell [1], has the chemical coding of ChAT+/NOS-. The same process is completed for all reconstructed HuC/D cell bodies.**

**Table 3-3 Surface Area of Each Type of Nerve Cell Body**

| Specimen | ChAT+/NOS- ($\mu m^2$) | ChAT-/NOS+ ($\mu m^2$) | ChAT+/NOS+ ($\mu m^2$) | ChAT-/NOS- ($\mu m^2$) |
|---|---|---|---|---|
| **H2211** | 3010 | 1666 | 3106 | 1508 |
| **H2234** | 3267 | 2796 | 3707 | 1533 |
| **H2236** | 3440 | 3895 | 5941 | 2384 |
| **H2239** | 1657 | 1358 | 2378 | 1068 |
| **H2241** | 4550 | 2217 | 4721 | 2360 |
| **H2242** | 1691 | 1188 | 2557 | 667 |
| **H2244** | 4273 | 2970 | 4686 | 1750 |
| ***Mean ± SEM*** | ***3127 ± 428*** | ***2299 ± 371*** | ***3871 ± 494*** | ***1610 ± 238*** |

*ChAT = choline acetyl transferase; NOS = nitric oxide synthase; SEM = standard error of the mean*

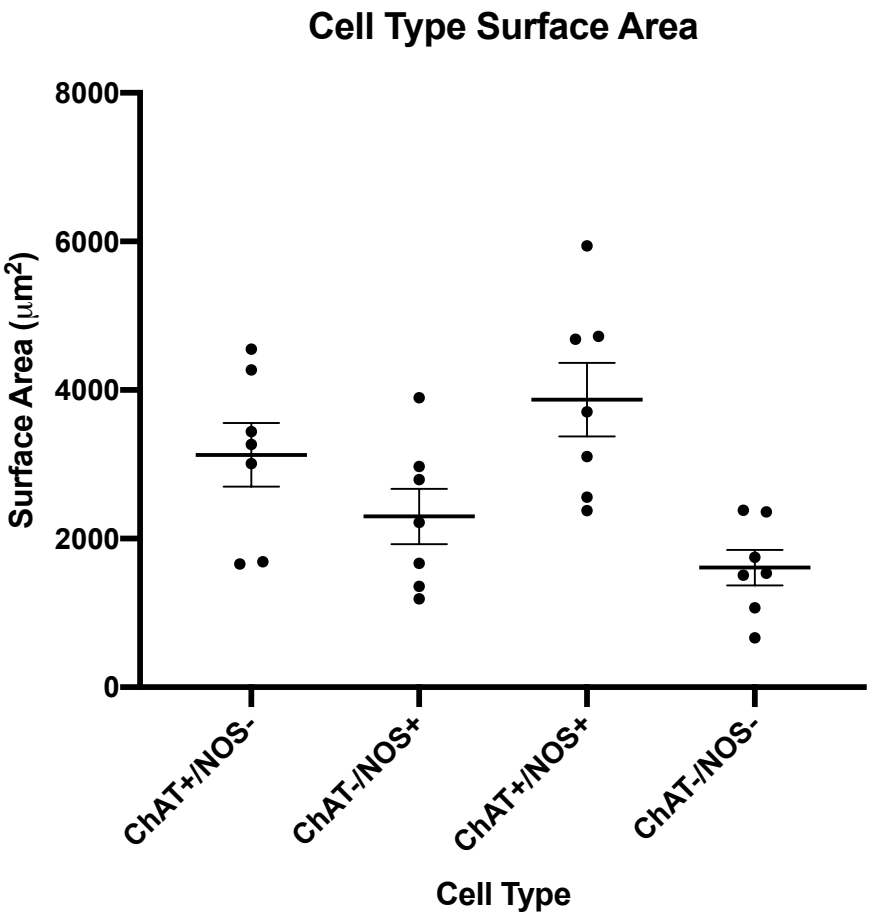


**Figure 3-7 Cell Type Surface Area.**

**Presented as mean area (thick horizontal bar) with standard error of the mean (thin horizontal lines). Mean values for each patient are shown as black circles. The mean surface area was greatest for ChAT+/NOS+ cells, followed by ChAT+/NOS- cells, ChAT-/NOS+ cells and finally smallest for ChAT-/NOS- cells. ChAT = choline acetyl transferase; NOS = nitric oxide synthase.**

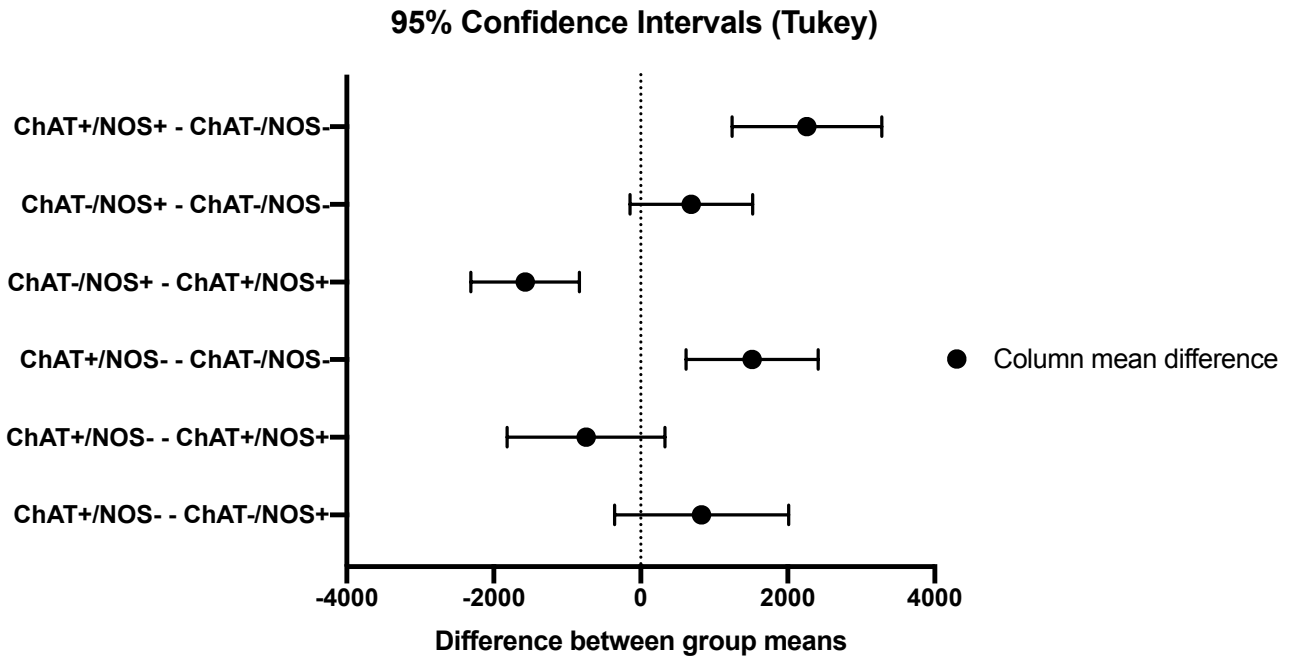


**Figure 3-8 Post Hoc Analysis comparing the surface area of different cell types with 95% confidence intervals. ChAT+/NOS+ cells were significantly larger than ChAT-/NOS- cells and ChAT-/NOS+ cells. ChAT+/NOS- cells were significantly larger than ChAT-/NOS- cells. ChAT = choline acetyltransferase; NOS = nitric oxide synthase.**

**Table 3-4 Volume of Each Type of Nerve Cell Body**

| Specimen | ChAT+/NOS- ($\mu m^3$) | ChAT-/NOS+ ($\mu m^3$) | ChAT+/NOS+ ($\mu m^3$) | ChAT-/NOS- ($\mu m^3$) |
|---|---|---|---|---|
| **H2211** | 5017 | 2349 | 5464 | 2575 |
| **H2234** | 5400 | 4591 | 7544 | 2040 |
| **H2236** | 4004 | 4524 | 6914 | 2791 |
| **H2239** | 3334 | 2524 | 5663 | 1946 |
| **H2241** | 6116 | 3109 | 6938 | 3005 |
| **H2242** | 3276 | 1977 | 4966 | 947 |
| **H2244** | 4813 | 3169 | 5057 | 1791 |
| ***Mean ± SEM*** | ***4566 ± 404*** | ***3178 ± 390*** | ***6078 ± 391*** | ***2156 ± 265*** |

*ChAT = choline acetyl transferase; NOS = nitric oxide synthase; SEM = standard error of the mean*

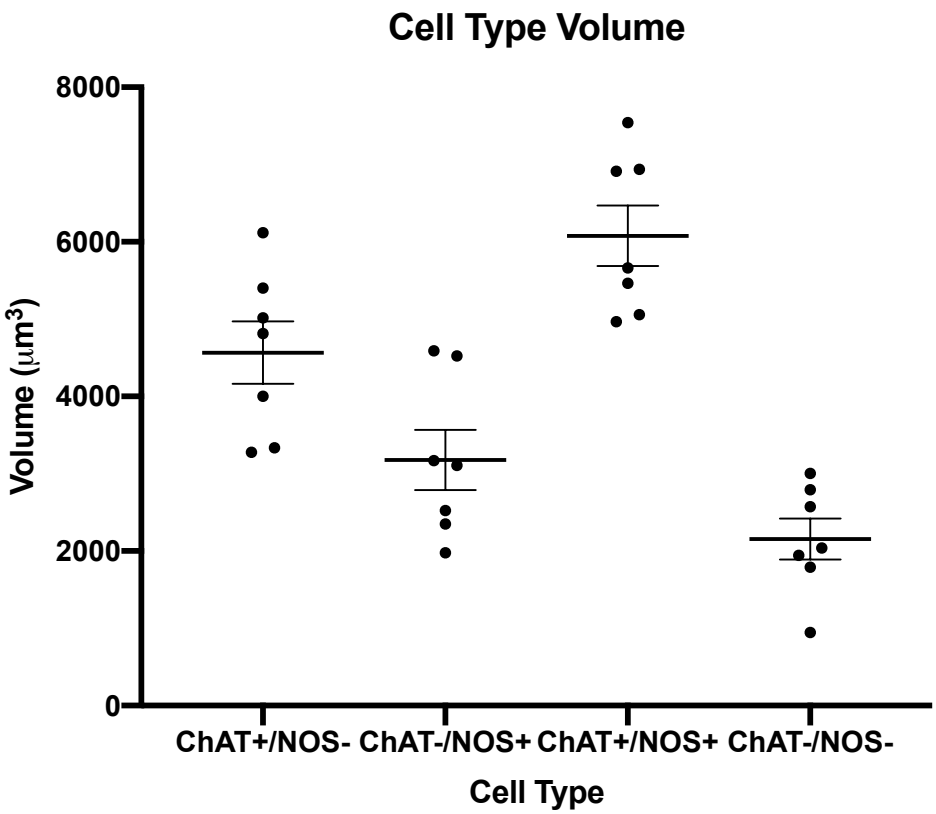


**Figure 3-9 Cell Type Volume.**

**Presented as mean cell volume (thick horizontal bar) with standard error of the mean (thin horizontal lines). Mean values for each patient are shown as black circles. Mean volume was greatest for ChAT+/NOS+ cells, followed by ChAT+/NOS- cells, ChAT-/NOS+ cells and finally smallest for ChAT-/NOS- cells. ChAT = choline acetyl transferase; NOS = nitric oxide synthase.**

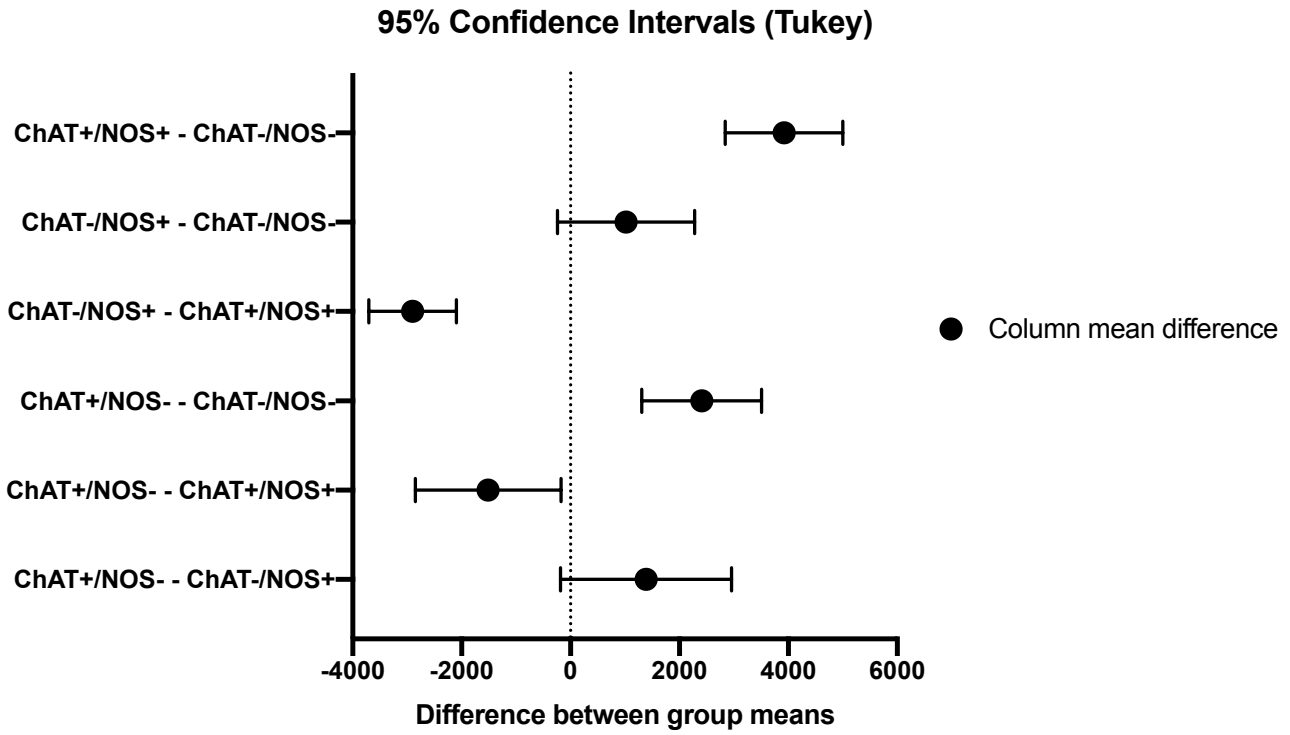


**Figure 3-10 Post Hoc Analysis.**

**Comparing the volume of different cell types with 95% confidence intervals. ChAT+/NOS+ cells were significantly larger than the three other cell types. ChAT+/NOS- cells were significantly larger than ChAT-/NOS- cells. ChAT = choline acetyltransferase; NOS = nitric oxide synthase.**

## 3.4 Discussion

The results with respect to ChAT and NOS immunoreactivity in human colonic myenteric neurons can be compared directly to immunohistochemical results in human colon determined Murphy et al., Wattchow et al., Beck et al. and Ng et al. These four prior studies report ChAT+/NOS- cells ranging from 36-51%, ChAT-/NOS+ cells from 34.5-51%, ChAT+/NOS+ cells from 3-10.3% and ChAT-/NOS- cells from 2.5-10% (Murphy et al., 2007; Wattchow et al., 2008]{Beck, 2009 #584; Ng et al., 2018). Two of these studies were performed in our research laboratory over a decade ago using the same antibodies. The present study found respective percentages of ChAT+/NOS- cells 38%, ChAT-/NOS+ cells 42%, ChAT+/NOS+ cells 12% and ChAT-/NOS- cells 8%. These values are overall similar to what has been reported previously, with the exception of the ChAT+/NOS+ cells, which made up a larger proportion in this study.

The reason for this discrepancy is unclear, however, several factors may have influenced the variability between datasets. Myenteric neurons in the human GIT are known to decrease in number with age (de Souza et al., 1993; Gomes et al., 1997). In both rats and humans it has been found that this decrease disproportionately affects the cholinergic neurons to a greater degree (Phillips et al., 2003; Bernard et al., 2009). However, this is unlikely to account for the differences shown in our study because the median age between the various studies is similar (range 63-68 years). A previous study of rats found a greater number of nitrergic neurons in the proximal colon compared to the distal colon, and therefore the colonic segment can affect the proportions of ChAT and NOS cells (Takahashi and Owyang, 1998). The study by Wattchow et al. also demonstrated regional variation, with more nitrergic cells in the ascending colon compared to other segments (Wattchow et al., 2008). Two of the four studies listed above used similar proportions of colonic specimens from each of the ascending, transverse and descending colon (Wattchow et al., 2008; Beck et al., 2009). The study by Murphy et al. did not have any specimens from the ascending colon, and the study by Ng et al. examined only the rectum and descending colon; both of these had a higher proportion of cholinergic neurons compared to studies with a more even spread of colonic regions (Murphy et al., 2007; Ng et al., 2018).

Another notable difference between the current study and the four previous studies is the use of confocal microscope; Beck et al. used confocal in 2009, while Murphy et al, Wattchow et al. and Ng et al. used conventional epifluorescence. It is possible that a newer confocal microscope (the Zeiss LSM 880) could detect lower intensities of NOS or ChAT, resulting in a higher proportion of

ChAT+/NOS+ cells (i.e. false negatives for NOS in previous studies). However, the NOS antibody (raised in sheep) generally provides intense labelling with a low background and is probably very well distinguished.

A more recent study investigated full thickness human colon after tissue clearing and immunohistochemistry (also with antibodies to HuC/D, ChAT and NOS, as well as VAChT) with confocal microscopy. The reported proportions were ChAT+/NOS- cells 28%; ChAT-/NOS+ cells 50%, ChAT+/NOS+ cells 5%; and ChAT-/NOS- cells 16% (Graham et al., 2020). The authors suggested that ChAT antibody staining may be weaker using their method with tissue clearing, accounting for the significantly lower estimate of cholinergic cells compared to previous studies. They also used a different commercial ChAT antiserum from the present study. Studies in our laboratory have shown this to give less intense labelling than the P03 Yeb antiserum used here. Interestingly, this study also used 3D reconstruction with Imaris software, but only for estimating the area of the myenteric ganglia as a whole, not the individual cells.

The cell sizes found in this study are in a similar sequence to those reported by Murphy et al., with ChAT+/NOS+ being the largest, followed by ChAT+/NOS- cells, ChAT-/NOS+ cells and the smallest being ChAT-/NOS- cells (Murphy et al., 2007). Graham et al. also found the diameter of cholinergic neurons to be significantly greater than that of nitrergic neurons (Graham et al., 2020). Notably, the finding that ChAT+/NOS+ cell bodies are largest in the human myenteric plexus contrasts with ChAT+/NOS+ neurons in the myenteric plexus of mice, which have been shown to have Dogiel type 1 morphology with relatively smaller cell bodies, representing an interspecies discrepancy (Qu et al., 2008).

Cell sizes in the present study however were calculated based on 3D reconstructed cells to calculate surface area and volume, whilst other studies have relied on calculating area using the 2D circumferential outline or the major axis through the greatest diameter of a cell. For this reason, the absolute values found in this study are not comparable to previous experiments, though they can be used as a baseline estimate for future investigation of these cell types using 3D reconstruction. Additionally, this data strengthens the need for choosing a method to analyse the juxtaposition of varicosities to myenteric neurons which accounts for the significant difference in size between cell types. It should also be noted that ChAT-immunoreactive and NOS-immunoreactive types are believed to comprise multiple functional types which may also differ in volume and surface area. For instance, intrinsic primary afferent neurons, which are known to be ChAT positive, have large

cell bodies and therefore could increase the overall average of cholinergic cell bodies.

Overall, these results for ChAT and NOS-immunoreactive cells were achieved for relatively small samples of neurons studied in detail with full 3D reconstruction. They provide comparable results to what has been reported previously in human colon, with the exception of a slightly higher proportion of ChAT+/NOS+ cells. Therefore, it is valid to use of this population of cells to as a representative sample to characterise the relationship between noradrenergic varicosities and myenteric neurons.

# Chapter 4 Characterisation of Noradrenergic Inputs in the Myenteric Plexus of the Human Colon

## 4.1 Introduction

The connectivity between noradrenergic nerve terminals and neurons of the myenteric plexus in the human colon remains unclear. Animal studies investigating this previously have varied in their conclusions. Electron microscopy studies on rabbit, guinea-pig and rat models have been conflicting. Some researchers have supported the presence of noradrenergic synapses with myenteric neurons, or specifically cholinergic or serotonergic neurons in rabbit and guinea-pig myenteric plexus (Manber and Gershon, 1979; Gershon and Sherman, 1982; 1987; Hayakawa et al., 2008), while others report the absence of noradrenergic synaptic connections in the guinea-pig model (Llewellyn-Smith et al., 1981; Gordon-Weeks, 1982). The only human electron microscopy study found noradrenergic baskets surrounding some myenteric neurons, with contacts between noradrenergic varicosities and intrinsic myenteric neurons processes or cell bodies (Llewellyn-Smith et al., 1984). These contacts had pre- and post-synaptic electron-dense membrane specialisations indicative of synapses. Contemporary animal studies using anterograde tracing of sympathetic fibres in extrinsic nerves also provided opposing results. Two studies found noradrenergic pericellular baskets suggestive of synapses around myenteric neurons in guinea-pig and mice (Tassicker et al., 1999; Tan et al., 2010), while another study of rats observed only a minority of noradrenergic axons that projected to myenteric plexus, the authors suggesting that noradrenergic connectivity does not occur via synaptic transmission (Walter et al., 2016).

Preferential targeting of one cell type compared to another would suggest that sympathetic innervation is “hardwired” and may involve synaptic neurotransmission. The alternative is that sympathetic innervation is less specific, with release of noradrenaline throughout the ganglia, giving rise to “volume transmission.” However, this does not rule out the possibility that some classes of neurons may preferentially receive greater amounts of input from volume transmission. In this study, the relative density of varicosities close to myenteric neurons was used to determine whether there was preferential targeting of particular cell types.

This chapter will address my first aim: to determine if postganglionic sympathetic (TH) varicosities preferentially target specific enteric neurons. My second, related aim was to quantify the density of

Enkephalin (Enk)-immunoreactive varicosities close to myenteric neurons, as these are likely to arise from enteric neuron pathways (i.e. intrinsic neurons) which may be more likely to form targeted synaptic connections with specific neurons.

## 4.2 Methods

The steps described in Chapter 2, section 2.1 to 2.7, were followed in order to determine and compare varicosity density close to myenteric neuronal cell types.

## 4.3 Results

### 4.3.1 Measurement of Varicosities Close to Myenteric Cells

From the original 673 HuC/D-immunoreactive cells that were reconstructed, 187 cells were excluded from density analysis because they were incomplete, their outline did not accurately represent the underlying cell or they could not be separated from a neighbouring cell. ChAT-/NOS- cells (33 cells) were not included in comparison of density analysis between cell types because they may possibly be mislabelled ChAT+/NOS- cells with poor labelling, and there were significantly smaller numbers in the sample. The remaining 190 ChAT+/NOS-, 205 ChAT-/NOS+ and 58 ChAT+/NOS+ cells were included in density analysis and comparison.

The density of TH and Enk varicosities was measured in concentric 1µm thick shells from -1µm to 10µm, in relation to each individual cell. Excluded and ChAT-/NOS- cells still had an effect in analysis, because varicosities near to them were attributed to those cells. This was done to preserve the spatial effect of these objects, and also to prevent double counting of varicosities. In the majority of cases varicosity density (for both TH and Enk) generally decreased as distance from the cell increased. However, in relatively fewer instances close packing of nearby cells with their associated varicosities meant that sometimes the varicosity density actually increased further from an individual cell because of the influence of a neighbouring cell.

Because of this variable close packing effect on the outer ranges, and also because varicosities close to the cell surface are likely to have greater post-junctional effects, the density in the range from -1µm to 1µm (a 2µm thick shell immediately apposed the cell surface) was used to assess functional varicosity density and compare between cell types.

### 4.3.2 Tyrosine Hydroxylase Varicosities Close to Cells

The TH varicosity mean density was greatest close to ChAT+/NOS- cells with a mean density of 7.43 varicosities per 1000µm$^3$, followed by ChAT+/NOS+ cells (6.02 varicosities per 1000µm$^3$) and ChAT-/NOS+ cells (5.59 varicosities per 1000µm$^3$). The mean density of TH varicosities close to cells is shown in Table 4-1 and the distribution of densities in Figure 4-1.

Mean densities were compared between different cell types, to determine if one was selectively targeted compared to another. There was a significantly greater density of TH varicosities close to ChAT+/NOS- versus ChAT-/NOS+ cells, with a median density ratio of 1.35, 95% credible interval 1.04-1.69 (see Table 4-2 and Figure 4-2). There was a trend towards there being a greater density of TH varicosities close to ChAT+/NOS- cells versus ChAT+/NOS+ cells. There was no difference between ChAT-/NOS+ cells and ChAT+/NOS+ cells.

**Table 4-1 Density of Tyrosine Hydroxylase (TH) Varicosities Close to Cells**

| Cell Type | Mean TH Varicosity Density ($1/1000\mu m^3$) | 95% Credible Interval |
|---|---|---|
| **ChAT+/NOS-** | 7.43 | 4.69 – 12.11 |
| **ChAT-/NOS+** | 5.59 | 3.53 – 9.38 |
| **ChAT+/NOS+** | 6.02 | 3.55 – 10.08 |

*ChAT = choline acetyl transferase; NOS = nitric oxide synthase; TH = Tyrosine Hydroxylase*

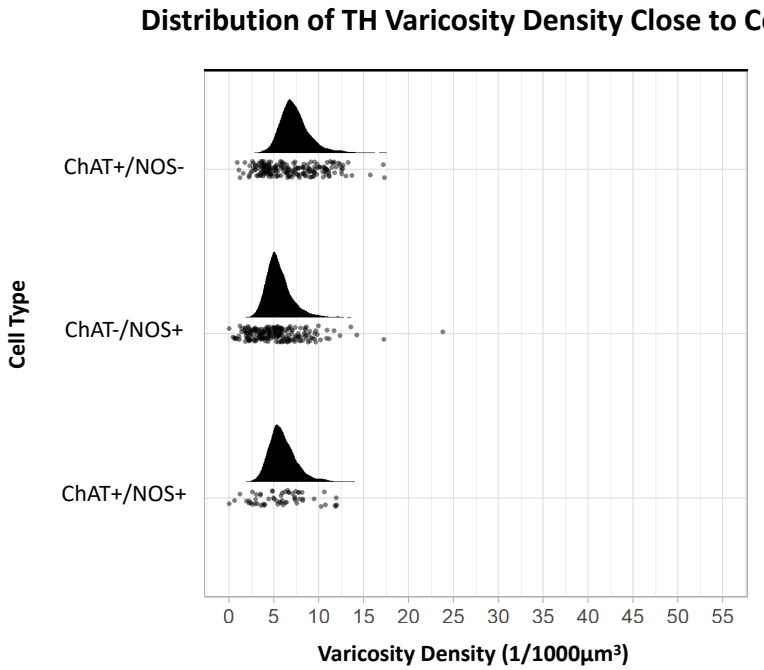


**Figure 4-1 Graph of the Distribution of Tyrosine Hydroxylase (TH) Varicosities Close to Cells.**

**The upright curve in each graph is the distribution of the mean density for each cell type. Every small black dot beneath represents the density of TH varicosities close to an individual cell. The mean varicosity density is greatest for the ChAT+/NOS- cell type at 7.43 varicosities per $1000\mu m^3$.**

**Table 4-2 Density Ratio of Tyrosine Hydroxylase (TH) Varicosities Close to Cells**

| Cell Type | Median TH Varicosity Density Ratio (1/1000µm$^3$) | 95% Credible Interval |
|---|---|---|
| **ChAT+/NOS- vs. ChAT-/NOS+** | 1.35 | 1.04 – 1.69 |
| **ChAT+/NOS- vs. ChAT+/NOS+** | 1.25 | 0.96 – 1.60 |
| **ChAT-/NOS+ vs. ChAT+/NOS+** | 0.94 | 0.67 – 1.31 |

*ChAT = choline acetyl transferase; NOS = nitric oxide synthase; TH = Tyrosine Hydroxylase*

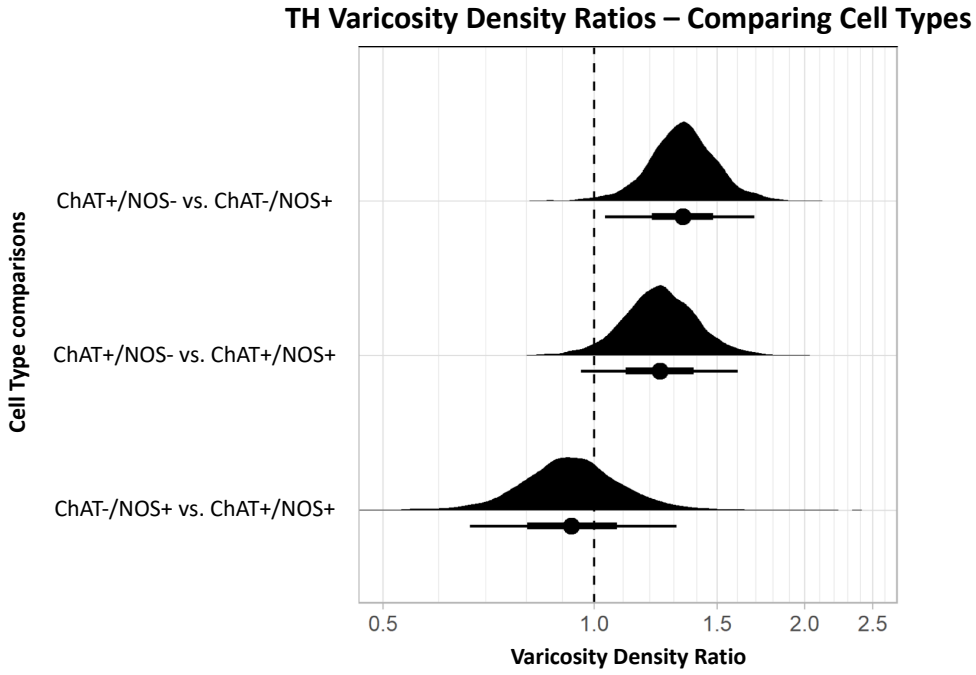


**Figure 4-2 Graph of Tyrosine Hydroxylase (TH) Varicosity Density Ratios Comparing Cell Types.**
**Density ratio is plotted on a logarithmic scale. The filled black curves indicate the ratio between the distributions of the mean of density (mean varicosity density of cell type divided by another). The bars beneath indicate the median (dot), the 66th percentiles and the 95th percentiles of the mean. A ratio of 1.0 indicates that the densities for the two types of cells compared are identical. In this graph, ChAT+/NOS- cells compared to the ChAT-/NOS+ cells have a mean density ratio and 95% percentile bar to the right of 1.0. This shows there is a significantly greater varicosity density close to ChAT+/NOS- cells compared to ChAT-/NOS+ cells.**

### 4.3.3 Enkephalin Varicosities Close to Cells

Like TH, the density of Enk-immunoreactive varicosities was also greatest close to ChAT+/NOS- cells, with a mean density of 19.52 varicosities per 1000µm$^3$ (95% credible interval 14.61 – 25.84), with lower densities for ChAT-/NOS+ cells and ChAT+/NOS+ cells. The mean density of Enk varicosities is shown in Table 4-3, and the distribution shown in Figure 4-3. The absolute density of Enk varicosities was considerably greater and the distribution wider than that of TH varicosities (see Figure 4-4).

Comparing different cells types, there was a greater density of Enk varicosities close to ChAT+/NOS- versus ChAT-/NOS+ cells, with a median density ratio of 1.51, 95% credible interval 1.23-1.83 (shown in Table 4-4 and Figure 4-5). The same is true of ChAT+/NOS- versus ChAT+/NOS+ cells with a median density ratio of 1.49, 95% credible interval 1.19-1.88. There was no difference between the ChAT-/NOS+ cells and the ChAT+/NOS+ cells.

**Table 4-3 Density of Enkephalin (Enk) Varicosities Close to Cells**

| Cell Type | Mean Enk Varicosity Density ($1/1000\mu m^3$) | 95% Credible Interval |
|---|---|---|
| **ChAT+/NOS-** | 19.52 | 14.61 – 25.84 |
| **ChAT-/NOS+** | 12.99 | 9.26 – 17.97 |
| **ChAT+/NOS+** | 13.22 | 9.17 – 18.42 |

*ChAT = choline acetyl transferase; NOS = nitric oxide synthase; Enk = Enkephalin*

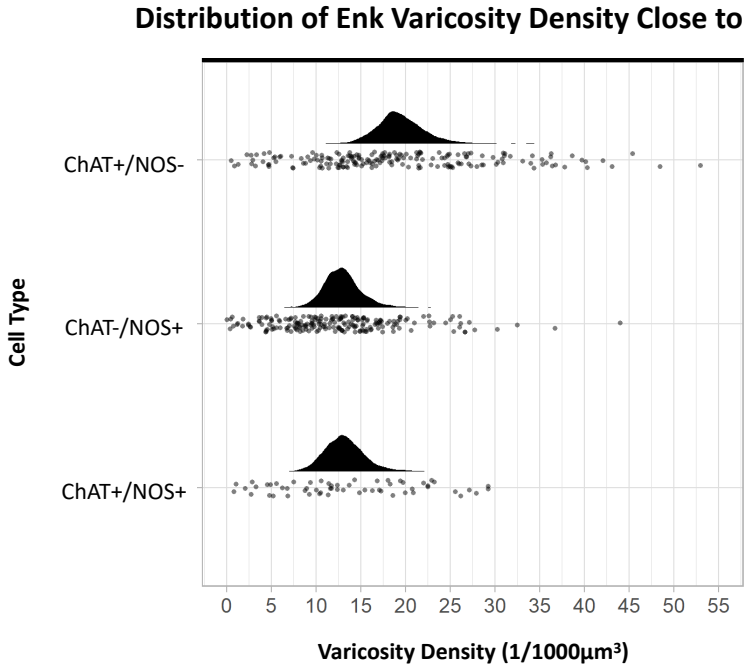


**Figure 4-3 Graph of the Distribution of Enkephalin (Enk) Varicosities Close to Cells.**

**The upright curve in each graph is the distribution of the mean density for each cell type. Every small black dot beneath represents the density of Enk varicosities close to an individual cell. The mean varicosity density is greatest for the ChAT+/NOS- cell type at 19.52 varicosities per $1000\mu m^3$.**

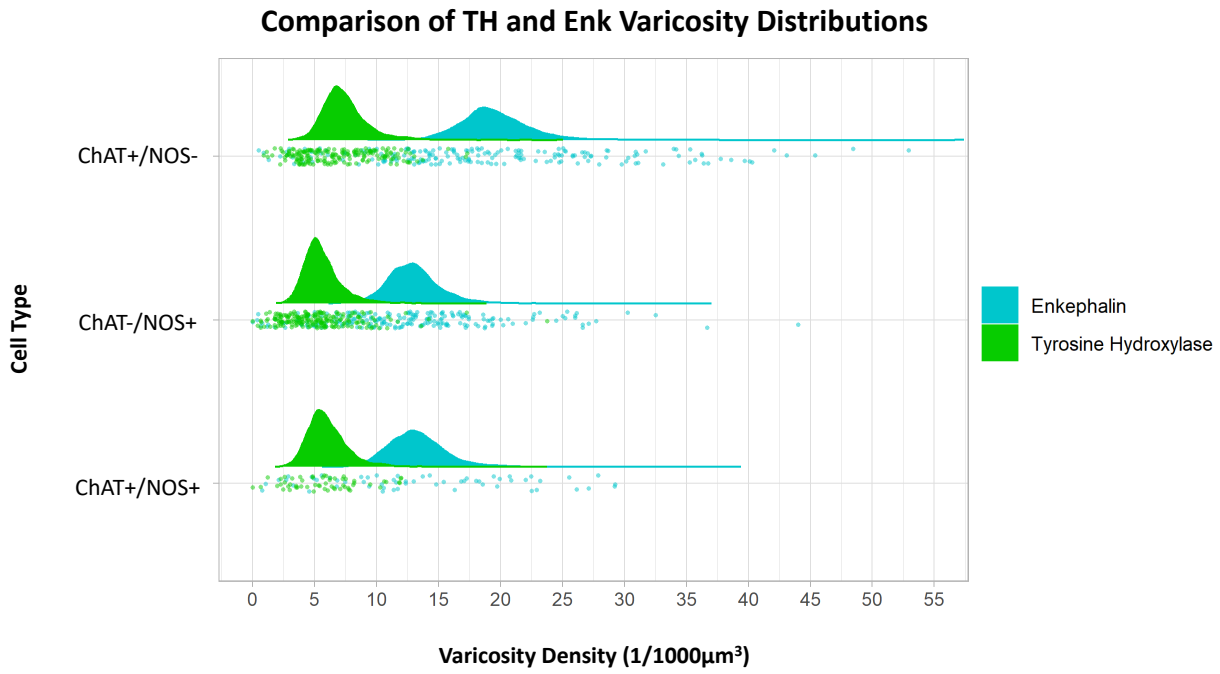


**Figure 4-4 Comparison of the absolute varicosity distributions for both varicosity markers.**

**Figure 4-1 and 4-3 have been stacked one above the other on the same scale, Tyrosine Hydroxylase (TH) is in bright green and Enkephalin (Enk) is in light blue. The upright curve in each graph is the distribution of the mean density for each cell type. Every small dot beneath represents the density of TH and Enk varicosities close to an individual cell. This comparison demonstrates the greater absolute mean density and wider distribution of Enk varicosities compared to TH varicosities in every cell type.**

**Table 4-4 Density Ratio of Enkephalin Varicosities Close to Cells**

| Cell Type | Median Enk Varicosity Density Ratio (1/1000µm$^3$) | 95% Credible Interval |
|---|---|---|
| **ChAT+/NOS- vs. ChAT-/NOS+** | 1.51 | 1.23 – 1.83 |
| **ChAT+/NOS- vs. ChAT+/NOS+** | 1.49 | 1.19 – 1.88 |
| **ChAT-/NOS+ vs. ChAT+/NOS+** | 1.00 | 0.75 – 1.31 |

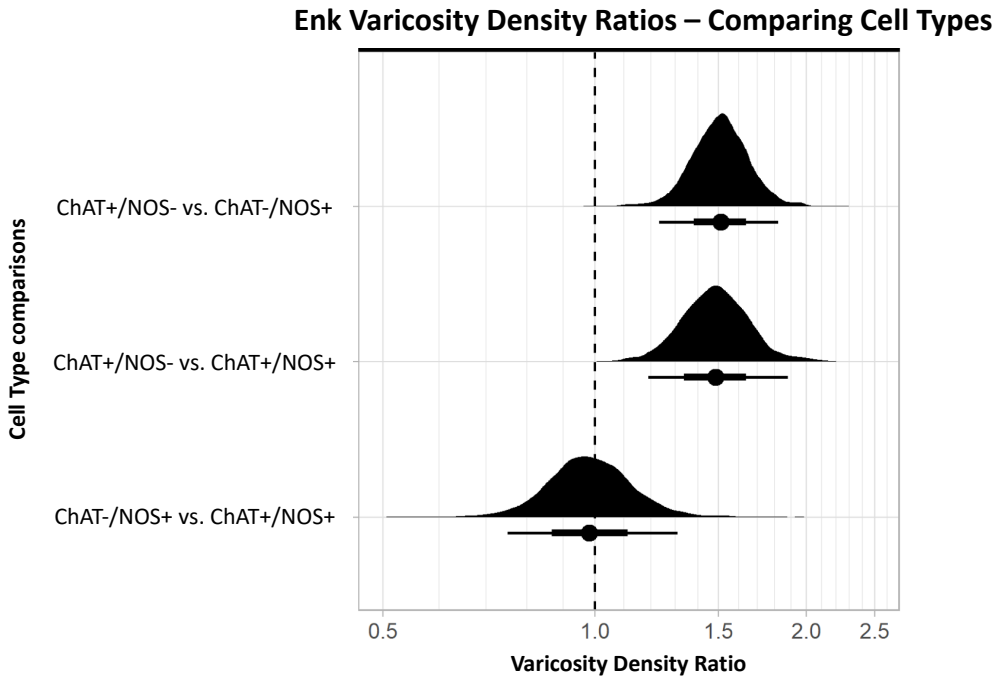


**Figure 4-5 Graph of Enkephalin (Enk) Varicosity Density Ratios Comparing Cell Types.**

**Density ratio is on a logarithmic scale. The filled black curves indicate the ratio between the distributions of the mean of density (mean varicosity density of cell type divided by another). The bars beneath indicate the median (dot), the 66th percentiles and the 95th percentiles of the mean. A ratio of 1.0 indicates that the densities for the two types of cells compared are identical. In this graph, ChAT+/NOS- cells compared to the ChAT-/NOS+ cells and also compared to the ChAT+/NOS+ cells have a mean density ratio and 95% percentile bar to the right of 1.0. This shows there is a significantly greater density of Enk varicosities close to ChAT+/NOS- cells compared to both ChAT-/NOS+ and ChAT+/NOS+ cells.**

## 4.4 Discussion

The density of TH varicosities is being used in this study as a quantitative measurement of close contacting nerve terminals, and thus the degree of noradrenergic input to individual cell types. A higher density of noradrenergic varicosities indicates greater connectivity, while lower density indicates lesser connectivity. A significant difference in the TH varicosity density suggests preferential targeting of one cell type over another.

TH varicosities were shown to have the greatest density close to ChAT+/NOS- in the myenteric plexus compared to ChAT-/NOS+ cells, and also to a slightly lesser degree, compared to the smaller population of ChAT+/NOS+ neurons. Such an arrangement suggests a slight preference by noradrenergic varicosities for close approaches to cholinergic neurons. Whether this reflects additional synaptic contacts is unclear; ultrastructural studies would be required to establish this. However, this finding is compatible with a previous investigation in myenteric plexus of human small intestine by Llewellyn-Smith et al. which identified ultrastructural synapses between noradrenergic neurons and some myenteric neurons. This was taken as evidence supporting the proposal of synaptic interaction between noradrenergic and cholinergic neurons put forward by Manber and Gershon from their studies of rabbit jejunum (Manber and Gershon, 1979; Llewellyn-Smith et al., 1984).

Enkephalin-immunoreactive varicosities were used in this study as a positive control, as it has been recently shown qualitatively that baskets of Enk positive varicosities are preferentially associated with cholinergic neurons (Brookes et al., 2020). Furthermore, Enk-immunoreactive cell bodies are nearly all also ChAT-immunoreactive, suggesting that Enk is a marker for some cholinergic synaptic release sites. Using a different method, the present study has confirmed quantitatively that there is a greater density of Enk varicosities close to cholinergic cells compared to both nitrergic and ChAT+/NOS+ cells. This finding satisfies the second aim of this research project and validates this method of quantitative analysis of varicosity density in determining preferential targeting of neurons.

It is well established that noradrenaline released by postganglionic sympathetic fibres binds to alpha-2a adrenergic receptors on cholinergic presynaptic terminals to inhibit the release of ACh. Noradrenaline is likely to have its direct action at the site of incoming cholinergic nerve terminals, rather than directly onto cholinergic cell bodies. The incoming cholinergic nerve terminals, with their

presynaptic alpha-2a adrenergic receptors, are likely to be positioned in close apposition to the dendrites of the next-in-line cholinergic cell body. Dendrites from cholinergic cell bodies are short in the human myenteric plexus, so the dendritic field area is very close to the cell body. (Brehmer, 2006) The incoming cholinergic nerve terminals are thus located in the dendritic field close the receiving ChAT+/NOS- cell body. This is supported by the finding in this and other studies that Enk varicosities, which are cholinergic neuronal terminals, have a greater density close to cholinergic cell bodies (Brookes et al., 2020). Therefore the position of TH varicosities in the same vicinity close to the cell bodies allows noradrenaline to act on the presynaptic membrane of the incoming cholinergic neurons to inhibit the release of ACh, and indirectly inhibit the action of the ChAT+/NOS- cell body. For this reason, the preferential innervation of TH varicosities to ChAT+/NOS- cell bodies indicates preferential targeting of those cells, though the mechanism is likely to be via an indirect pathway. The finding of a greater density of noradrenergic varicosities close to cholinergic neurons is likely to be functionally significant in causing an inhibitory effect in the myenteric plexus and subsequently inhibiting motility.

Together, ChAT and NOS-immunoreactive cell bodies account for almost all of the intrinsic myenteric neurons (Murphy et al., 2007; Ng et al., 2018). Noradrenergic varicosities appear to target cholinergic neurons preferentially. However, ChAT-immunoreactive neurons include many functional classes of enteric neurons, including excitatory motor neurons to both muscle layers, ascending interneurons, primary afferent neurons, some descending interneurons, vasomotor neurons and secretomotor neurons (Murphy et al., 2007). It is possible that noradrenergic terminals preferentially target one or several of these subtypes of ChAT-immunoreactive neurons, rather than every class of cholinergic cell, which would be almost half of the myenteric neurons. This would require extensive testing beyond the scope of this study. The same is true for Enkephalin varicosities, which likely come from ascending interneurons and form baskets around one or more specific functional classes of myenteric neurons (Humenick et al., 2020). To account for effects on motility, the intuitively simplest pathway would be for noradrenergic varicosities to surround the cell bodies and dendrites of the excitatory motor neurons to the longitudinal and circular smooth muscle layers. This would position them ideally to exert presynaptic inhibitory control of synaptic drive to these cholinergic neurons, thus inhibiting colonic motility. Whether this is the case or not cannot be confirmed from the present study.

ChAT+/NOS+ neurons have been shown comprise at least three to four classes of descending

interneurons, making up 29% of this functional pathway (Porter et al., 2002). Interestingly, these cells have a lower density of TH varicosities compared to ChAT+/NOS-cells, with density more similar to that of ChAT-/NOS+ cells. Of the other descending interneurons, 46% are ChAT-/NOS+, while 20% are ChAT+/NOS-. It is not clear whether ChAT+/NOS- descending interneurons have a higher density of TH inputs. Although this study gives strong evidence for denser close contacts between noradrenergic varicosities and some cholinergic cells, noradrenaline may still act substantially by diffuse volume transmission as well. There is also some direct innervation of the smooth muscle by noradrenergic fibres (Walter et al., 2016). Therefore, a number of distinct mechanisms may be involved in mediating the effects of sympathetic pathways on colonic function.

Throughout this study, the density of TH varicosities was measured relative to nerve cell bodies labelled with HuC/D antisera. These are known to label the great majority, if not all enteric nerve cell bodies (Murphy et al., 2007). However, while HuC/D labels the nerve soma effectively, it does not visualise completely the dendrites of enteric neurons. In most cases, the dendrites are not extensive, (Brehmer, 2006) but this may impose a limit on the resolution of the techniques used in the present study. Furthermore, no account was taken of glial cells that surround enteric neurons in the myenteric plexus. Thin glial cell leaflets can be interposed between axonal varicosities and nearby nerve cell bodies and these may prevent access by released neurotransmitter to post-synaptic receptors or at least increase the tortuosity of some extracellular pathways (Llewellyn-Smith et al., 1984). Nevertheless, it seems likely that the higher density of TH varicosities within 1µm of the surface of cholinergic nerve cell bodies will translate to a higher local concentration of noradrenaline to cause inhibition of those cells.

Enk-immunoreactive varicosities were also denser around cholinergic compared to nitrergic neurons, similar to TH. However, two differences were very striking. First, the absolute density of Enk varicosities was considerably higher than TH varicosities. Second, the preference of Enk varicosities for cholinergic neurons (ChAT+/NOS-) over nitrergic neurons (ChAT-/NOS+) was more extreme than for TH varicosities. Thus, the median ratio for Enk varicosity density was 1.51 (51% difference) compared to 1.35 for TH varicosities (35% difference). This suggests that the enteric-enteric connectivity for Enk-immunoreactive varicosities may be more tightly hard-wired than the sympathetic-enteric connectivity. It is worth pointing out that Enk varicosities often formed dense “baskets” around particular enteric nerve cell bodies (most of which were cholinergic) whereas TH varicosities appeared to be more evenly distributed throughout the ganglia, with few visible

"baskets." This may differ between species and regions however. TH varicosities form clear baskets around 5-HT-immunoreactive enteric neurons in the guinea-pig small intestine myenteric plexus, (Gershon and Sherman, 1982; 1987; Tassicker et al., 1999) and baskets have also been described in human small intestine (Llewellyn-Smith et al., 1984).

Some of the TH-immunoreactive varicosities that have been interpreted as belonging to noradrenergic extrinsic sympathetic neurons could be derived from intrinsic dopaminergic cells (Eaker et al., 1988; Anlauf et al., 2003). However, these are thought to make up only a very small proportion of the TH varicosities in the myenteric plexus and were considered to have a negligible effect on the total pool of varicosities. Indeed, few TH-immunoreactive nerve cell bodies were identified during these studies (see Chapter 6), suggesting that intrinsic dopaminergic pathways in human colon are likely to be sparse.

Lastly, this study had a relatively small sample size of 7 patients and only a limited number of specimens from each colonic region. However, each specimen was examined in detail and a large number of reconstructed cells generated from which to gather data. There was also a relatively equal number of specimens from each colonic region, preventing data from being skewed by an individual region should there be a significant difference.

Further research is required to determine which functional class of cholinergic cells receive the greatest density of synaptic input from noradrenergic terminals. This could be accomplished using multiple layer immunohistochemistry with elution to better classify the cholinergic cell subtypes that have the greatest noradrenergic varicosity density, using the same method of density analysis. Another method might include anterograde labelling of extrinsic colonic nerves to identify the postganglionic sympathetic neurons entering the myenteric plexus and subsequent multi-layer immunohistochemistry to identify cell types receiving the most significant innervation. Furthermore, electrical stimulation of extrinsic colonic nerves and calcium imaging of the activated neurons, once again followed by multilayer immunohistochemistry, would also be an elegant way to determine the specific cell type receiving sympathetic inhibition in the colon.

In conclusion, noradrenergic varicosities preferentially target cholinergic neurons in the myenteric plexus of the human colon, demonstrating a specific neural pathway of inhibition of colonic motility by sympathetic modulation. This interaction may utilise synaptic transmission based on close contacting varicosities. The method of density analysis presented here is valid for determining

preferential targeting of neurons in the ENS.

# Chapter 5 Baskets of Varicosities within the Myenteric Plexus of the Human Colon

## 5.1 Introduction

Baskets of varicosities surrounding nerve cell bodies can often be seen in immunofluorescence preparations (Tassicker et al., 1999; Smolilo et al., 2018). They represent a high density of nerve endings in close apposition to individual cells and often correlate with dense with synaptic contacts (Pompolo and Furness, 1995). Qualitatively, identifying baskets around particular cells can reveal targeted innervation and the hard-wired connectivity of the enteric nervous system. Baskets of varicose nerve fibres in the myenteric plexus of guinea-pig were described in 1968 by Read and Burnstock (Read and Burnstock, 1968).

This chapter examines the cells with baskets of inputs by TH and Enk varicosities. The data derived here from visual examination would be expected to correlate with what has been determined quantitatively by 3D reconstruction and density analysis in the Chapter 4. Enkephalin varicosities are already known to form high density baskets surrounding ChAT+/NOS- cells, suggesting synaptic contact to a cholinergic functional class within the human myenteric plexus (Brookes et al., 2020). Noradrenergic baskets have been observed in human small intestine around undefined myenteric cells, and in guinea-pig surrounding cholinergic and serotonergic neurons (Llewellyn-Smith et al., 1984; Tassicker et al., 1999).

## 5.2 Methods

The steps described in Chapter 2, section 2.1 to 2.6, and section 2.8 were followed to determine visually defined varicosity baskets. Only those cells reconstructed for the density analysis in Chapter 4 were used for analysis so the same group of cells could be observed.

## 5.3 Results

### 5.3.1 Tyrosine Hydroxylase Baskets around Cells

Of the HuC/D labelled cells used for density analysis, 10 visually identified TH baskets were seen to surround nerve cell bodies (10/486 cells, 2.10%). An example of a TH basket is shown in Figure 5-1.

Of the cells surrounded by TH baskets, all 10 were identified as ChAT+, even though only 51% (248/486 cells) of enteric neurons in the sample were ChAT-immunoreactive (Table 5-1). This result is statistically significant (Fisher Exact Test comparing ChAT+ and ChAT- cells, df=1, p=0.0018). Furthermore, all 10 cells were specifically ChAT+/NOS-. Interestingly, 4 of these cholinergic cells with a TH basket also received an Enkephalin varicosity basket.

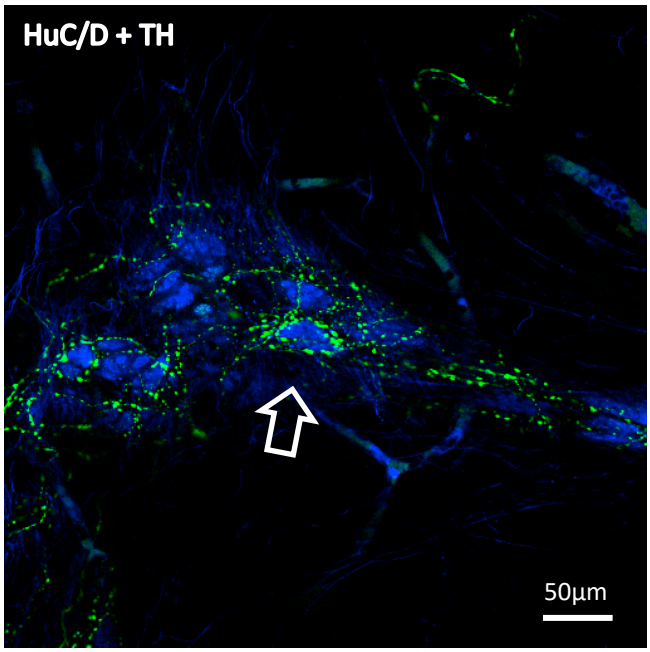


**Figure 5-1 Example of a TH basket around a HuC/D labelled cell (arrow).**

**Single slice confocal image from H2239, sigmoid colon of a 45 year old female. TH (tyrosine hydroxylase) is in green and HuC/D cells in blue. TH varicosity baskets indicate a high density of nerve terminal close contacts to cells and are suggestive of synaptic contacts.**

**Table 5-1 Tyrosine Hydroxylase Baskets surrounding Myenteric Neuron Cell Bodies**

| Subject | TH (ChAT+/NOS-) | TH (ChAT-/NOS+) | TH (ChAT+/NOS+) | TH (ChAT-/NOS-) | TH baskets (total) |
|---|---|---|---|---|---|
| **H2211** | 0 | 0 | 0 | 0 | 0 |
| **H2234** | 0 | 0 | 0 | 0 | 0 |
| **H2236** | 3 | 0 | 0 | 0 | 3 |
| **H2239** | 2 | 0 | 0 | 0 | 2 |
| **H2241** | 0 | 0 | 0 | 0 | 0 |
| **H2242** | 5 | 0 | 0 | 0 | 5 |
| **H2244** | 0 | 0 | 0 | 0 | 0 |
| *Total* | ***10*** | ***0*** | ***0*** | ***0*** | ***10*** |
| *Percentage* | ***100%*** | ***0%*** | ***0%*** | ***0%*** | |

*TH = tyrosine hydroxylase; ChAT = choline acetyltransferase; NOS = nitric oxide synthase.*

### 5.3.2 Enkephalin Baskets around Cells

A larger number of Enkephalin baskets were identified visually. An example of an Enk basket is shown in Figure 5-2. 61 cells with Enk baskets were identified, of which 53 were ChAT+/NOS-, 5 were ChAT+/NOS+ and only 3 were ChAT-/NOS- (Table 5-2). There were no ChAT-/NOS+ cells with surrounding Enk baskets. There was a statistically significantly larger number of Enk baskets surrounding ChAT-immunoreactive cells compared to cells not immunoreactive for ChAT (Fisher Exact Test, df=1, $p<0.00001$). Many ganglia contained multiple Enk baskets.

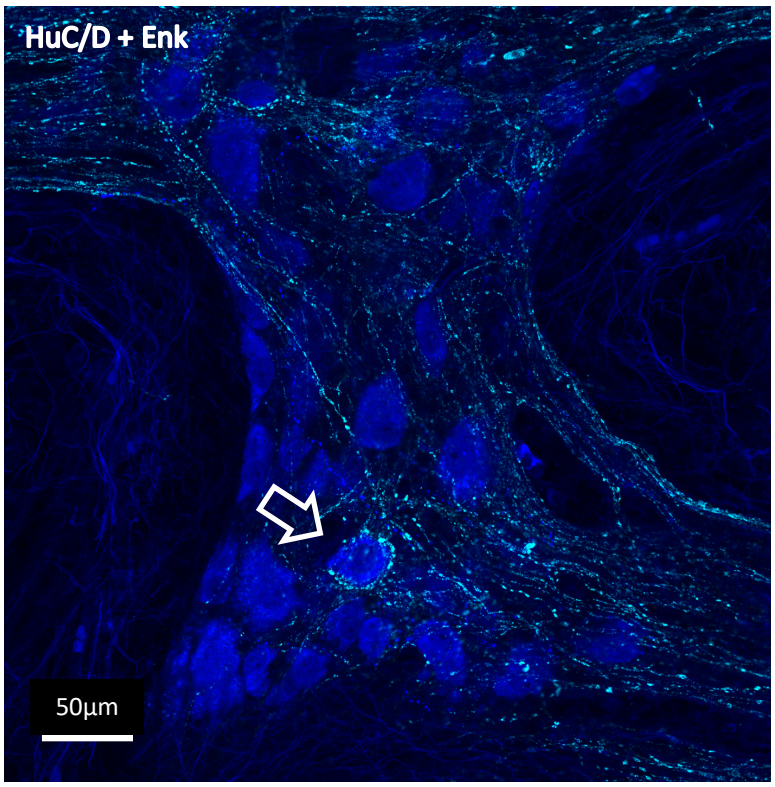


**Figure 5-2 Example of a HuC/D Cell body surrounded by a basket of Enk-immunoreactive varicosities (arrow). Single slice confocal Image from H2236, descending colon from 67 year old man. HuC/D in blue and Enk (Enkephalin) in cyan.**

**Table 5-2 Enkephalin Baskets surrounding Myenteric Neuron Cell Bodies**

| **Subject** | **Enk (ChAT+/NOS-)** | **Enk (ChAT-/NOS+)** | **Enk (ChAT+/NOS+)** | **Enk (ChAT-/NOS-)** | **Enk baskets (total)** |
|---|---|---|---|---|---|
| **H2211** | 8 | 0 | 0 | 3 | 11 |
| **H2234** | 3 | 0 | 0 | 0 | 3 |
| **H2236** | 6 | 0 | 0 | 0 | 6 |
| **H2239** | 4 | 0 | 2 | 0 | 6 |
| **H2241** | 10 | 0 | 0 | 0 | 10 |
| **H2242** | 13 | 0 | 2 | 0 | 15 |
| **H2244** | 9 | 0 | 1 | 0 | 10 |
| *Totals* | ***53*** | ***0*** | ***5*** | ***3*** | ***61*** |
| *Percentage* | ***87%*** | ***0%*** | ***8%*** | ***5%*** | |

### 5.3.3 Comparison of Visually Defined Varicosity Baskets and Quantified Varicosity Density Close to ChAT+/NOS- Cells

A post-hoc analysis of ChAT+/NOS- cells was performed to compare the quantified Enk and TH varicosity density found in Chapter 4 with the presence of visually defined varicosity baskets. For ChAT+/NOS- cell bodies with Enk varicosity baskets the calculated density was 26.75 compared to 16.43 varicosities per 1000µm$^3$ for cells without baskets. For ChAT+/NOS- cell bodies with TH varicosity baskets the calculated density was 9.59 compared to 7.13 varicosities per 1000µm$^3$ (see Figure 5-3).

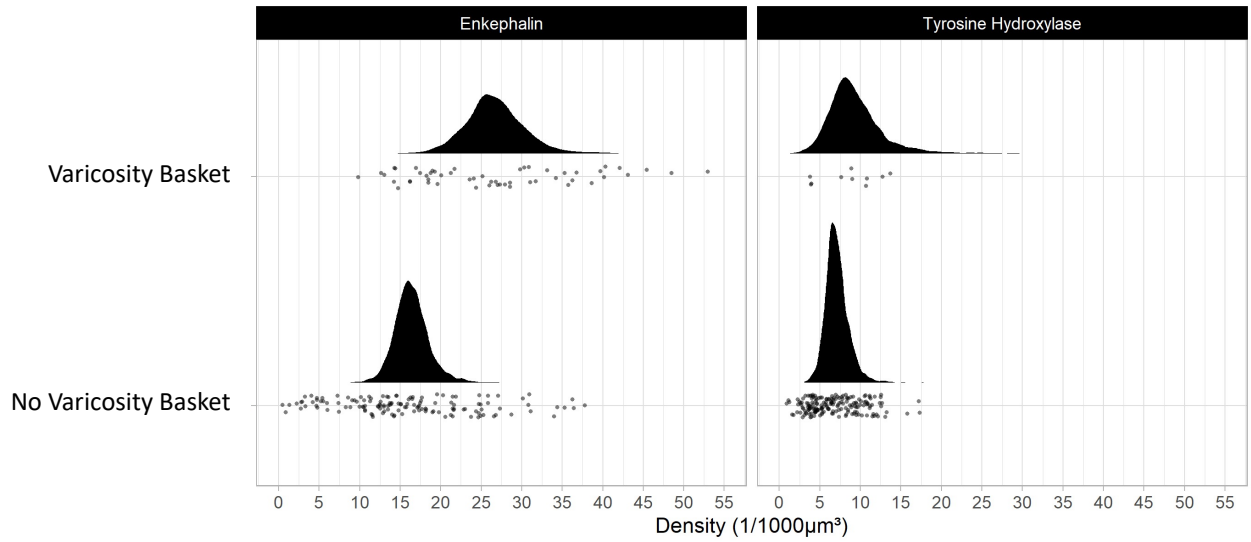


**Figure 5-3 Comparison of Enk (Enkephalin) and TH (Tyrosine Hydroxylase) varicosity density in ChAT+/NOS- cells with and without varicosity baskets.**

**Cell bodies with Enk baskets had a varicosity density of 26.75 varicosities per 1000µm$^3$ (95% credible interval 19.75 – 35.22) versus 16.43 varicosities per 1000µm$^3$ in cells without an Enk basket (95% credible interval 12.52 – 21.37). Cell bodies with TH baskets had a varicosity density of 9.59 varicosities per 1000µm$^3$ (95% credible interval 4.37 – 19.38) versus 7.13 varicosities per 1000µm$^3$ for cells without a TH basket (95% credible interval 4.73 – 10.55).**

The density ratio was calculated for cells with varicosity baskets compared to no baskets, using the same method detailed in Section 2.7.4. ChAT+/NOS- cells had an Enk varicosity density ratio of 1.63 (95% credible interval 1.38 – 1.91), demonstrating a higher calculated density for those cells with Enk baskets. ChAT+/NOS- cells had a TH varicosity density ratio of 1.35 (95% credible interval 0.68 – 2.63), which showed a less significant trend towards there being a greater calculated density for those cells with TH baskets (see Figure 5-4).

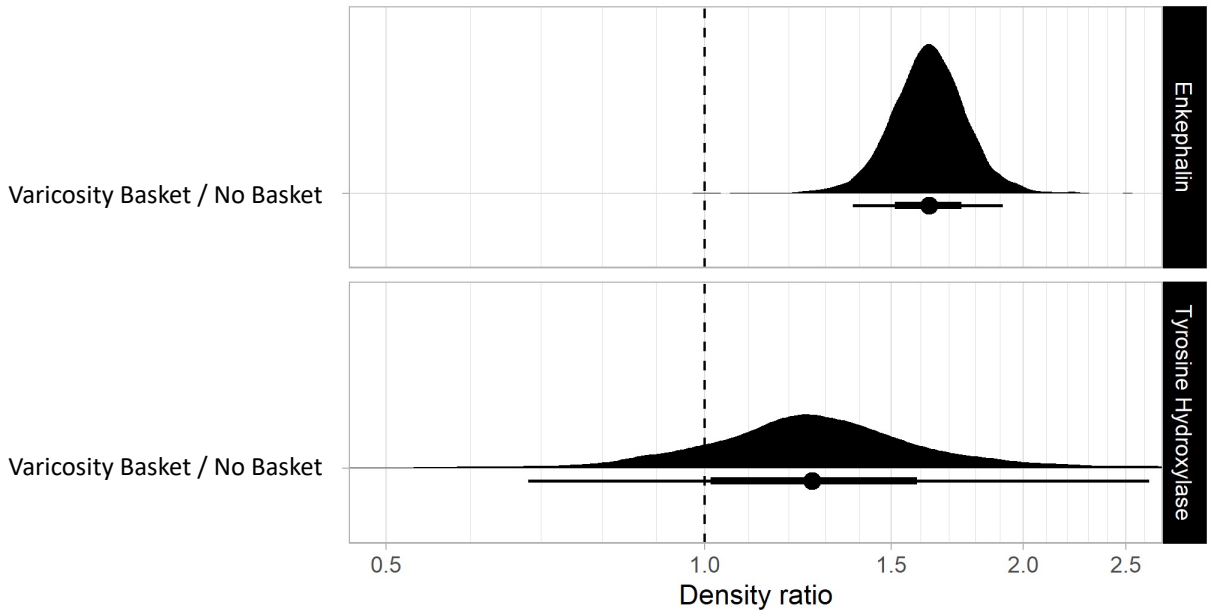


**Figure 5-4 Varicosity density ratio for ChAT+/NOS- cells with and without Enkephalin and Tyrosine Hydroxylase baskets.**

**There appears to be a greater calculated Enk varicosity density in those cells with visually defined Enk baskets compared to cells without baskets. The same relationship is less well defined for cells with and without visually defined TH baskets.**

## 5.4 Discussion

Only 10 baskets of TH-immunoreactive varicosities were identified during this study, from a sample of 486 neurons. Each of the cells receiving a TH basket was ChAT-immunoreactive and hence likely to be cholinergic. This was despite the fact that only 51% of all 486 neurons were ChAT-immunoreactive. This result is consistent with the overall greater density of TH varicosities close to ChAT cells found quantitatively in Chapter 4. The data for Enk baskets also correlates well with the results from Chapter 4, with the majority of Enk baskets being present around cholinergic neurons, and none being present around ChAT-/NOS+ cells. Previously, 93.6% of Enk baskets have been seen to encircle cholinergic neurons in human colonic myenteric plexus (Brookes et al., 2020). The above results support the idea that visually identified associations are consistent with quantitatively measured associations using our novel density analysis method.

When the quantified varicosity density of ChAT+/NOS- cells with and without visually identified baskets were compared, cells that had Enk baskets had a significantly greater varicosity density. However, cells that had TH baskets did not have a similarly greater varicosity density compared with cells without baskets. There were however, 53 ChAT+/NOS- cell bodies with visually defined Enk baskets compared to just 10 ChAT+/NOS- cell bodies with TH baskets, and the low sample size of the latter may have influenced our findings.

Tassicker et al. found that nerve cell bodies in the myenteric plexus of guinea-pig small intestine that received TH baskets were immunoreactive for ChAT or 5-HT (Tassicker et al., 1999). The present study similarly found TH baskets around myenteric cholinergic neurons in human colon, however 5-HT immunoreactivity was not tested. In contrast however, Tan et al. reported noradrenergic varicosities in apposition with NOS-immunoreactive myenteric neurons in rat jejunum (Tan et al., 2010). Whether this reflects inter-species or inter-regional differences remains to be determined.

Observation of baskets of varicosities relies on subjective visual observation. Additionally, while baskets in the horizontal 2-dimensional plane can be readily determined, it is more difficult to determine whether a 3-dimensional distribution of varicosities actually form a basket around a nerve cell body. This factor, combined with the lower density of varicosities, may explain why relatively few TH baskets were observed in this and other studies. 3-dimensional reconstructive analysis may allow such targeted connections to be better perceived and quantified. The reliance on visual identification of baskets makes this approach susceptible to unconscious bias. This is

unlikely to be significant in the present study because both TH and Enk baskets were first located around unidentified HuC/D-immunoreactive cell bodies. Only after further processing (i.e. elution of TH and Enk staining) was ChAT and NOS immunoreactivity tested in the basket-receiving cells. Another consideration is that some of the TH immunoreactive baskets seen visually could have arisen from the intrinsic catecholaminergic neurons. However, there are very few enteric derived catecholamingeric neurons, therefore it is more likely that visually identified TH baskets are derived from the extensive innervation of extrinsic postganglionic sympathetic inputs.

In conclusion, of the few noradrenergic varicosity baskets seen, all surrounded cholinergic neurons, in keeping with preferential innervation of cholinergic neurons identified by the novel method of density analysis in Chapter 4. Additionally, results for Enk baskets showed a similar preference for cholinergic over nitrergic neurons.

# Chapter 6 Intrinsic Catecholaminergic Cells in the Myenteric Plexus of the Human Colon

## 6.1 Introduction

Intrinsic catecholaminergic cells have been identified in the human small and large intestine in several studies and are reported as most likely to be dopaminergic. Dopaminergic neurons may have a role in modulating gastrointestinal motility (Wakabayashi et al., 1989; Anlauf et al., 2003). The specific nature and underlying functional cell type of these dopaminergic cells remains unclear.

TH has been used in the previous chapters as a marker of extrinsic noradrenergic neuron fibres and varicosities, but will also label the intrinsic catecholaminergic (dopaminergic) cells in the ENS. This chapter will focus on intrinsic TH-immunoreactive cell bodies in order to investigate the third aim in this research project: to classify intrinsic TH-immunoreactive cells in the myenteric plexus of the human colon into the broad groups of cholinergic and nitrergic cells.

## 6.2 Methods

The steps in Chapter 2, sections 2.1-2.4, 2.6 and 2.9 were followed in order to classify the TH positive cell bodies. 3D reconstruction was not required for analysis of TH positive cell bodies, therefore every visualised cell body from each specimen could be counted.

## 6.3 Results

Forty-four ganglia from 7 patients were included in the analysis of intrinsic TH positive cell bodies. TH cell bodies were found in 13 ganglia from 5 patients; 31 ganglia did not contain any TH positive cell bodies (see Figure 6-1 with an example of a TH positive cell body). The greatest number of TH cell bodies found in a single ganglion was 5. Of 2252 counted HuC/D cell bodies, only 22 (1%) were TH positive (see Table 6-1). After elution of TH and relabelling with NOS and ChAT antisera, 21 of 22 TH cells were ChAT+/NOS-, while 1 was ChAT-/NOS-. None contained NOS immunoreactivity. The breakdowns of cell types for each subject are summarised in Table 6-2.

HuC/D and TH immunoreactivity do not label cell processes, therefore it was not possible to determine the morphological of the intrinsic catecholaminergic cells. There was variability in the

intensity of TH immunoreactivity; some cell bodies had strong labelling, however others were more difficult to define amongst the many bright TH positive varicosities. 16 out of 22 cells were located within the ganglion while the other 6 were peripherally located at the edge. 10 TH+ cell bodies had a single long axon visible coming from one pole of the cell, while in the other cells no axons were seen (see Figure 6-2). The 2-dimensional mean area of TH-immunoreactive cell bodies was 1324 ± 143$\mu m^2$ SEM with a range from 477 to 2602$\mu m^2$. 1 of the 22 cells was not included in the measurement of cell area because it was on the border of the captured image and therefore incomplete.

Interestingly, there was a gradient of decreasing proportions of TH positive cells from proximal to distal colonic segments, however small numbers of cells and patients preclude statistical testing of this trend.

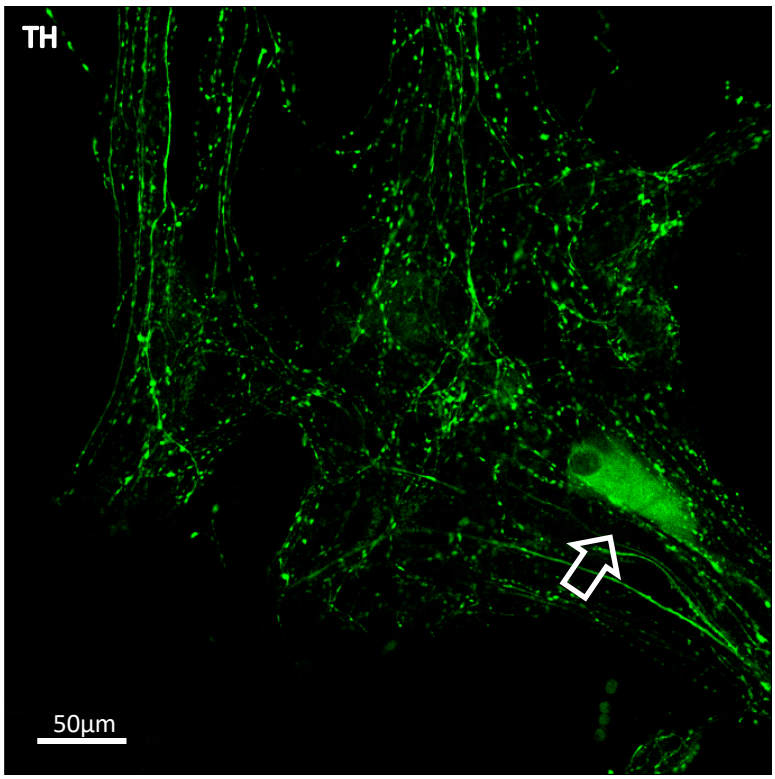


**Figure 6-1 Example of a TH positive cell body (white arrow).**

**Single slice confocal image from H2234, ascending colon from a 90 year old female. TH immunoreactivity in axons and varicosities seen elsewhere in the ganglion is largely from the extrinsic noradrenergic nerves. TH = Tyrosine Hydroxylase.**

**Table 6-1 Intrinsic TH positive cells**

| Subject | Age/Gender | Segment | Total HuC/D cells | Total TH cells | Percentage |
|---|---|---|---|---|---|
| **H2211** | 66 F | Ascending | 226 | 4 | 1.8% |
| **H2234** | 90 F | Ascending | 227 | 6 | 2.6% |
| **H2236** | 67 M | Descending | 331 | 0 | 0% |
| **H2239** | 45 F | Sigmoid | 285 | 0 | 0% |
| **H2241** | 66 F | Transverse | 388 | 5 | 1.3% |
| **H2242** | 37 M | Transverse | 387 | 4 | 1.0% |
| **H2244** | 80 F | Descending | 408 | 3 | 0.7% |
| *Totals* | | | ***2252*** | ***22*** | ***1.0%*** |

*TH = Tyrosine Hydroxylase.*

**Table 6-2 Breakdown of TH positive cells by ChAT/NOS immunoreactivity**

| Subject | TH (ChAT+/NOS-) | TH (ChAT-/NOS+) | TH (ChAT+/NOS+) | TH (ChAT-/NOS-) |
|---|---|---|---|---|
| **H2211** | 4 | 0 | 0 | 0 |
| **H2234** | 6 | 0 | 0 | 0 |
| **H2236** | 0 | 0 | 0 | 0 |
| **H2239** | 0 | 0 | 0 | 0 |
| **H2241** | 4 | 0 | 0 | 1 |
| **H2242** | 4 | 0 | 0 | 0 |
| **H2244** | 3 | 0 | 0 | 0 |
| *Totals* | ***21*** | ***0*** | ***0*** | ***1*** |
| *Percentage* | ***95%*** | ***0%*** | ***0%*** | ***5%*** |

*TH = Tyrosine Hydroxylase; ChAT = Choline Acetyl Transferase; NOS = Nitric Oxide Synthase.*

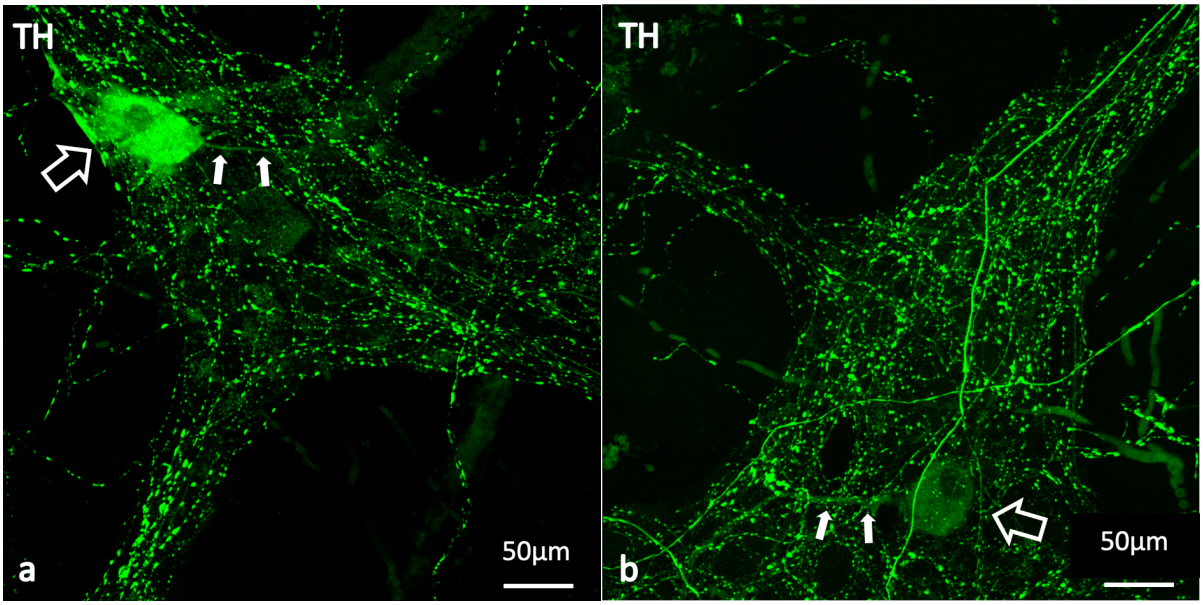


**Figure 6-2 Two examples of the typical morphology found of TH-immunoreactive cell bodies.**

**(a) Maximum projection confocal image from H2244, descending colon from an 80 year old female; and (b) maximum projection confocal image from H2241, transverse colon from a 66 year old female. In both images TH-immunoreactive (green) cell bodies are present (larger hollow arrows) with an oval shape and a single long axonal process projecting into the ganglion (small white arrows). TH = tyrosine hydroxylase.**

## 6.4 Discussion

This study has shown that TH-immunoreactive cells comprise approximately 1% of the intrinsic neurons in the human colon myenteric plexus. They appear to be cholinergic, with the exception of 1 from 22 TH positive cells that apparently lacked immunoreactivity for both ChAT and NOS.

In an earlier study of human bowel, 0-3.1% of all counted myenteric cells in the colon were reported to be immunoreactive for TH (Wakabayashi et al., 1989). In comparison, Singaram et al. reported 12.4 (standard error 2.1) TH-immunoreactive neurons per 100 myenteric neurons (12.4%) in specimens of human ascending colon from normal controls (Singaram et al., 1995). In another study, up to 6% of neurons in the ileum and large intestine were immunoreactive for the catecholaminergic marker VMAT2 (vesicular monoamine transporter 2) and these cells largely co-labelled for TH which was present in 4% of neurons (Anlauf et al., 2003). The present study found a relatively low number of intrinsic TH positive cells, in keeping with the first study by Wakabayashi et al. The reasons for the discrepancies are not clear, however Singaram et al. only studied ascending colon. In the present study, the TH antisera intensely labelled varicose axons in blood vessels and ganglia with a high signal to noise ratio.

The low number of TH-immunoreactive myenteric nerve cell bodies makes it difficult to statistically compare proportions of TH positive cells between colonic segments. However, in this study there was a notable trend towards greater percentages of catecholaminergic cells proximally compared to distally: ascending colon 2.6% and 1.8%; transverse colon 1.3% and 1.0%, descending colon 0.7% and 0%; and sigmoid colon 0%. The same trend was reported by Wakabayashi, who found more TH positive cells in the ascending colon compared to other regions (Wakabayashi et al., 1989). A later study in mice has also reported a comparatively lower proportion of enteric cells expressing transcripts encoding TH in the distal colon (Li et al., 2004). The functional significance of this distribution is currently not clear.

Minimal information could be acquired regarding the morphology of these TH-immunoreactive cells. However, it was found that most are located within the bodies of the ganglia rather than at the periphery and that approximately half had a single axon. The morphology and size of TH-immunoreactive cells has been noted to vary greatly between regions of the GIT (Wakabayashi et al., 1989). Murphy et al. demonstrated a mean area of ChAT+/NOS- cells of 537$\mu m^2$ with a wide distribution relative to other cell types (Murphy et al., 2007). By comparison, TH+ cells in the present

study (of which 21 from 22 are ChAT+/NOS-) had a substantially larger mean area of 1324μm$^2$, with a range of 477 to 2602μm$^2$. This finding may help in narrowing down the possible functional subtype that TH-immunoreactive cells belong to.

Studies in animals and humans have shown that some TH positive neurons in the myenteric plexus are likely to be dopaminergic (Eaker et al., 1988). It was reported that many TH-immunoreactive enteric neurons lack dopamine beta hydroxylase immunoreactivity, suggesting a dopaminergic phenotype (Anlauf et al., 2003). An exception to this is an early study in animal models, in which some enteric neurons were immunoreactive for dopamine beta-hydroxylase (DBH, the enzyme responsible for conversion from dopamine to noradrenaline) in guinea-pig stomach and rat oesophagus, stomach and colon (Schultzberg et al., 1980). The present study is the first to demonstrate that intrinsic TH positive myenteric cells are also immunoreactive for ChAT and thus likely to be cholinergic. Interestingly, Anlauf et al. did not find co-existence of TH and VAChT (vesicular acetylcholine transporter, another cholinergic marker) in human enteric neurons, and therefore stated that catecholaminergic (dopaminergic) and cholinergic cells are in separate classes (Anlauf et al., 2003). However, VAChT is localised predominantly within vesicles in varicosities, and is often difficult to detect in enteric nerve cell bodies because of low expression and the high intensity labelling of varicosities throughout the ganglia.

Dopamine can modulate colonic motility. In animal models, it has been reported as predominantly an inhibitory effect throughout the GIT. Exogenous dopamine applied to isolated rat colon has been shown to reduce spontaneous motility and also cause relaxation of depolarised colon (Aguilar et al., 2005; Zhang et al., 2012). Studies of mice similarly show dopamine inhibiting colonic motility (Walker et al., 2000; Auteri et al., 2016). Conversely, early studies in humans *in* vivo showed that exogenous dopamine stimulates motor function of the sigmoid colon (Lanfranchi et al., 1978). A recent study in healthy human colonic preparations *in vitro* has demonstrated that dopamine causes opposing effects in the two external muscle layers (Zizzo et al., 2020). Exogenously applied dopamine activates $D_1$-like receptors in the circular smooth muscle layer to cause contractile activity, while in the longitudinal smooth muscle layer it activates $D_2$-like receptors to cause relaxation and inhibition. At high concentrations, dopamine caused relaxation mediated by $D_2$-like receptors in the circular muscle as well. This study also made the important claim that dopamine is likely to act within the smooth muscle layers. Neural blockade with tetrodotoxin and ω-conotoxin resulted in no change in the effects induced by exogenous dopamine, implying that its site of action

is within the muscularis propria. Additionally, dopaminergic receptor subtypes are located within smooth muscle, with transcripts identified by reverse transcription polymerase chain reaction (rt-PCR) in those layers (Zizzo et al., 2020).

Relating those findings to the present results, endogenous dopamine appears to be synthesised in a few TH positive myenteric cells. If it acts solely on dopaminergic receptors in the circular and smooth muscle layers this would suggest that some of the TH+/ChAT+ neurons are a subset of cholinergic excitatory motor neurons. Some could also be ascending interneurons, descending interneurons, primary afferent neurons, or vaso/secretomotor neurons. However, further research is required to classify the neurochemical code of these cells and determine their projections. This could be achieved using retrograde tracing from the muscle layers to find myenteric motor neurons, followed by immunohistochemical staining with TH to identify any dopaminergic cells among them, and then use the multi-layer immunohistochemical technique to distinguish the individual cell type.

A limitation of this study is that the purported dopaminergic cells have been identified by TH alone; it would be necessary to establish the absence of DBH immunoreactivity in the same cells to clinch their classification as dopaminergic. However, previous studies using human tissue have already established that TH positive cells do not co-label with DBH, meaning these cells are likely to be dopaminergic rather than noradrenergic (Anlauf et al., 2003). There was also a limited sample of TH+ cells that could be analysed in this study, which is a problem inherent with a scarce cell type in the colon; greater patient numbers would be required to yield more cells.

In conclusion, 1% of the total number of myenteric cell bodies counted in the human colon were TH positive and thus intrinsic catecholaminergic cells likely to be dopaminergic. The present study has found this limited cell type to be almost exclusively cholinergic, narrowing the neurochemical code of these distinct cells. Some of these neurons may give rise to TH-immunoreactive varicosities in enteric ganglia, however given their scarcity, it is unlikely that they contribute more than a small proportion.

# Chapter 7 Discussion

## 7.1 Major Findings

Prior to this research, the neural connectivity between extrinsic noradrenergic nerves and enteric cells of the myenteric plexus was largely unclear, especially in the human bowel. This connectivity is a significant component for understanding the sympathetic inhibition of colonic motility. The major aims and findings of this study are summarised here.

**Aim 1: To determine if noradrenergic (postganglionic sympathetic) varicosities preferentially target specific neurons (ChAT-immunoreactive versus NOS-immunoreactive) in the myenteric plexus of the human colon.**

1. Extrinsic noradrenergic (postganglionic sympathetic) nerve terminals preferentially target cholinergic cells in the myenteric plexus of the human colon compared to non-cholinergic, NOS-containing cells. This demonstrates that there is a specific neural pathway of inhibition of colonic motility by sympathetic modulation of cholinergic neurons in the myenteric plexus. From the close proximity of noradrenergic varicosities to the surfaces of cholinergic neurons, this may involve synaptic transmission. This is a new finding in relation to sympathetic interaction with the myenteric plexus.

**Aim 2: To quantitatively analyse the density of Enkephalin-immunoreactive varicosities close to myenteric neurons in the human colon and compare varicosity density between cholinergic and nitrergic cell types.**

2. Enkephalin nerve terminals were shown to have a greater varicosity density close to cholinergic cells in the myenteric plexus of the human colon, compared to nitrergic cells. This correlates with what has been demonstrated by visually-defined varicosity baskets in the current and previous studies and therefore validates the novel method of quantitative varicosity density analysis.

**Aim 3: To classify intrinsic tyrosine hydroxylase-immunoreactive cells in the myenteric plexus of the human colon into the broad groups of cholinergic and nitrergic cells.**

3. Intrinsic catecholaminergic (likely dopaminergic) neurons comprise approximately 1% of

the myenteric neurons in the human colon, and these cells are cholinergic. This has not been reported previously and further defines this relatively unknown population of cells.

The importance of these findings as well as comparison to previously literature is discussed at length in Chapters 3-6. Aspects of the methodology, challenges, limitations and implications for future directions are discussed in the following sections.

## 7.2 Rationale for the Methodology

### 7.2.1 Rationale for Antibody Elution and Multiple Layer Immunohistochemistry

Immunohistochemistry has been established as a reliable method for morphologically and chemically coding individual neurons over many decades. However, it is limited by the number of antibodies that can be applied at one time (up to a maximum of four) and the combinations of primary antibodies that can be used together. If two primary antibodies are both raised in the same species e.g., mouse, then cross-reactivity of the secondary antibody-fluorophores prevents specific double-labelling. Antibody elution allows for more than four primary antibodies to be applied to a single specimen, without the issue of cross-reactivity between layers, resulting in a much more specific chemical code for an individual cell in a single specimen. This has been applied to study multiple markers in tumour but has not been widely used in neural tissue (Gerdes et al., 2013; Gendusa et al., 2014).

A recent study in our laboratory has modified these techniques to identify the detailed immunohistochemical codes of myenteric neurons in the human colon using the antibody elution technique detailed in section 2.4 of Chapter 2 (Unpublished data). In the future, this technique will provide a powerful tool for researchers to define individual cells based on only their immunohistochemistry. Using HuC/D-immunoreactive cells provides a useful denominator for the total number of myenteric neurons and also a marker that can be used as a reference point when combined with the Biotin-Streptavidin secondary antibody not removed by the 2-ME/SDS elution buffer. A reference point is essential when working in multiple layers so that the same structures can be re-identified. HuC/D is also useful because it labels neuronal soma and not the cell processes.

My study utilised only 5 markers (HuC/D, TH, Enk, ChAT and NOS) from 2 layers, but this still generated a wealth of information. Sequential layers of immunohistochemistry with additional markers have the potential to expand on our knowledge of the ENS even more. Furthermore,

identifying a high density of varicosities around an individual cell type can be performed for any neuronal cell type with visible varicosities, for instance cholinergic varicosities labelled with VAChT.

Another advantage of the multiple layer immunohistochemistry technique used in my study is that ChAT and NOS immunoreactivity was only identified in the second layer of immunohistochemistry, therefore effectively blinding the observer when looking at varicosities in apposition to undefined HuC/D cells in the first layer. However, the technique has limitations. It is useful for examining the presence of multiple antigens in large structures such as nerve cell bodies, but it is much more difficult to identify small structures such as individual varicosities in different layers.

### 7.2.1 Rationale for Confocal Microscopy

Light microscopy, confocal microscopy and electron microscopy have all been used to image the enteric nervous system previously and each have their own merits and disadvantages. Confocal microscopes provide a high-resolution image of a single focal plane and reject light that is out of focus. This results in less blurring in images than those seen with light microscopy, and confocal microscopy enables a plane in the middle of a thick preparation to be seen without interference from the intervening tissue. Furthermore, the in-focus plane of interest can be moved up or down in the "Z-axis," where the X-axis represents width, the Y-axis represents height, and the Z-axis represents depth in a 3D structure. It is then possible to create "Z-stack" of consecutive images, which provides a 3D representation of the object imaged. Appropriate confocal fluorescence filters then enable the visualisation of immunohistochemically stained structures (Elliott, 2020).

Electron microscopy (EM) provides very fine detail of cellular structures and is considered the gold standard to define the presence of synaptic specialisations on cell membranes. However, EM allows only a small number of cells to be observed in a single 2-diminsional image, so quantifying a larger number of close appositions between nerve terminals and neurons is time consuming (Mann et al., 1997; Neal and Bornstein, 2007). Furthermore, EM does not provide any 3D information. Confocal microscopy takes less time, and in the present study captured an image of an entire ganglion in approximately 15 to 25 minutes. Additionally, confocal provided the Z-stack of images and allowed the 3D architecture of the tissue preparation to be appreciated. As such, this represents an advance on conventional brightfield or fluorescence microscopy, and also enables quantitative analysis of many more close appositions than EM.

Several studies have validated the use of confocal microscopy in demonstrating appositions

between varicosities and neurons in the ENS. Research by Mann et al. used light, confocal and electron microscopy to observe close contacts between nerve terminals and neurons (Mann et al., 1997). Confocal observed many more close contacts than light microscopy. Numerous direct appositions between varicosities and neurons seen on confocal microscopy corresponded to the presence of synaptic connections confirmed on EM. This suggests that close appositions determined by confocal may be indicative of synapses.

Another study, performed by Li and Furness, aimed to characterise the appositions between intrinsic primary afferent neurons (IPANs) with descending interneurons (ChAT+/NOS+) and inhibitory motor neurons (ChAT-/NOS+) and used both confocal and EM (Li and Furness, 2000). The EM studies observed the IPAN varicosities in proximity to nerve cell bodies: varicosities within 300nm (the commonly quoted resolution of confocal) made synapses or close contacts in 84% of cases, whereas in the other 16% the varicosities were separate from the neurons with an intervening glial process. This is important because thin glial processes would be expected to prevent transmission from a closely apposed varicosity, but this only occurs in a minority of cases. Overall, this suggests that varicosities that appear to directly contact neurons on images acquired by confocal microscopy (i.e. separated by less than 300nm) make synapses or direct close contacts determined ultrastructurally by EM in most cases. Therefore, although EM remains the gold-standard for defining close contacts and synapses, appositions between varicosities and neurons seen on confocal microscopy are also likely to represent close contacts and synapses, although the specific ultrastructural features needed to define them cannot be visualised on confocal.

### 7.2.2 Rationale for 3D Reconstruction

Previous studies using light and electron microscopy have been able to view only one plane at a time, demonstrating appositions to cells in 2 dimensions. However, varicosities may make contact at any point on the 3D surface of a cell and therefore can be misleading in a single plane of view. 3D reconstruction of the Z-stack images produced by the confocal microscope enables 3D rendering, which better reveals varicosities apposing cell surfaces. In this way a more accurate estimation of varicosity connectivity can be attained.

An example of 3D reconstruction being used for neural connectivity is provided by Fogarty et al., who described a method using Imaris software to map specific synaptic inputs to a single neuron, in combination with immunohistochemical staining and confocal microscopy (Fogarty et al., 2013).

They identified a Neurobiotin filled hypoglossal motor neuron from a mouse and rendered its surface using Imaris. With immunohistochemical markers, the presynaptic and postsynaptic terminals were reconstructed as “spots” in the same way as varicosities were reconstructed in spots in my study. In their analysis, they examined only a single cell and colocalised the pre- and postsynaptic terminals to determine the number of synaptic connections.

More recently, 3D reconstruction of confocal images has been applied to the human colon. Yuan et al. used a modified tissue clearing technique and human peripheral ChAT antibody staining to examine four preparations of human colon (Yuan et al., 2020). 3D reconstruction and analysis demonstrated a higher density of cholinergic fibres in the circular compared to longitudinal muscle. Individual cholinergic nerve cell bodies and fibres were rendered and their cell processes followed, showing the 3D architecture of cholinergic neurons in the colon wall.

In my study, cells labelled with the pan-neuronal marker HuC/D were rendered because this marker labels all nerve cell bodies. Combined with the multiple layer immunohistochemistry technique using antibody elution, these HuC/D neurons can be subsequently identified by their chemical coding. Furthermore, the Imaris program can determine the distance between rendered objects in an automated fashion, reducing observer bias.

## 7.3 Alternate Attempted Methods for Quantifying Close Appositions

A major challenge in my research project was determining how to quantify the number of close appositions between varicosities and myenteric cell bodies. The method of varicosity density analysis detailed in Chapter 2, section 2.7 prevailed as the most pragmatic approach, however it is worth discussing some of the other means explored to test this relationship and the problems encountered.

### 7.3.1 Counting Varicosities within Set Distance Ranges

My first approach was a simple count of varicosities within a set distance from the cell surface using the “Find Spots Close to Surface” function on Imaris. In this method the number of varicosities within “shells” 1µm 3µm, 5µm and 10µm from the cell surface were collected for each cell. The “within 1µm” category also included varicosities within 1µm inside the cell surface (i.e. to -1µm). Cell volumes and surface areas were also calculated based on 3D reconstructions of cell bodies, and it was found that ChAT+/NOS- cells were significantly larger than ChAT-/NOS+ cells, based on

preliminary data (6 ganglia from 4 patients). Therefore, the volume of space for varicosities to occupy at set distances from the cell surface (e.g. the "shell" from 0 to 1µm) was significantly larger for ChAT+/NOS- cells compared to ChAT-/NOS+. There were inherently more varicosities in this space, even if they were distributed uniformly throughout the ganglion. Therefore, there was a need to incorporate a correction for cell size for all counts of varicosities.

### 7.3.2 Varicosities per unit Surface Area

As an extension of the above method, varicosity counts within 1µm were divided by the surface area of the reconstructed cell, giving a unit of varicosities/$\mu m^2$. Surface area seemed to be a more reasonable parameter than volume, because the relationship of interest is the apposition between the varicosity and the cell surface. Using the same 6 ganglia from 4 patients, there was a slight increase apparent for varicosities per unit surface area for ChAT+/NOS- cells versus to ChAT-/NOS+ cells using the student T test to compare. However, high variability in measurements of surface area, and interactions between neighbouring cells (including double counting of varicosities, see below) led me to settle on the density analysis given in Chapter 3.

### 7.3.3 Varicosities within 1µm as a Proportion within 10µm

Another way tested to correct for cell size was to calculate the varicosities within 1µm as a proportion of the population of varicosities within 10µm. The varicosities at 10µm were considered far enough away to not be specifically related to a cell. This method relied on quantifying close appositions as a proportion from a pool of varicosities thought to be uniformly distributed throughout the ganglion. In my work from 6 ganglia in 4 specimens, the range of close appositions by this method was 8-30% in TH varicosities, and 9-28% in Enk varicosities.

The three methods described immediately above relied on the "Find Spots close to Surfaces" function on Imaris. Within the frame of the confocal image, this function counted any varicosity that was within a set distance from the cell. However, this was performed for each cell exclusive of other cells, therefore a varicosity that was within the set distances of two cells (e.g. 3µm from cell A and 5µm from cell B where cell A and B are 8µm apart) would be counted twice; once for each cell. At the close distances of interest (e.g. 1µm) there would be fewer varicosities that would be double-counted compared with greater set distances, however there were many cells that were adjacent or touching, meaning a proportion of varicosities would inevitably be double counted. These close appositions are the most important because they are most likely to have the most post-synaptic

effect, therefore double counting could skew the data.

### 7.3.4 The Concept of using Density

An alternative method to quantify close appositions was to determine the absolute density of varicosities. A density measurement is beneficial because it takes into account the size of the cell that the varicosities are associated with. The difficulty in obtaining the density was in calculating the volume of the space enclosing the varicosities within a particular distance from the cell, which are referred to as concentric shells (see Figure 2-1 in Chapter 2, demonstrating a shell at 1µm from a cell).

An attempt was made to approximate cells as ellipsoids, based on data from Imaris (each cell had an ellipsoid length, width and depth) and using the following formula for ellipsoid volume.

$$V = \frac{4}{3}\pi abc$$

Then, the ellipsoid volume was expanded by adding the set distance to each of the dimensions. After subtracting the volume of the original ellipsoid, this approximated the volume of concentric shells. However, it was found that this method oversimplified the complexity and variety of nerve cell shapes and led to large errors.

The method detailed in "Varicosity Density Analysis," Chapter 2 section 2.7, allowed accurate volumes of the concentric shells to be calculated. This required exporting data from Imaris of the 3D shape of each reconstructed cell surface. The surface is encoded as small triangles recorded by triplets of 3D coordinates. The positions of varicosities, represented as single points, were similarly encoded. Using this density analysis method, the density of varicosities in concentric 1µm thick shells was calculated out to 10µm. This resulted in a graph illustrating the relationship between distance from the cell and density of a varicosity type. A further benefit of using density measurements was that varicosities were associated with a single cell only, and this prevented double counting of varicosities. To ensure this benefit remained, cell surfaces that were excluded because they were incomplete, unable to be separated from neighbouring cells or where the 3D rendered surface did not represent the true cell shape, had their varicosities also excluded.

Initially, it was thought a decay function over distance could be fitted to this graph and used to compare between cell types. If an individual cell was surrounded by varicosities with no other

nearby cells, then the density of varicosities (of any type) was highest in the closest shells and declined as distance from the surface increased. However, many cells are not isolated in space, therefore in some instances the density of varicosities in more distant shells (e.g. shell from 5µm to 6µm) may be higher than very close to the cell – an effect of close packing within the shape of the ganglion. This was particularly marked when a tract of axons ran through a ganglion and was interpreted by Imaris as a dense cloud of varicosities. Because of this effect, the decay function did not accurately reflect the relationship between varicosities and enteric neurons, and it would not be reasonable to compare the decay function between cell types. Therefore, the decay function was not used to analyse varicosity densities.

My final decision was to use varicosities that were within 1µm from the cell surface, because these closest varicosities were most likely to be an indicator of preferential targeting and are likely to have the greatest physiological effect on cells.

### 7.3.5 Attempts at Randomisation of Varicosities

In my analysis several attempts were made to generate a random distribution of varicosities throughout myenteric ganglia to compare against actual distributions of varicosities. First, flipping the Enkephalin-immunoreactive varicosity Z-stack on all 3 axes (x, y, z) was attempted, so the varicosities were no longer associated with cells. This method has been used in 2-dimensional data in the Neurogastroenterology laboratory previously. However, many varicosities ended up outside the boundaries of the ganglion (i.e. varicosities appeared in the inter-ganglionic space). Also, the spaces previously occupied by cells were devoid of varicosities, and this was not a workable way to generate a random distribution.

A more complex approach was then attempted. Using the existing pattern of varicosities (both Enk and TH), the shape of the ganglion was established, and a “bounding box” was created that represented the space where ganglionic varicosities could be located. Rendered cells could occupy space in this bounding box. By random generation of coordinates, randomised spots were inserted only within the bounding box of the ganglion. This was continued until there was an equivalent number of varicosities to the actual number of TH or Enk varicosities in the ganglion. This produced a randomised collection of varicosities, adjacent to true cells within a ganglion shaped bounding box. From here the same method of density analysis described above could be used to calculate the density of randomised varicosities close to cells, which could be compared to the true density of TH

or Enk in the equivalent range. Unfortunately, it was then discovered that altering the parameters for random sampling of varicosities in relation to the border of the ganglion bounding box substantially impacted on the distribution, and thus density, of the randomised varicosities. This meant that the randomised varicosity density model, was strongly influenced by our selection of arbitrary parameters for random sampling. Thus, it introduced substantial bias that affected any comparison made with true varicosities.

Overall, a randomised varicosity model was abandoned, and it was decided the most reliable method was to simply compare varicosity densities between the cell types (ChAT+/NOS-; ChAT-/NOS+; ChAT+/NOS+) using the shell method described in Chapter 2, section 2.7.

## 7.4 Significant Difficulties Encountered in This Study

### 7.4.1 Immunohistochemistry Difficulties

In my study, I routinely encountered significant difficulties in obtaining high quality immunohistochemical staining. Initially, the antibodies for HuC/D were applied in the first layer, and antibodies for ChAT, NOS and either of the varicosity staining antibodies TH or Enk applied in the second layer. It was intended that Enk and TH be analysed in separate pieces of tissue. Unfortunately, staining of varicosities was uneven in the majority of tissue specimens. A third layer of staining was attempted with TH, NPY and SOM (somatostatin) in one arm, and Enk, VIP and VAChT in another. The aim of that additional study would have been to colocalise TH and Enk with other neurotransmitters. This has not been reported in human tissue previously. Once again, the staining was highly variable between ganglia, and mostly poor. We identified that the antibodies used to observe varicosities (i.e. TH and Enk) were best applied in the first layer of staining, before elution which slightly increased background autofluorescence. Significant amounts of debris of an unknown source accumulated on the surface of some preparations during the elution process, adding to poor visualisation of structures in the ENS. For these reasons, the first set of 8 tissue samples was abandoned 4 months into the study and the experiments were restarted with a different protocol.

Changes were made to the sequence of antibodies applied to the tissue. Antibodies for varicosities Enk and TH were used in the first layer, in addition to HuC/D. This had several advantages. First, it removed any possibility of bias in deciding which cells were surrounding by baskets, as the only cell body marker was HuC/D at the time of identification. The best staining for Enk had been with rabbit-

raised antibodies, and in sheep-raised antibodies for TH. Neither of these cross-reacted with the HuC/D antibody raised in mouse. However, due to a broken laser (CY3) on the confocal microscope (see Appendix A) secondary antibodies using the CY3 fluorophore were avoided in the first layer until the laser was repaired (during the Coronavirus Disease pandemic).

There were also some changes made to detailed techniques for immunohistochemistry. Due to the larger size of the colonic tissue preparation the antibody solution volume was doubled from 200µL to 400µL to ensure that the tissue was thoroughly immersed and not folded upon itself. Meticulous attention was given to rinses with 1% PBS between layers of antibodies. This evolved into five episodes of rinsing with 1% PBS for 5 minutes each (from a previous 3x 5 minute routine). Additionally, specimens were rinsed in 1% PBS overnight after being removed from glycerol, and before being put into PBS/0.5% Triton™ X-100, because of concerns that this combination led to precipitation of debris. Filtered glycerol (50%, 70% and 100%) used for mounting was changed frequently because dust particles accumulated quickly in this solution.

These changes significantly improved the consistency and quality of immunohistochemistry, notably the TH varicosity labelling. Using this protocol, only small amounts of debris were present on the surface of subsequent preparations and these did not interfere with analysis.

### 7.4.2 3D Reconstruction Difficulties

Reconstructing the HuC/D-labelled myenteric neuron cell bodies was challenging for a number of reasons. The intensity threshold was determined and set to best match the immunohistochemically defined cell bodies, however the background noise in some regions reached a similar intensity. Many artefactual structures could be rendered, in particular non-cellular filaments. In addition, some varicose axons were labelled with HuC/D antisera, which did not correspond to TH+ or Enk+ varicosities. HuC/D labelled axons were more intensely stained than the cell bodies. The “cutting” function in Imaris enabled these to be deleted manually, though this process was time-consuming, taking up to 3 hours for a single ganglion. In preparations where the background noise was high, large numbers of artefactual structures had to be removed in this way.

Cells that were very close together were not easily distinguished by Imaris as separate structures. In these cases, they could be cut apart to be recognised as two discrete cells. In cases where there were only small points of contact between cell bodies the resulting cut surface was very small allowing the software to retain an accurate shape of each cell. However, where two cells were

contacting with a broad face (e.g. “sandwiched” on top of each other) cutting did not produce representative cell surfaces, so these cells had to be excluded from analysis.

The initial intention was to keep the confocal microscope and Imaris parameters identical for all specimens imaged and reconstructed. This was possible with the confocal settings but not for Imaris due to differential staining of human bowel tissue probably caused by variations in the thickness of tissue, the quality of dissection, or inherent properties of the specimen itself. As an example, setting the intensity threshold correctly in one specimen and then applying the same threshold to the another would produce cell surfaces too small or with holes in place of the nucleus – essentially not representative reconstructions of the cell size, volume and shape. For this reason, some settings were optimised on a preparation-by-preparation basis. However, this was done before any measurements were made, so it is unlikely to have introduced any systematic bias.

## 7.5 General Limitations of my Study Protocol

Although the aims of this study were achieved, in addition to the limitations already discussed in Chapters 3-6, there are some additional limitations that need to be addressed.

3D reconstruction has some caveats to bear in mind. The intensity thresholding of rendering HuC/D-labelled cell bodies is observer dependent, and thresholding too high or too low could result in undersized or oversized cells respectively, or otherwise incorporating non-cellular material (e.g. background autofluorescence). The same is true of varicosities, where the intensity threshold would determine the number of “spots” generated as rendered varicosities.

The main issue arose with the reconstruction of the cell surface. Accurate reconstruction was critical because this determined the catchment for varicosities within the -1µm to 1µm range. To limit observer error, the intensity threshold was set within each subject so that the edges of the rendered cell matched, as closely as possible, the edges of the immunohistochemically defined cell.

Unfortunately, there was no negative control distribution of varicosities (either true or randomly generated) to compare against noradrenergic varicosity density distribution. Though the randomised varicosity model had promise, at this stage it would still be unable to reliably indicate a distribution with no association between varicosities and cells bodies. Instead, Enkephalin varicosities, which are known to form baskets around some cholinergic cells, were used as a positive control. Chapter 5 presented results demonstrating that Enk varicosities form baskets around

cholinergic neurons. This correlated with the results of Enk varicosities having a quantifiably greater density around cholinergic neurons presented in Chapter 4, which helped to validate the novel method of varicosity density analysis.

## 7.6 Future Directions for these Non-Clinical, Laboratory Based Studies

The findings of this study have increased the current knowledge regarding connectivity of noradrenergic sympathetic axons to the myenteric plexus. However, there remain many questions and avenues for further research to gain a more comprehensive understanding of how the sympathetic nervous system modulates colonic motility and other functions.

### 7.6.1 Further Determination of the Sympathetic Modulation of Colonic Motility

#### *7.6.1.1 Anatomical and morphological studies*

As discussed in Chapter 4, it is now known that noradrenergic nerve terminals preferentially target cholinergic neurons, but whether all cholinergic cells receive equal innervation or only a subset of cell types remains to be determined. Furthermore, the extent to which anatomical proximity predicts functional effects remains to be determined.

A further study to investigate this could use the novel protocol for measuring varicosity density, focussing on defining cholinergic neurons in the myenteric plexus. Subsequent layers of immunohistochemistry would aim to discriminate between different types of cholinergic cells, i.e. excitatory motor neurons to longitudinal and circular muscle, ascending interneurons, some descending interneurons, and intrinsic primary afferent neurons. Although neurochemical coding of myenteric cells in humans is not as complete as it is in the guinea-pig, previous human studies have demonstrated that Tachykinin, Enkephalin, Substance P and Calbindin are markers for some populations of excitatory motor neurons and ascending interneurons, therefore these would be reasonable markers to begin with (Wattchow et al., 1997; Humenick et al., 2020). When cell types have been determined by the combinations of these markers, varicosity density could be compared between classes to find if one or several functional cell types is preferentially targeted. A larger sample size of cholinergic neurons from a greater number of subjects would be needed to make such a study robust, because there are likely to be multiple functional classes intermingled in the ganglia.

In addition to neurochemical coding, retrograde and anterograde labelling is able to highlight some

individual cell types in the myenteric plexus. Retrograde labelling techniques have previously identified motor neurons to the muscular layers and interneurons (Wattchow et al., 1995; Porter et al., 1997). Combining retrograde labelling with noradrenergic varicosity density analysis, it could be determined if there is preferential targeting of these specific cell types.

Anterograde labelling of extrinsic nerves with Biotinamide has recently demonstrated promise in human colonic tissue (Unpublished data). This technique is only possible with very careful microdissection of colonic nerves in the short segments of mesentery attached to colonic specimens. After labelling, the branching pattern of fibres coming from colonic nerves can be seen, and a significant proportion of these are thought to be sympathetic postganglionic fibres (Tassicker et al., 1999). As a further study, anterograde labelling could also determine which myenteric cell types are preferentially targeted by the noradrenergic fibres comprised within the labelled extrinsic nerve fibres. Additionally, this technique also causes retrograde filling of fibres of viscerofugal neurons, which would allow examination of the morphology and projections of this cell type in humans.

Appreciating any variation in the sympathetic input between colonic regions (ascending, transverse, descending, sigmoid colon) would be useful in understanding the functional differences between regions. A recent study in mice suggested that extrinsic sympathetic innervation regulates the proximal colon differently compared to the distal colon, specifically promoting mixing of faecal content proximally and suppression of propulsion distally (Smith-Edwards et al., 2020). Further studies could be performed to compare the noradrenergic varicosity density between regions of colon by the novel method developed in this thesis. This would require a greater sample size (n = 10) of tissue samples from each regionally distinct section of the human colon. The small sample size in my study (2 or less tissue samples from each region) was insufficient for any meaningful analysis.

#### *7.6.1.2 Functional studies*

The above proposed studies examine noradrenergic inputs to myenteric cells from an anatomical point of view. Functional studies on *in vitro* human colonic tissue can also progress our knowledge of the pathways of sympathetic inhibition of colonic motility. Calcium imaging offers the ability to view activated neurons and has been utilised in previous studies of enteric sensory neurons in the ENS in mice (Hibberd et al., 2018).

Human colonic tissue would be retrieved and kept immersed in oxygenated Krebs solution. The preparation would then be dissected to a wholemount of myenteric plexus and longitudinal muscle, along with an attached and isolated colonic extrinsic nerve. The tissue would be incubated with a fluorescent calcium indicator (e.g. Fluo-4). Calcium imaging of myenteric ganglia would be performed, first observing the baseline activity of myenteric neurons and then the activity induced by pulses of transmural electrical stimulation (to activate excitatory enteric neural inputs). Next, the dissected extrinsic colonic nerve would be repetitively stimulated (stimulating the significant proportion of fibres that are noradrenergic) and the response to further pulses of transmural electrical stimulation of the colonic tissue would be recorded. Preliminary results from anterograde labelling studies in our laboratory suggest that there are few parasympathetic fibres in the colonic nerves, meaning that mostly sympathetic fibres would be activated (Unpublished data). Neurons that are preferentially targeted by noradrenergic inputs should be inhibited by the extrinsic colonic nerve stimulation and thus demonstrate a lack of activation to the transmural stimulation. Adrenergic receptor blockers would be used to confirm that the effects were mediated by sympathetic pathways. After calcium imaging, these preparations would undergo fixation and multiple layer immunohistochemistry to define the cell types by their neurochemical codes. Cell types could then be compared based on their relative activation and inactivation by transmural stimulation and extrinsic nerve stimulation respectively. The objective of this study would be to determine the neurochemical codes of those myenteric neurons that are functionally inhibited by the sympathetic postganglionic fibres in extrinsic colonic nerves.

The overall purpose of all the above proposed anatomical and functional studies is to better define the specific targeted pathway of noradrenergic inhibition that has been identified in this thesis. This knowledge would improve the understanding of the gastrointestinal physiology and possibly reveal new targets for therapy for functional gastrointestinal disorders, such as slow transit constipation or postoperative ileus.

### 7.6.2 Further Defining Intrinsic Catecholaminergic (Dopaminergic) Cells

Intrinsic catecholaminergic cell bodies labelled by TH make up a small subset of enteric neurons in the myenteric plexus. They have been suggested to lack dopamine beta hydroxylase (DBH) immunoreactivity and therefore to be dopaminergic in a single human study, and may have a role in modulating colonic motility (Anlauf et al., 2003). Interestingly this same study by Anlauf showed no overlap between TH and VAChT (vesicular acetylcholine transporter) immunoreactivity in nerve

cell bodies, whereas my present study showed that almost all were immunoreactive for ChAT. These results from Chapter 6 have revealed that these cells are also likely to be cholinergic.

The aim of a subsequent study could be to further define this small population of intrinsic catecholaminergic cells. Once again, this could be performed by multiple labelling immunohistochemistry. Antisera to TH and dopamine would demonstrate dopaminergic fibres, while visualising DBH-immunoreactive fibres would help to exclude noradrenergic fibres that also label for TH. Subsequent layers of immunohistochemistry would determine the specific neurochemical code of these intrinsic catecholaminergic cells. Staining with the marker for Neurofilament would additionally provide details regarding the morphology of these cells, which could not be attained in my study.

The distribution of TH-immunoreactive varicosities without DBH immunoreactivity could be used to identify potential targets in the gut wall. It would be interesting to elucidate whether there is truly a gradient in the distribution of this cell type between colonic regions (i.e. ascending, transverse, descending, sigmoid) as suggested in Chapter 6 (more TH positive cell bodies in the proximal colon compared to distally).

There is already interest in the role of these dopaminergic cells in the pathophysiology of constipation experienced in patients with Parkinson's disease, and further defining this population of cells may reveal more about their functional role.

### 7.6.3 Implications of the Novel Varicosity Density Analysis Method

My research has demonstrated that evaluating varicosity density can detect preferential innervation of one cell type over another. The method presented in this thesis could potentially be used for any immunohistochemical marker that is expressed in varicosities, and therefore could determine a significant proportion of the connectivity within the ENS. As an example, VAChT is present in varicosities that release acetylcholine, so the same method could be employed to identify neurons receiving cholinergic inputs.

Technically, the novel varicosity density method used to determine preferential targeting in Chapter 4 requires good immunohistochemistry, antibody elution, confocal microscopy, 3D reconstruction software and software to analyse the relative varicosity densities. Knowledge of the chemical coding of myenteric neurons is also required in order to tell which functional cell type has preferential

innervation over other cell types. Recent work by my colleagues at Flinders University has comprehensively defined the most frequent neurochemical codes for human colonic myenteric neurons using multiple layer immunohistochemistry with 13 neuronal markers (Unpublished data). A combination of this varicosity density method and the “key” for neurochemical coding allows preferential targeting to be determined for any marker of varicose axons, and thus a great deal of information on the connectivity within the ENS to be discerned.

### 7.6.4 Investigation of Functional Gastrointestinal Disorders

The pathophysiology underlying functional gastrointestinal disorders is poorly understood and a better appreciation of normal colonic physiology in relation to motility is required before the pathology can be properly elucidated. Therefore, this study sought to define the sympathetic inputs to the colonic myenteric plexus in healthy tissue, which are hypothesised to be implicated in slow transit constipation and postoperative ileus. The methods presented here are research tools only at this stage.

In a research setting, the same protocol could be followed in colonic specimens from patients suffering from slow transit constipation, to determine if there is any relative difference in the degree of sympathetic input to the myenteric plexus. For example, a higher relative density of noradrenergic innervation to the myenteric plexus could functionally result in a greater level of inhibition to colonic motility. However, this protocol requires full thickness colonic tissue, which can only be obtained from colonic resection, an invasive procedure with operative risks. The most important part of this research is establishing the normal physiology of sympathetic interaction with the myenteric plexus, which can then form the basis for further investigation of functional gastrointestinal disorders.

# Conclusion

My analysis of varicosity density close to enteric cells has shown that noradrenergic inputs preferentially target cholinergic neurons in the human colonic myenteric plexus. This finding suggests “hard-wired” innervation of a subset of cholinergic cells. Noradrenaline release from postganglionic sympathetic varicosities is most likely to act on the alpha-2a adrenergic receptors on the presynaptic membrane of cholinergic nerve terminals, inhibiting release of acetylcholine and thereby preventing activation of the next-in-line cholinergic cell body. This neurotransmission may be indicative of synaptic neurotransmission by sympathetic inputs onto enteric neurons, however the likelihood of volume transmission cannot be excluded. The connectivity demonstrated here may represent an important pathway in the modulation of colonic motility by the sympathetic nervous system, specifically indirect inhibition of non-sphincteric smooth muscle via the myenteric plexus.

A novel method of determining preferential targeting of enteric cells by varicose nerve terminals has been developed, utilising confocal microscopy and 3D reconstruction to quantitatively analyse varicosity density close to cell bodies. This method was validated by comparing the results to a previously described method in which visually observed baskets of varicosities surrounding neurons represent targeted innervation. Enkephalin varicosities, which are known to form baskets surrounding cholinergic neurons, had the same relationship demonstrated with the novel method described in this thesis. In the future, this technique may be used to assist in mapping the connectivity of neural pathways in the enteric nervous system.

Lastly, a small population of intrinsic catecholaminergic neurons, likely to be dopaminergic, were found to comprise approximately 1% of the myenteric neurons in the human colon. These few tyrosine hydroxylase-immunoreactive cells were classified as cholinergic.

# References


Agnati, L.F., Guidolin, D., Guescini, M., Genedani, S., and Fuxe, K. (2010). Understanding wiring and volume transmission. *Brain Res Rev* 64(1)**,** 137-159. doi: 10.1016/j.brainresrev.2010.03.003.

Aguilar, M.J., Estan, L., Martinez-Mir, I., Martinez-Abad, M., Rubio, E., and Morales-Olivas, F.J. (2005). Effects of dopamine in isolated rat colon strips. *Can J Physiol Pharmacol* 83(6)**,** 447-452. doi: 10.1139/y05-031.

Allescher, H.D., Storr, M., Brechmann, C., Hahn, A., and Schusdziarra, V. (2000). Modulatory effect of endogenous and exogenous opioids on the excitatory reflex pathway of the rat ileum. *Neuropeptides* 34(1)**,** 62-68. doi: 10.1054/npep.1999.0789.

Anlauf, M., Schafer, M.K., Eiden, L., and Weihe, E. (2003). Chemical coding of the human gastrointestinal nervous system: cholinergic, VIPergic, and catecholaminergic phenotypes. *J Comp Neurol* 459(1)**,** 90-111. doi: 10.1002/cne.10599.

Auteri, M., Zizzo, M.G., Amato, A., and Serio, R. (2016). Dopamine induces inhibitory effects on the circular muscle contractility of mouse distal colon via D1- and D2-like receptors. *J Physiol Biochem* 73(3)**,** 395-404. doi: 10.1007/s13105-017-0566-0.

Barrett, K.E., Barman, S.M., Boitano, S., and Brooks, H.L. (2016). *Ganong's Review of Medical Physiology.* McGraw-Hill Education.

Bass, L.M., and Wershil, B.K. (2016). "Anatomy, Histology, Embryology, and Developmental Anomalies of the Small and Large Intestine," in *Sleisenger and Fordtran's Gastrointestinal and Liver Disease*. 10th edn. ed (1600 John F. Kennedy Blvd. Ste 1800, Philadelphia, PA: Saunders Elsevier), 1551-1579.

Bauer, A.J., and Boeckxstaens, G.E. (2004). Mechanisms of postoperative ileus. *Neurogastroenterology and Motility* 16**,** 54-60. doi: DOI 10.1111/j.1743-3150.2004.00558.x.

Bayliss, W.M., and Starling, E.H. (1899). The movements and innervation of the small intestine. *J Physiol* 24(2)**,** 99-143. doi: 10.1113/jphysiol.1899.sp000752.

Beani, L., Bianchi, C., and Crema, A. (1969). The effect of catecholamines and sympathetic stimulation on the release of acetylcholine from the guinea-pig colon. *Br J Pharmacol* 36(1)**,** 1-17. doi: 10.1111/j.1476-5381.1969.tb08298.x.

Beck, M., Schlabrakowski, A., Schrodl, F., Neuhuber, W., and Brehmer, A. (2009). ChAT and NOS in human myenteric neurons: co-existence and co-absence. *Cell Tissue Res* 338(1)**,** 37-51. doi: 10.1007/s00441-009-0852-4.

Behm, B., and Stollman, N. (2003). Postoperative ileus: etiologies and interventions. *Clin*

*Gastroenterol Hepatol* 1(2)**,** 71-80. doi: 10.1053/cgh.2003.50012.

Bennett, E.J., Evans, P., Scott, A.M., Badcock, C.A., Shuter, B., Hoschl, R., et al. (2000). Psychological and sex features of delayed gut transit in functional gastrointestinal disorders. *Gut* 46(1)**,** 83-87. doi: 10.1136/gut.46.1.83.

Bernard, C.E., Gibbons, S.J., Gomez-Pinilla, P.J., Lurken, M.S., Schmalz, P.F., Roeder, J.L., et al. (2009). Effect of age on the enteric nervous system of the human colon. *Neurogastroenterol Motil* 21(7)**,** 746-e746. doi: 10.1111/j.1365-2982.2008.01245.x.

Brehmer, A. (2006). Structure of enteric neurons. *Adv Anat Embryol Cell Biol* 186**,** 1-91.

Brehmer, A., Lindig, T.M., Schrodl, F., Neuhuber, W., Ditterich, D., Rexer, M., et al. (2005). Morphology of enkephalin-immunoreactive myenteric neurons in the human gut. *Histochem Cell Biol* 123(2)**,** 131-138. doi: 10.1007/s00418-005-0757-6.

Brookes, S.J. (2001). Classes of enteric nerve cells in the guinea-pig small intestine. *Anat Rec* 262(1)**,** 58-70. doi: 10.1002/1097-0185(20010101)262:1<58::AID-AR1011>3.0.CO;2-V.

Brookes, S.J., Humenick, A., Chen, B.N., Dinning, P.G., Costa, M., and Wattchow, D. (2020). Multiplexed Immunohistochemistry to Identify Systematically Classes of Human Colonic Myenteric Neurons. *The FASEB Journal* 34(S1).

Bürkner, P.-C. (2017). brms: An R Package for Bayesian Multilevel Models Using Stan. *2017* 80(1)**,** 28. doi: 10.18637/jss.v080.i01.

Chung, D.H. (2017). "Pediatric Surgery," in *Sabiston Textbook of Surgery,* eds. C.M. Townsend, R.D. Beauchamp, M. Evers & K.L. Mattox. (1600 John F. Kennedy Blvd, Ste 1800, Philadelphia, PA: Elsevier), 1858-1899.

Corsetti, M., Costa, M., Bassotti, G., Bharucha, A.E., Borrelli, O., Dinning, P., et al. (2019). First translational consensus on terminology and definitions of colonic motility in animals and humans studied by manometric and other techniques. *Nat Rev Gastroenterol Hepatol* 16(9)**,** 559-579. doi: 10.1038/s41575-019-0167-1.

Costa, M., Brookes, S.J., and Hennig, G.W. (2000). Anatomy and physiology of the enteric nervous system. *Gut* 47 Suppl 4**,** iv15-19; discussion iv26. doi: 10.1136/gut.47.suppl_4.iv15.

Costa, M., and Furness, J.B. (1971). Storage, uptake and synthesis of catecholamines in the intrinsic adrenergic neurones in the proximal colon of the guinea-pig. *Z Zellforsch Mikrosk Anat* 120(3)**,** 364-385. doi: 10.1007/BF00324898.

Costa, M., and Furness, J.B. (1973). The simultaneous demonstration of adrenergic fibres and enteric ganglion cells. *Histochem J* 5(4)**,** 343-349. doi: 10.1007/BF01004802.

Costa, M., and Furness, J.B. (1976). The peristaltic reflex: an analysis of the nerve pathways and their pharmacology. *Naunyn Schmiedebergs Arch Pharmacol* 294(1)**,** 47-60. doi: 10.1007/BF00692784.

Costa, M., and Furness, J.B. (1984). Somatostatin is present in a subpopulation of noradrenergic nerve fibres supplying the intestine. *Neuroscience* 13(3)**,** 911-919. doi: 10.1016/0306-4522(84)90105-2.

Costa, M., and Gabella, G. (1971). Adrenergic innervation of the alimentary canal. *Z Zellforsch Mikrosk Anat* 122(3)**,** 357-377. doi: 10.1007/BF00935995.

Costanzo, L.S. (2018). "Autonomic Nervous System," in *Physiology*. 6 ed (Philadelphia, PA: Elsevier), 47-67.

De Ponti, F., Giaroni, C., Cosentino, M., Lecchini, S., and Frigo, G. (1996). Adrenergic mechanisms in the control of gastrointestinal motility: from basic science to clinical applications. *Pharmacol Ther* 69(1)**,** 59-78. doi: 10.1016/0163-7258(95)02031-4.

de Souza, R.R., Moratelli, H.B., Borges, N., and Liberti, E.A. (1993). Age-induced nerve cell loss in the myenteric plexus of the small intestine in man. *Gerontology* 39(4)**,** 183-188. doi: 10.1159/000213532.

De Winter, B.Y., Boeckxstaens, G.E., De Man, J.G., Moreels, T.G., Herman, A.G., and Pelckmans, P.A. (1997). Effect of adrenergic and nitrergic blockade on experimental ileus in rats. *Br J Pharmacol* 120(3)**,** 464-468. doi: 10.1038/sj.bjp.0700913.

Del Tacca, M., Soldani, G., Selli, M., and Crema, A. (1970). Action of catecholamines on release of acetylcholine from human taenia coli. *Eur J Pharmacol* 9(1)**,** 80-84. doi: 10.1016/0014-2999(70)90323-7.

Deloose, E., Janssen, P., Depoortere, I., and Tack, J. (2012). The migrating motor complex: control mechanisms and its role in health and disease. *Nat Rev Gastroenterol Hepatol* 9(5)**,** 271-285. doi: 10.1038/nrgastro.2012.57.

Dinning, P.G. (2018). A new understanding of the physiology and pathophysiology of colonic motility? *Neurogastroenterol Motil* 30(11)**,** e13395. doi: 10.1111/nmo.13395.

Dinning, P.G., Costa, M., and Brookes, S.J. (2016a). "Colonic Motor and Sensory Function and Dysfunction," in *Sleisenger and Fordtran's Gastrointestinal and Liver Disease*. 10th edn. ed (1600 John F. Kennedy Blvd. Ste 1800, Philadelphia, PA: Saunders Elsevier), 1696-1712.

Dinning, P.G., Sia, T.C., Kumar, R., Mohd Rosli, R., Kyloh, M., Wattchow, D.A., et al. (2016b). High-resolution colonic motility recordings in vivo compared with ex vivo recordings after colectomy, in patients with slow transit constipation. *Neurogastroenterol Motil* 28(12)**,** 1824-1835. doi: 10.1111/nmo.12884.

Dinning, P.G., Wiklendt, L., Maslen, L., Gibbins, I., Patton, V., Arkwright, J.W., et al. (2014a). Quantification of in vivo colonic motor patterns in healthy humans before and after a meal revealed by high-resolution fiber-optic manometry. *Neurogastroenterol Motil* 26(10)**,** 1443-1457. doi: 10.1111/nmo.12408.

Dinning, P.G., Wiklendt, L., Omari, T., Arkwright, J.W., Spencer, N.J., Brookes, S.J., et al. (2014b). Neural mechanisms of peristalsis in the isolated rabbit distal colon: a neuromechanical loop hypothesis. *Front Neurosci* 8**,** 75. doi: 10.3389/fnins.2014.00075.

Dogiel, A.S. (1899). Über den Bau der Ganglien in den Geflechten des Darmes und der Gallenblase des Menschen und der Säugetiere. *Arch Anat Physiol Leipzig Anat Abt Jg***,** 130-158.

Drew, G.M. (1978). Pharmacological characterization of the presynaptic alpha-adrenoceptors regulating cholinergic activity in the guinea-pig ileum. *Br J Pharmacol* 64(2)**,** 293-300. doi: 10.1111/j.1476-5381.1978.tb17303.x.

Drossman, D.A., and Hasler, W.L. (2016). Rome IV-Functional GI Disorders: Disorders of Gut-Brain Interaction. *Gastroenterology* 150(6)**,** 1257-1261. doi: 10.1053/j.gastro.2016.03.035.

Eaker, E.Y., Bixler, G.B., Dunn, A.J., Moreshead, W.V., and Mathias, J.R. (1988). Dopamine and norepinephrine in the gastrointestinal tract of mice and the effects of neurotoxins. *J Pharmacol Exp Ther* 244(2)**,** 438-442.

Eccles, J. (1976). From electrical to chemical transmission in the central nervous system. *Notes Rec R Soc Lond* 30(2)**,** 219-230. doi: 10.1098/rsnr.1976.0015.

Elliott, A.D. (2020). Confocal Microscopy: Principles and Modern Practices. *Curr Protoc Cytom* 92(1)**,** e68. doi: 10.1002/cpcy.68.

Evans, R.J., and Surprenant, A. (1992). Vasoconstriction of guinea-pig submucosal arterioles following sympathetic nerve stimulation is mediated by the release of ATP. *Br J Pharmacol* 106(2)**,** 242-249. doi: 10.1111/j.1476-5381.1992.tb14323.x.

Falck, B., Hillarp, N.A., Thieme, G., and Torp, A. (1982). Fluorescence of catechol amines and related compounds condensed with formaldehyde. *Brain Res Bull* 9(1-6)**,** xi-xv. doi: 10.1016/0361-9230(82)90113-7.

Falck, B., and Torp, A. (1962). New evidence for the localization of noradrenalin in the adrenergic nerve terminals. *Med Exp Int J Exp Med* 6**,** 169-172. doi: 10.1159/000135153.

Ferraz, A.A., Wanderley, G.J., Santos, M.A., Jr., Mathias, C.A., Araujo, J.G., Jr., and Ferraz, E.M. (2001). Effects of propranolol on human postoperative ileus. *Dig Surg* 18(4)**,** 305-310. doi: 10.1159/000050157.

Fogarty, M.J., Hammond, L.A., Kanjhan, R., Bellingham, M.C., and Noakes, P.G. (2013). A method for the three-dimensional reconstruction of Neurobiotin-filled neurons and the location of their

synaptic inputs. *Front Neural Circuits* 7**,** 153. doi: 10.3389/fncir.2013.00153.

Frankel, A., Gillespie, C., Lu, C.T., Hewett, P., and Wattchow, D. (2019). Subcutaneous neostigmine appears safe and effective for acute colonic pseudo-obstruction (Ogilvie's syndrome). *ANZ J Surg* 89(6)**,** 700-705. doi: 10.1111/ans.15265.

Frattini, J.C., and Nogueras, J.J. (2008). Slow transit constipation: a review of a colonic functional disorder. *Clin Colon Rectal Surg* 21(2)**,** 146-152. doi: 10.1055/s-2008-1075864.

Fukuda, H., Tsuchida, D., Koda, K., Miyazaki, M., Pappas, T.N., and Takahashi, T. (2007). Inhibition of sympathetic pathways restores postoperative ileus in the upper and lower gastrointestinal tract. *J Gastroenterol Hepatol* 22(8)**,** 1293-1299. doi: 10.1111/j.1440-1746.2007.04915.x.

Furness, J.B. (2000). Types of neurons in the enteric nervous system. *J Auton Nerv Syst* 81(1-3)**,** 87-96. doi: 10.1016/s0165-1838(00)00127-2.

Furness, J.B. (2006). *The Enteric Nervous System.* 350 Main Street, Malden, Massachusetts, USA: Blackwell Publishing, Inc.

Furness, J.B. (2012). The enteric nervous system and neurogastroenterology. *Nat Rev Gastroenterol Hepatol* 9(5)**,** 286-294. doi: 10.1038/nrgastro.2012.32.

Furness, J.B., and Costa, M. (1973). The ramifications of adrenergic nerve terminals in the rectum, anal sphincter and anal accessory muscles of the guinea-pig. *Z Anat Entwicklungsgesch* 140(1)**,** 109-128. doi: 10.1007/BF00520721.

Fuxe, K., Agnati, L.F., Marcoli, M., and Borroto-Escuela, D.O. (2015). Volume Transmission in Central Dopamine and Noradrenaline Neurons and Its Astroglial Targets. *Neurochem Res* 40(12)**,** 2600-2614. doi: 10.1007/s11064-015-1574-5.

Gendusa, R., Scalia, C.R., Buscone, S., and Cattoretti, G. (2014). Elution of High-affinity (>10-9 KD) Antibodies from Tissue Sections: Clues to the Molecular Mechanism and Use in Sequential Immunostaining. *J Histochem Cytochem* 62(7)**,** 519-531. doi: 10.1369/0022155414536732.

Gerdes, M.J., Sevinsky, C.J., Sood, A., Adak, S., Bello, M.O., Bordwell, A., et al. (2013). Highly multiplexed single-cell analysis of formalin-fixed, paraffin-embedded cancer tissue. *Proc Natl Acad Sci U S A* 110(29)**,** 11982-11987. doi: 10.1073/pnas.1300136110.

Gershon, M.D. (1998). *The Second Brain.* New York: Harper-Collins.

Gershon, M.D., and Sherman, D.L. (1982). Identification of and interactions between noradrenergic and serotonergic neurites in the myenteric plexus. *J Comp Neurol* 204(4)**,** 407-421. doi: 10.1002/cne.902040411.

Gershon, M.D., and Sherman, D.L. (1987). Noradrenergic innervation of serotoninergic neurons in

the myenteric plexus. *J Comp Neurol* 259(2)**,** 193-210. doi: 10.1002/cne.902590203.

Gibbins, I.L., Teo, E.H., Jobling, P., and Morris, J.L. (2003). Synaptic density, convergence, and dendritic complexity of prevertebral sympathetic neurons. *J Comp Neurol* 455(3)**,** 285-298. doi: 10.1002/cne.10404.

Gillespie, J.S., and Maxwell, J.D. (1971). Adrenergic innervation of sphincteric and nonsphincteric smooth muscle in the rat intestine. *J Histochem Cytochem* 19(11)**,** 676-681. doi: 10.1177/19.11.676.

Glynn, H., Moller, S.P., Wilding, H., Apputhurai, P., Moore, G., and Knowles, S.R. (2021). Prevalence and Impact of Post-traumatic Stress Disorder in Gastrointestinal Conditions: A Systematic Review. *Dig Dis Sci*. doi: 10.1007/s10620-020-06798-y.

Gomes, O.A., de Souza, R.R., and Liberti, E.A. (1997). A preliminary investigation of the effects of aging on the nerve cell number in the myenteric ganglia of the human colon. *Gerontology* 43(4)**,** 210-217. doi: 10.1159/000213852.

Gordon-Weeks, P.R. (1982). Noradrenergic and non-noradrenergic nerves containing small granular vesicles in Auerbach's plexus of the guinea-pig: evidence against the presence of noradrenergic synapses. *Neuroscience* 7(11)**,** 2925-2936. doi: 10.1016/0306-4522(82)90115-4.

Goyal, R.K., and Chaudhury, A. (2013). Structure activity relationship of synaptic and junctional neurotransmission. *Auton Neurosci* 176(1-2)**,** 11-31. doi: 10.1016/j.autneu.2013.02.012.

Goyal, R.K., and Rattan, S. (1978). Neurohumoral, hormonal, and drug receptors for the lower esophageal sphincter. *Gastroenterology* 74(3)**,** 598-619.

Gradus, J.L., Farkas, D.K., Svensson, E., Ehrenstein, V., Lash, T.L., and Toft Sorensen, H. (2017). Posttraumatic Stress Disorder and Gastrointestinal Disorders in the Danish Population. *Epidemiology* 28(3)**,** 354-360. doi: 10.1097/EDE.0000000000000622.

Graham, K.D., Lopez, S.H., Sengupta, R., Shenoy, A., Schneider, S., Wright, C.M., et al. (2020). Robust, 3-Dimensional Visualization of Human Colon Enteric Nervous System Without Tissue Sectioning. *Gastroenterology* 158(8)**,** 2221-2235 e2225. doi: 10.1053/j.gastro.2020.02.035.

Hall, J.E., and Hall, M.E. (2016a). "The Autonomic Nervous System and the Adrenal Medulla," in *Guyton and Hall Textbook of Medical Physiology,* ed. J.E. Hall. 13th edn. ed (1600 John F. Kennedy Blv. Ste 1800, Philadelphia, PA: Elsevier), 773-785.

Hall, J.E., and Hall, M.E. (2016b). "General Principles of Gastrointestinal Function - Motility, Nervous Control, and Blood Circulation," in *Guyton and Hall Textbook of Medical Physiology,* ed. J.E. Hall. 13th edn. ed (1600 John F. Kennedy Blvd. Ste 1800, Philadelphia, PA: Elsevier, Inc), ???

Hallerback, B., Ander, S., and Glise, H. (1987a). Effect of combined blockade of beta-adrenoceptors and acetylcholinesterase in the treatment of postoperative ileus after cholecystectomy. *Scand J*

*Gastroenterol* 22(4)**,** 420-424. doi: 10.3109/00365528708991484.

Hallerback, B., Carlsen, E., Carlsson, K., Enkvist, C., Glise, H., Haffner, J., et al. (1987b). Beta-adrenoceptor blockade in the treatment of postoperative adynamic ileus. *Scand J Gastroenterol* 22(2)**,** 149-155. doi: 10.3109/00365528708991872.

Hanman, A., Chen, J.H., Parsons, S.P., and Huizinga, J.D. (2019). Noradrenaline inhibits neurogenic propulsive motor patterns but not neurogenic segmenting haustral progression in the rabbit colon. *Neurogastroenterol Motil* 31(5)**,** e13567. doi: 10.1111/nmo.13567.

Harris, J.W., and Evers, B.M. (2017). "Small Intestine," in *Sabiston Textbook of Surgery,* eds. C.M. Townsend, R.D. Beauchamp, M. Evers & K.L. Mattox. 20th edn. ed (1600 John F. Kennedy Blvd, Ste 1800, Philadelphia, PA: Elsevier), 1237-1295.

Hayakawa, T., Kuwahara, S., Maeda, S., Tanaka, K., and Seki, M. (2008). Fine structural survey of tyrosine hydroxylase immunoreactive terminals in the myenteric ganglion of the rat duodenum. *J Chem Neuroanat* 36(3-4)**,** 191-196. doi: 10.1016/j.jchemneu.2008.04.005.

He, C.L., Burgart, L., Wang, L., Pemberton, J., Young-Fadok, T., Szurszewski, J., et al. (2000). Decreased interstitial cell of cajal volume in patients with slow-transit constipation. *Gastroenterology* 118(1)**,** 14-21. doi: 10.1016/s0016-5085(00)70409-4.

Heinicke, E.A., and Kiernan, J.A. (1990). An immunohistochemical study of the myenteric plexus of the colon in the rat and mouse. *J Anat* 170**,** 51-62.

Hibberd, T.J., Travis, L., Wiklendt, L., Costa, M., Brookes, S.J.H., Hu, H., et al. (2018). Synaptic activation of putative sensory neurons by hexamethonium-sensitive nerve pathways in mouse colon. *Am J Physiol Gastrointest Liver Physiol* 314(1)**,** G53-G64. doi: 10.1152/ajpgi.00234.2017.

Hibberd, T.J., Zagorodnyuk, V.P., Spencer, N.J., and Brookes, S.J. (2012). Identification and mechanosensitivity of viscerofugal neurons. *Neuroscience* 225**,** 118-129. doi: 10.1016/j.neuroscience.2012.08.040.

Hirst, G.D., and McKirdy, H.C. (1974). Presynaptic inhibition at mammalian peripheral synapse? *Nature* 250**,** 430-431.

Howard, E.R., and Garrett, J.R. (1973). The intrinsic myenteric innervation of the hind-gut and accessory muscles of defaecation in the cat. *Z Zellforsch Mikrosk Anat* 136(1)**,** 31-44. doi: 10.1007/BF00307678.

Hu, H.Z., and Spencer, N.J. (2018). "Enteric Nervous System Structure and Neurochemistry Related to Function and Neuropathology," in *Physiology of the Gastrointestinal Tract,* ed. H. Said. Elsevier), 337-360.

Hulten, L. (1969). Extrinsic nervous control of colonic motility and blood flow. An experimental study in the cat. *Acta Physiol Scand Suppl* 335**,** 1-116.

Humenick, A., Chen, B.N., Lauder, C.I.W., Wattchow, D.A., Zagorodnyuk, V.P., Dinning, P.G., et al. (2019). Characterization of projections of longitudinal muscle motor neurons in human colon. *Neurogastroenterol Motil* 31(10)**,** e13685. doi: 10.1111/nmo.13685.

Humenick, A., Chen, B.N., Wattchow, D.A., Zagorodnyuk, V.P., Dinning, P.G., Spencer, N.J., et al. (2020). Characterization of putative interneurons in the myenteric plexus of human colon. *Neurogastroenterol Motil***,** e13964. doi: 10.1111/nmo.13964.

Humenick, A., Chen, B.N., Wattchow, D.A., Zagorodnyuk, V.P., Dinning, P.G., Spencer, N.J., et al. (2021). Characterization of putative interneurons in the myenteric plexus of human colon. *Neurogastroenterol Motil* 33(1)**,** e13964. doi: 10.1111/nmo.13964.

Jacobowitz, D. (1965). Histochemical studies of the autonomic innervation of the gut. *J Pharmacol Exp Ther* 149(3)**,** 358-364.

Jansson, G., Lisander, B., and Martinson, J. (1969). Hypothalamic control of adrenergic outflow to the stomach in the cat. *Acta Physiol Scand* 75(1)**,** 176-186. doi: 10.1111/j.1748-1716.1969.tb04370.x.

Jansson, G., and Martinson, J. (1966). Studies on the Ganglionic Site of Action of Sympathetic Outflow to the Stomach. *Acta Physiologica Scandinavica* 68(2)**,** 184-192.

Kaestner, C.L., Smith, E.H., Peirce, S.G., and Hoover, D.B. (2019). Immunohistochemical analysis of the mouse celiac ganglion: An integrative relay station of the peripheral nervous system. *J Comp Neurol* 527(16)**,** 2742-2760. doi: 10.1002/cne.24705.

Kewenter, J. (1965). The vagal control of the jejunal and ileal motility and blood flow. *Acta Physiol Scand* 257**,** 1-68.

Knoll, J., and Vizi, E.S. (1970). Presynaptic inhibition of acetylcholine release by endogenous and exogenous noradrenaline at high rate of stimulation. *Br J Pharmacol* 40(3)**,** 554P-555P.

Kotecha, N. (1998). Modulation of submucosal arteriolar tone by neuropeptide Y Y2 receptors in the guinea-pig small intestine. *J Auton Nerv Syst* 70(3)**,** 157-163. doi: 10.1016/s0165-1838(98)00049-6.

Kram, B., Greenland, M., Grant, M., Campbell, M.E., Wells, C., and Sommer, C. (2018). Efficacy and Safety of Subcutaneous Neostigmine for Ileus, Acute Colonic Pseudo-obstruction, or Refractory Constipation. *Ann Pharmacother* 52(6)**,** 505-512. doi: 10.1177/1060028018754302.

Krokhina, E.M., and Chuvil'skaia, I.M. (1975). [The neuronal composition of the intramural nerve plexi of the gastrointestinal tract]. *Biull Eksp Biol Med* 79(3)**,** 110-113.

Kuntz, A. (1938). The structural organization of the celiac ganglia. *J. Comp. Neurol.* 69**,** 1-12.

Kuntz, A., and Saccomanno, G. (1944). Reflex inhibition of intestinal motility mediated through decentralized prevertebral ganglia. *J Neurophysiol* 7**,** 163-170.

Kuntz, A., and Van Buskirk, C. (1941). Reflex inhibition of bile flow and intestinal motility mediated through decentralized celiac plexus. . *Proc. Soc. Exp. Biol. Med.* 46**,** 519-523.

Lanfranchi, G.A., Marzio, L., Cortini, C., and Osset, E.M. (1978). Motor effect of dopamine on human sigmoid colon. Evidence for specific receptors. *Am J Dig Dis* 23(3)**,** 257-263. doi: 10.1007/BF01072326.

Langley, J.N. (1898). On the Union of Cranial Autonomic (Visceral) Fibres with the Nerve Cells of the Superior Cervical Ganglion. *J Physiol* 23(3)**,** 240-270. doi: 10.1113/jphysiol.1898.sp000726.

Li, Z.S., and Furness, J.B. (2000). Inputs from intrinsic primary afferent neurons to nitric oxide synthase-immunoreactive neurons in the myenteric plexus of guinea pig ileum. *Cell Tissue Res* 299(1)**,** 1-8. doi: 10.1007/s004419900125.

Li, Z.S., Pham, T.D., Tamir, H., Chen, J.J., and Gershon, M.D. (2004). Enteric dopaminergic neurons: definition, developmental lineage, and effects of extrinsic denervation. *J Neurosci* 24(6)**,** 1330-1339. doi: 10.1523/JNEUROSCI.3982-03.2004.

Li, Z.S., Schmauss, C., Cuenca, A., Ratcliffe, E., and Gershon, M.D. (2006). Physiological modulation of intestinal motility by enteric dopaminergic neurons and the D2 receptor: analysis of dopamine receptor expression, location, development, and function in wild-type and knock-out mice. *J Neurosci* 26(10)**,** 2798-2807. doi: 10.1523/JNEUROSCI.4720-05.2006.

Lin, H.C., Neevel, C., Chen, P.S., Suh, G., and Chen, J.H. (2003). Slowing of intestinal transit by fat or peptide YY depends on beta-adrenergic pathway. *Am J Physiol Gastrointest Liver Physiol* 285(6)**,** G1310-1316. doi: 10.1152/ajpgi.00230.2003.

Llewellyn-Smith, I.J., Furness, J.B., O'Brien, P.E., and Costa, M. (1984). Noradrenergic nerves in human small intestine. Distribution and ultrastructure. *Gastroenterology* 87(3)**,** 513-529.

Llewellyn-Smith, I.J., Wilson, A.J., Furness, J.B., Costa, M., and Rush, R.A. (1981). Ultrastructural identification of noradrenergic axons and their distribution within the enteric plexuses of the guinea-pig small intestine. *J Neurocytol* 10(2)**,** 331-352. doi: 10.1007/BF01257975.

Lomax, A.E., Sharkey, K.A., and Furness, J.B. (2010). The participation of the sympathetic innervation of the gastrointestinal tract in disease states. *Neurogastroenterol Motil* 22(1)**,** 7-18. doi: 10.1111/j.1365-2982.2009.01381.x.

Lundgren, O. (2000). Sympathetic input into the enteric nervous system. *Gut* 47 Suppl 4**,** iv33-35; discussion iv36. doi: 10.1136/gut.47.suppl_4.iv33.

Lyford, G.L., He, C.L., Soffer, E., Hull, T.L., Strong, S.A., Senagore, A.J., et al. (2002). Pan-colonic decrease in interstitial cells of Cajal in patients with slow transit constipation. *Gut* 51(4)**,** 496-501.

doi: 10.1136/gut.51.4.496.

Macrae, I.M., Furness, J.B., and Costa, M. (1986). Distribution of subgroups of noradrenaline neurons in the coeliac ganglion of the guinea-pig. *Cell Tissue Res* 244(1)**,** 173-180. doi: 10.1007/BF00218395.

Mahmoud, N.N., Bleier, J.I.S., Aarons, C.B., Paulson, E.C., Shanmugan, S., and Fry, D. (2017). "Colon and Rectum," in *Sabiston Textbook of Surgery - The Biologic Basis of Modern Surgical Practice,* eds. C.M. Townsend, R.D. Beauchamp, M. Evers & K.L. Mattox. 20th ed (Philadelphia, PA: Elsevier), 1312-1393.

Manber, L., and Gershon, M.D. (1979). A reciprocal adrenergic-cholinergic axoaxonic synapse in the mammalian gut. *Am J Physiol* 236(6)**,** E738-745. doi: 10.1152/ajpendo.1979.236.6.E738.

Mann, P.T., Southwell, B.R., Young, H.M., and Furness, J.B. (1997). Appositions made by axons of descending interneurons in the guinea-pig small intestine, investigated by confocal microscopy. *J Chem Neuroanat* 12(3)**,** 151-164. doi: 10.1016/s0891-0618(96)00189-5.

McCorry, L.K. (2007). Physiology of the autonomic nervous system. *Am J Pharm Educ* 71(4)**,** 78. doi: 10.5688/aj710478.

Mearin, F., Lacy, B.E., Chang, L., Chey, W.D., Lembo, A.J., Simren, M., et al. (2016). Bowel Disorders. *Gastroenterology*. doi: 10.1053/j.gastro.2016.02.031.

Miller, L., Roland, B.C., Whitson, M., Passi, M., Cheung, M., and Vegesna, A. (2018). "Clinical and Translational Aspects of Normal and Abnormal Motility in the Esophagus, Small Intestine and Colon," in *Physiology of the Gastrointestinal Tract,* ed. H. Said. 6th edh. ed: Elsevier), 485-516.

Miller, S.M., and Szurszewski, J.H. (2002). Relationship between colonic motility and cholinergic mechanosensory afferent synaptic input to mouse superior mesenteric ganglion. *Neurogastroenterol Motil* 14(4)**,** 339-348. doi: 10.1046/j.1365-2982.2002.00338.x.

Murphy, E.M., Defontgalland, D., Costa, M., Brookes, S.J., and Wattchow, D.A. (2007). Quantification of subclasses of human colonic myenteric neurons by immunoreactivity to Hu, choline acetyltransferase and nitric oxide synthase. *Neurogastroenterol Motil* 19(2)**,** 126-134. doi: 10.1111/j.1365-2982.2006.00843.x.

Nasser, Y., Ho, W., and Sharkey, K.A. (2006). Distribution of adrenergic receptors in the enteric nervous system of the guinea pig, mouse, and rat. *J Comp Neurol* 495(5)**,** 529-553. doi: 10.1002/cne.20898.

Natale, G., Ryskalin, L., Busceti, C.L., Biagioni, F., and Fornai, F. (2017). The nature of catecholamine-containing neurons in the enteric nervous system in relationship with organogenesis, normal human anatomy and neurodegeneration. *Arch Ital Biol* 155(3)**,** 118-130. doi: 10.12871/00039829201733.

Neal, K.B., and Bornstein, J.C. (2007). Mapping 5-HT inputs to enteric neurons of the guinea-pig small intestine. *Neuroscience* 145(2)**,** 556-567. doi: 10.1016/j.neuroscience.2006.12.017.

Neely, J., and Catchpole, B. (1971). Ileus: the restoration of alimentary-tract motility by pharmacological means. *Br J Surg* 58(1)**,** 21-28. doi: 10.1002/bjs.1800580104.

Ng, K.S., Montes-Adrian, N.A., Mahns, D.A., and Gladman, M.A. (2018). Quantification and neurochemical coding of the myenteric plexus in humans: No regional variation between the distal colon and rectum. *Neurogastroenterol Motil* 30(3). doi: 10.1111/nmo.13193.

Ng, Q.X., Soh, A.Y.S., Loke, W., Venkatanarayanan, N., Lim, D.Y., and Yeo, W.S. (2019). Systematic review with meta-analysis: The association between post-traumatic stress disorder and irritable bowel syndrome. *J Gastroenterol Hepatol* 34(1)**,** 68-73. doi: 10.1111/jgh.14446.

Nishi, S., and North, R.A. (1973). Presynaptic action of noradrenaline in the myenteric plexus. *J Physiol* 231(1)**,** 29P-30P.

Norberg, K.A. (1964). Adrenergic Innervation of the Intestinal Wall Studied by Fluorescence Microscopy. *Int J Neuropharmacol* 3**,** 379-382. doi: 10.1016/0028-3908(64)90067-x.

Olsson, C., Chen, B.N., Jones, S., Chataway, T.K., Costa, M., and Brookes, S.J. (2006). Comparison of extrinsic efferent innervation of guinea pig distal colon and rectum. *J Comp Neurol* 496(6)**,** 787-801. doi: 10.1002/cne.20965.

Pahlin, P.E., and Kewenter, J. (1976). Sympathetic nervous control of cat ileocecal sphincter. *Am J Physiol* 231(2)**,** 296-305. doi: 10.1152/ajplegacy.1976.231.2.296.

Paton, W.D., and Vizi, E.S. (1969). The inhibitory action of noradrenaline and adrenaline on acetylcholine output by guinea-pig ileum longitudinal muscle strip. *Br J Pharmacol* 35(1)**,** 10-28. doi: 10.1111/j.1476-5381.1969.tb07964.x.

Phillips, R.J., Kieffer, E.J., and Powley, T.L. (2003). Aging of the myenteric plexus: neuronal loss is specific to cholinergic neurons. *Auton Neurosci* 106(2)**,** 69-83. doi: 10.1016/S1566-0702(03)00072-9.

Pompolo, S., and Furness, J.B. (1995). Sources of inputs to longitudinal muscle motor neurons and ascending interneurons in the guinea-pig small intestine. *Cell Tissue Res* 280(3)**,** 549-560. doi: 10.1007/BF00318359.

Porter, A.J., Wattchow, D.A., Brookes, S.J., and Costa, M. (1997). The neurochemical coding and projections of circular muscle motor neurons in the human colon. *Gastroenterology* 113(6)**,** 1916-1923. doi: 10.1016/s0016-5085(97)70011-8.

Porter, A.J., Wattchow, D.A., Brookes, S.J., and Costa, M. (2002). Cholinergic and nitrergic interneurones in the myenteric plexus of the human colon. *Gut* 51(1)**,** 70-75. doi: 10.1136/gut.51.1.70.

Porter, A.J., Wattchow, D.A., Hunter, A., and Costa, M. (1998). Abnormalities of nerve fibers in the circular muscle of patients with slow transit constipation. *Int J Colorectal Dis* 13(5-6)**,** 208-216. doi: 10.1007/s003840050163.

Qu, Z.D., Thacker, M., Castelucci, P., Bagyanszki, M., Epstein, M.L., and Furness, J.B. (2008). Immunohistochemical analysis of neuron types in the mouse small intestine. *Cell Tissue Res* 334(2)**,** 147-161. doi: 10.1007/s00441-008-0684-7.

Rae, M.G., Fleming, N., McGregor, D.B., Sanders, K.M., and Keef, K.D. (1998). Control of motility patterns in the human colonic circular muscle layer by pacemaker activity. *Journal of Physiology-London* 510(1)**,** 309-320. doi: DOI 10.1111/j.1469-7793.1998.309bz.x.

Rayner, C.K., and Hughes, P.A. (2016). "Small Intestinal Motor and Sensory Function and Dysfunction," in *Seisenger and Fortdran's Gastrointestinal and Liver Disease*. 10th edn ed (1600 John F. Kennedy Blvd. Ste 1800, Philadelphia, PA: Saunders Elsevier), 1580-1594.

Read, J.B., and Burnstock, G. (1968). Comparative histochemical studies of adrenergic nerves in the enteric plexuses of vertebrate large intestine. *Comp Biochem Physiol* 27(2)**,** 505-517. doi: 10.1016/0010-406x(68)90247-8.

Sanders, K.M., and Ward, S.M. (2019). Nitric oxide and its role as a non-adrenergic, non-cholinergic inhibitory neurotransmitter in the gastrointestinal tract. *Br J Pharmacol* 176(2)**,** 212-227. doi: 10.1111/bph.14459.

Schapiro, H., and Woodward, E.R. (1959). Pathway of enterogastric reflex. *Proc Soc Exp Biol Med* 101(3)**,** 407-409. doi: 10.3181/00379727-101-24960.

Scheibner, J., Trendelenburg, A.U., Hein, L., Starke, K., and Blandizzi, C. (2002). Alpha 2-adrenoceptors in the enteric nervous system: a study in alpha 2A-adrenoceptor-deficient mice. *Br J Pharmacol* 135(3)**,** 697-704. doi: 10.1038/sj.bjp.0704512.

Schemann, M., Sann, H., Schaaf, C., and Mader, M. (1993). Identification of cholinergic neurons in enteric nervous system by antibodies against choline acetyltransferase. *Am J Physiol* 265(5 Pt 1)**,** G1005-1009. doi: 10.1152/ajpgi.1993.265.5.G1005.

Schultzberg, M., Hokfelt, T., Nilsson, G., Terenius, L., Rehfeld, J.F., Brown, M., et al. (1980). Distribution of peptide- and catecholamine-containing neurons in the gastro-intestinal tract of rat and guinea-pig: immunohistochemical studies with antisera to substance P, vasoactive intestinal polypeptide, enkephalins, somatostatin, gastrin/cholecystokinin, neurotensin and dopamine beta-hydroxylase. *Neuroscience* 5(4)**,** 689-744. doi: 10.1016/0306-4522(80)90166-9.

Scott, S.M., Simren, M., Farmer, A.D., Dinning, P.G., Carrington, E.V., Benninga, M.A., et al. (2020). Chronic constipation in adults: Contemporary perspectives and clinical challenges. 1: Epidemiology, diagnosis, clinical associations, pathophysiology and investigation. *Neurogastroenterol Motil***,** e14050. doi: 10.1111/nmo.14050.

Semba, T. (1954). Studies on the enterogastric reflexes. *Hiroshima J Med Sci* 2**,** 323-327.

Serra, J., Pohl, D., Azpiroz, F., Chiarioni, G., Ducrotte, P., Gourcerol, G., et al. (2020). European society of neurogastroenterology and motility guidelines on functional constipation in adults. *Neurogastroenterol Motil* 32(2)**,** e13762. doi: 10.1111/nmo.13762.

Singaram, C., Ashraf, W., Gaumnitz, E.A., Torbey, C., Sengupta, A., Pfeiffer, R., et al. (1995). Dopaminergic defect of enteric nervous system in Parkinson's disease patients with chronic constipation. *Lancet* 346(8979)**,** 861-864. doi: 10.1016/s0140-6736(95)92707-7.

Sinnatamby, C.S. (2011). "Abdomen," in *Last's Anatomy Regional and Applied*. 12 ed (London, UK: Elsevier), 247-258.

Smith-Edwards, K.M., Edwards, B.S., Wright, C.M., Schneider, S., Meerschaert, K.A., Ejoh, L.L., et al. (2020). Sympathetic Input to Multiple Cell Types in Mouse and Human Colon Produces Region-Specific Responses. *Gastroenterology*. doi: 10.1053/j.gastro.2020.09.030.

Smolilo, D.J., Costa, M., Hibberd, T.J., Wattchow, D.A., and Spencer, N.J. (2018). Morphological evidence for novel enteric neuronal circuitry in guinea pig distal colon. *J Comp Neurol* 526(10)**,** 1662-1672. doi: 10.1002/cne.24436.

Spencer, N.J., Dinning, P.G., Brookes, S.J., and Costa, M. (2016). Insights into the mechanisms underlying colonic motor patterns. *Journal of Physiology-London* 594(15)**,** 4099-4116. doi: 10.1113/Jp271919.

Stakenborg, N., Labeeuw, E., Gomez-Pinilla, P.J., De Schepper, S., Aerts, R., Goverse, G., et al. (2019). Preoperative administration of the 5-HT4 receptor agonist prucalopride reduces intestinal inflammation and shortens postoperative ileus via cholinergic enteric neurons. *Gut* 68(8)**,** 1406-1416. doi: 10.1136/gutjnl-2018-317263.

Stebbing, M., Johnson, P., Vremec, M., and Bornstein, J. (2001). Role of alpha(2)-adrenoceptors in the sympathetic inhibition of motility reflexes of guinea-pig ileum. *J Physiol* 534(Pt. 2)**,** 465-478. doi: 10.1111/j.1469-7793.2001.00465.x.

Steele, P.A., Brookes, S.J., and Costa, M. (1991). Immunohistochemical identification of cholinergic neurons in the myenteric plexus of guinea-pig small intestine. *Neuroscience* 45(1)**,** 227-239. doi: 10.1016/0306-4522(91)90119-9.

Strata, P., and Harvey, R. (1999). Dale's principle. *Brain Res Bull* 50(5-6)**,** 349-350. doi: 10.1016/s0361-9230(99)00100-8.

Sykova, E. (2004). Extrasynaptic volume transmission and diffusion parameters of the extracellular space. *Neuroscience* 129(4)**,** 861-876. doi: 10.1016/j.neuroscience.2004.06.077.

Szurszewski, J.H. (1969). A migrating electric complex of canine small intestine. *Am J Physiol* 217(6)**,** 1757-1763. doi: 10.1152/ajplegacy.1969.217.6.1757.

Szurszewski, J.H., Ermilov, L.G., and Miller, S.M. (2002). Prevertebral ganglia and intestinofugal afferent neurones. *Gut* 51 Suppl 1**,** i6-10. doi: 10.1136/gut.51.suppl_1.i6.

Takahashi, T., and Owyang, C. (1998). Regional differences in the nitrergic innervation between the proximal and the distal colon in rats. *Gastroenterology* 115(6)**,** 1504-1512. doi: 10.1016/s0016-5085(98)70029-0.

Tan, L.L., Bornstein, J.C., and Anderson, C.R. (2010). The neurochemistry and innervation patterns of extrinsic sensory and sympathetic nerves in the myenteric plexus of the C57Bl6 mouse jejunum. *Neuroscience* 166(2)**,** 564-579. doi: 10.1016/j.neuroscience.2009.12.034.

Tanila, H., Kauppila, T., and Taira, T. (1993). Inhibition of intestinal motility and reversal of postlaparotomy ileus by selective alpha 2-adrenergic drugs in the rat. *Gastroenterology* 104(3)**,** 819-824. doi: 10.1016/0016-5085(93)91018-d.

Tassicker, B.C., Hennig, G.W., Costa, M., and Brookes, S.J. (1999). Rapid anterograde and retrograde tracing from mesenteric nerve trunks to the guinea-pig small intestine in vitro. *Cell Tissue Res* 295(3)**,** 437-452. doi: 10.1007/s004410051250.

Tillou, J., and Poylin, V. (2017). Functional Disorders: Slow-Transit Constipation. *Clin Colon Rectal Surg* 30(1)**,** 76-86. doi: 10.1055/s-0036-1593436.

Trendelenburg, P. (2006). Physiological and pharmacological investigations of small intestinal peristalsis. Translation of the article "Physiologische und pharmakologische Versuche uber die Dunndarmperistaltik", Arch. Exp. Pathol. Pharmakol. 81, 55-129, 1917. *Naunyn Schmiedebergs Arch Pharmacol* 373(2)**,** 101-133. doi: 10.1007/s00210-006-0052-7.

Vanhatalo, S., and Soinila, S. (1998). The concept of chemical neurotransmission--variations on the theme. *Ann Med* 30(2)**,** 151-158. doi: 10.3109/07853899808999398.

Vather, R., Trivedi, S., and Bissett, I. (2013). Defining postoperative ileus: results of a systematic review and global survey. *J Gastrointest Surg* 17(5)**,** 962-972. doi: 10.1007/s11605-013-2148-y.

Vizi, E.S., and Knoll, J. (1971). The effects of sympathetic nerve stimulation and guanethidine on parasympathetic neuroeffector transmission; the inhibition of acetylcholine release. *J Pharm Pharmacol* 23(12)**,** 918-925. doi: 10.1111/j.2042-7158.1971.tb09893.x.

Wakabayashi, K., Takahashi, H., Ohama, E., and Ikuta, F. (1989). Tyrosine hydroxylase-immunoreactive intrinsic neurons in the Auerbach's and Meissner's plexuses of humans. *Neurosci Lett* 96(3)**,** 259-263. doi: 10.1016/0304-3940(89)90388-1.

Walker, J.K., Gainetdinov, R.R., Mangel, A.W., Caron, M.G., and Shetzline, M.A. (2000). Mice lacking the dopamine transporter display altered regulation of distal colonic motility. *Am J Physiol Gastrointest Liver Physiol* 279(2)**,** G311-318. doi: 10.1152/ajpgi.2000.279.2.G311.

Walter, G.C., Phillips, R.J., McAdams, J.L., and Powley, T.L. (2016). Individual sympathetic

postganglionic neurons coinnervate myenteric ganglia and smooth muscle layers in the gastrointestinal tract of the rat. *J Comp Neurol* 524(13)**,** 2577-2603. doi: 10.1002/cne.23978.

Wattchow, D., Brookes, S., Murphy, E., Carbone, S., de Fontgalland, D., and Costa, M. (2008). Regional variation in the neurochemical coding of the myenteric plexus of the human colon and changes in patients with slow transit constipation. *Neurogastroenterol Motil* 20(12)**,** 1298-1305. doi: 10.1111/j.1365-2982.2008.01165.x.

Wattchow, D., Heitmann, P., Smolilo, D., Spencer, N.J., Parker, D., Hibberd, T., et al. (2020). Postoperative ileus-An ongoing conundrum. *Neurogastroenterol Motil***,** e14046. doi: 10.1111/nmo.14046.

Wattchow, D.A., Brookes, S.J., and Costa, M. (1995). The morphology and projections of retrogradely labeled myenteric neurons in the human intestine. *Gastroenterology* 109(3)**,** 866-875. doi: 10.1016/0016-5085(95)90396-8.

Wattchow, D.A., Porter, A.J., Brookes, S.J., and Costa, M. (1997). The polarity of neurochemically defined myenteric neurons in the human colon. *Gastroenterology* 113(2)**,** 497-506. doi: 10.1053/gast.1997.v113.pm9247469.

Wood, J.D. (1999). Neurotransmission at the interface of sympathetic and enteric divisions of the autonomic nervous system. *Chin J Physiol* 42(4)**,** 201-210.

Wood, J.D. (2011). *Enteric Nervous System: The Brain-in-the-Gut.* New Jersey, USA: Morgan & Claypool Life Sciences.

Wright, C.M., Schneider, S., Smith-Edwards, K.M., Mafra, F., Leembruggen, A.J.L., Gonzalez, M.V., et al. (2021). scRNA-Seq Reveals New Enteric Nervous System Roles for GDNF, NRTN, and TBX3. *Cell Mol Gastroenterol Hepatol* 11(5)**,** 1548-1592 e1541. doi: 10.1016/j.jcmgh.2020.12.014.

Yuan, P.Q., Bellier, J.P., Li, T., Kwaan, M.R., Kimura, H., and Tache, Y. (2020). Intrinsic cholinergic innervation in the human sigmoid colon revealed using CLARITY, three-dimensional (3D) imaging, and a novel anti-human peripheral choline acetyltransferase (hpChAT) antiserum. *Neurogastroenterol Motil***,** e14030. doi: 10.1111/nmo.14030.

Zhang, X., Guo, H., Xu, J., Li, Y., Li, L., Zhang, X., et al. (2012). Dopamine receptor D1 mediates the inhibition of dopamine on the distal colonic motility. *Transl Res* 159(5)**,** 407-414. doi: 10.1016/j.trsl.2012.01.002.

Zhang, Z.W., Kang, J.I., and Vaucher, E. (2011). Axonal varicosity density as an index of local neuronal interactions. *PLoS One* 6(7)**,** e22543. doi: 10.1371/journal.pone.0022543.

Zizzo, M.G., Bellanca, A., Amato, A., and Serio, R. (2020). Opposite effects of dopamine on the mechanical activity of circular and longitudinal muscle of human colon. *Neurogastroenterol Motil* 32(6)**,** e13811. doi: 10.1111/nmo.13811.

# Appendix A Laboratory Based Research During COVID-19

2020 has been a unique year in modern history due to the global COVID-19 (Coronavirus Disease 2019) pandemic. There are few facets of society that have not been impacted and laboratory-based research is no exception.

This research project formally commenced on 3 February 2020. Just over a month later, concern regarding the seriousness and impact of the pandemic was at its peak and Australian borders were closed to non-residents on 20 March. Soon after, interstate borders were also closed to varying degrees, or otherwise allowing people to cross the border and quarantine in isolation for 14 days. Through the rest of the year, interstate borders intermittently opened and closed in response to regional outbreaks. Non-essential services were closed and many people were required to work from home.

Access to human colonic tissue ceased from the middle of March due to the potential risk of aerosolisation of SARS-CoV2 (Severe Acute Respiratory Syndrome coronavirus 2) virus particles via faeces and possible transmission. Tissue retrieval only recommenced in late July. Additional precautions were taken to avoid having colonic tissue (with faecal residue) in bubbled oxygenated Krebs solution. During this time, there was fortunately enough banked tissue collected from my time in the lab between early January and mid-March which allowed for the experiment to be restarted after the first failed run of immunohistochemistry.

Social distancing measures meant that for brief periods the laboratory was closed, and for 2 months the weekly in-house laboratory team meetings were cancelled. On a larger scale, the Federation of Neurogastroenterology and Motility international meeting, scheduled to be held in Adelaide on 14-17 April was cancelled. Several other significant conferences were transferred to a virtual online format, including two that this research was presented at: the Royal Australasian College of Surgeons Academic Surgery Conference (November) and the General Surgery Australia SA/NT Registrar's Paper Day (December).

The Zeiss LSM880 confocal microscope being used to acquire high-resolution image stacks presented a technical issue. In early April the CY3 laser broke and produced poor immunofluorescence. It was determined that the laser needed replacement, however the Zeiss engineer was based in Sydney and could not travel to Adelaide due to travel restrictions. During this

time, the first batch of immunohistochemistry was failing and the experiment was restarted with a new protocol, in which fluorophores requiring the CY3 laser were avoided in the first layer because of the confocal issue. An exemption was eventually granted to allow the engineer to travel to Adelaide without quarantining to fix the CY3 laser, in time for the second layer of immunohistochemistry allowing for the optimal ChAT-CY3 combination.

Through these significant challenges there were multiple workarounds and modifications required which enabled the project to be completed on a slightly delayed timeline.